AD____________________

Award Number: W81XWH-07-1-0306

TITLE: PROSPECT (Profiling of Resistance Patterns & Oncogenic Signaling Pathways in Evaluation of Cancers of the Thorax and Therapeutic Target Identification)

PRINCIPAL INVESTIGATOR: Waun Ki Hong, M.D.
David J. Stewart, M.D.

CONTRACTING ORGANIZATION: University of Texas M. D. Anderson Cancer Center
Houston, Texas 77030

REPORT DATE: June 2008

TYPE OF REPORT: Annual

PREPARED FOR: U.S. Army Medical Research and Materiel Command
Fort Detrick, Maryland 21702-5012

DISTRIBUTION STATEMENT: Approved for Public Release;
Distribution Unlimited

REPORT DOCUMENTATION PAGE

Form Approved
OMB No. 0704-0188

1. REPORT DATE *(DD-MM-YYYY)*
01-06-2008

2. REPORT TYPE
Annual

3. DATES COVERED *(From - To)*
1 June 2007- 30 May 2008

4. TITLE AND SUBTITLE
PROSPECT (Profiling of Resistance Patterns & Oncogenic Signaling Pathways in Evaluation of Cancers of the Thorax and Therapeutic Target Identification)

5a. CONTRACT NUMBER

5b. GRANT NUMBER
W81XWH-07-1-0306

5c. PROGRAM ELEMENT NUMBER

6. AUTHOR(S)
Waun Ki Hong, M.D., David J. Stewart, M.D.

5d. PROJECT NUMBER

5e. TASK NUMBER

5f. WORK UNIT NUMBER

7. PERFORMING ORGANIZATION NAME(S) AND ADDRESS(ES)
University of Texas M. D. Anderson Cancer Center
Houston, Texas 77030

8. PERFORMING ORGANIZATION REPORT NUMBER

9. SPONSORING / MONITORING AGENCY NAME(S) AND ADDRESS(ES)
U.S. Army Medical Research and Materiel Command
Fort Detrick, Maryland 21702-5012

10. SPONSOR/MONITOR'S ACRONYM(S)

11. SPONSOR/MONITOR'S REPORT NUMBER(S)

12. DISTRIBUTION / AVAILABILITY STATEMENT
Approved for Public Release; Distribution Unlimited

13. SUPPLEMENTARY NOTES

14. ABSTRACT
We will develop a high throughput therapeutic-target focused (TTF) profiling platform and will combine this with tumor genome wide mRNA profiling and with serum or plasma profiling of phosphopeptides and DNA. We will use these molecular profiles to help define how various molecular factors alone and in combination relate to resistance to therapy, to prognosis, and to metastatic patterns at relapse. Using tumor and blood samples from non-small cell lung cancer (NSCLC) patients as well as NSCLC cell lines with defined chemotherapy resistance patterns, we will examine how molecular profiles may confer resistance and will identify new, potential therapeutic targets. The PROSPECT approach will be novel in that we will assess tumors from NSCLC patients undergoing surgical resection after having received neoadjuvant therapy as a model of resistance. Tumor surviving neoadjuvant therapy would be expected to be enriched for resistant cells. We will define what combinations of targeted therapies are most effective against resistant cell lines with similar molecular profiles, and this will drive later clinical trials (beyond the scope of this Program). Similar studies will be conducted in patients with mesotheliomas undergoing surgical resection of tumor after neoadjuvant therapy with the new Src inhibitor dasatinib.

15. SUBJECT TERMS
Lung Cancer, Mesothelioma; Target-focused profiling; Resistance

16. SECURITY CLASSIFICATION OF:			17. LIMITATION OF ABSTRACT	18. NUMBER OF PAGES	19a. NAME OF RESPONSIBLE PERSON
					USAMRMC
a. REPORT	b. ABSTRACT	c. THIS PAGE			19b. TELEPHONE NUMBER *(include area code)*
U	U	U	UU	73	

Standard Form 298 (Rev. 8-98)
Prescribed by ANSI Std. Z39.18

Table of Contents

INTRODUCTION

Lung cancer is the leading cause of cancer death in the world. Non-small cell lung cancer (NSCLC) accounts for 85% of all lung cancer cases. Only 15% of patients diagnosed with lung cancer survive five years from diagnosis. Therapy for advanced disease increases average life expectancy by only a few months, and slightly improves quality of life. Similarly, adjuvant chemotherapy for resected disease has only a modest impact on survival rates. More effective therapy is needed. We believe that applying state-of-the-art molecular tools to carefully conducted clinical trials will lead to the identification of molecular mechanisms that contribute to lung cancer therapeutic resistance and that drive prognosis, and that this in turn will lead to the development of drugs with novel biological and therapeutic functions. Therefore, we have undertaken a translational research program named **PROSPECT**: Profiling of Resistance Patterns & Oncogenic Signaling Pathways in Evaluation of Cancers of the Thorax and Therapeutic Target Identification. The goal of PROSPECT is to use therapeutic target-focused (TTF) profiling along with genome-wide mRNA and serum phosphopeptide profiling to identify and evaluate molecular targets and pathways that contribute to therapeutic sensitivity or resistance, prognosis, and recurrence patterns, and to use this information to guide formulation of new rational therapeutic strategies for NSCLC and mesotheliomas. In the Program, we have 5 research projects and 3 Cores to address 3 central issues: therapeutic resistance, prognosis and new therapeutic targets and strategies.

PROGRESS REPORT (BODY):

Project 1: Therapeutic target-focused (TTF) profiling for the identification of molecular targets and pathways that contribute to drug sensitivity or resistance *in vitro* and the development of rational treatment strategies for NSCLC.

(Leader: Dr. John Heymach; Co-Leaders: Drs. Li Mao, John Minna)

Hypotheses:

We hypothesize that a broad, systematic molecular profiling of NSCLC cell lines, using both TTF and global approaches, will lead to the following results:

1. The identification of new potential therapeutic targets for NSCLC
2. The development of predictive markers for *in vitro* sensitivity to targeted agents, which will form the starting point for the development of a predictive model of *in vivo* sensitivity using clinical specimens as described in Aim 3.
3. Insights into the molecular mechanism underlying therapeutic resistance and into the relationship of resistance mechanisms to factors innately affecting tumor growth rate and prognosis
4. Identification of readily translatable therapeutic strategies to combat these resistance mechanisms.

Specific Aims:

In this project we will develop and validate a novel therapeutic target-focused (TTF) profiling platform at M.D. Anderson Cancer Center. The platform will provide a high throughput, quantitative, scalable, and highly sensitive set of assays to assess activation of key signaling pathways (eg, PI3K/AKT, STAT, RAS-RAF-ERK) as well as other potential therapeutic targets such as receptor tyrosine kinases (RTKs). It will be coupled with global profiling of gene expression using Affymetrix 2.0 array. These molecular profiles will then be coupled with information from a broad DATS (drug and therapeutic target siRNA) screen to develop markers for predicting drug sensitivity *in vitro* based on molecular profiles, elucidate the molecular determinants of sensitivity or resistance to a given therapeutic agent, and identify potential therapeutic targets for tumor cells resistant to a given agent. This project lays the foundation for Project 3, where the same TTF and global profiling approaches will be used to characterize clinical tumor specimens and investigate molecular markers identified in this project, for Project 4 in which the profiles and therapeutic targets for mesothelioma will be explored, and for Project 2 in which the profiles will be correlated with patient prognosis and metastatic patterns. The specific aims of this project are as follows:

Specific Aim 1: To develop a TTF profile for assessing critical signaling pathways and potential therapeutic targets, and to apply TTF and gene expression profiling to NSCLC and mesothelioma cell lines.

1.1. Development and technical validation of a TTF profile using reverse phase lysate arrays (RPPA) and multiplexed bead array technology.

1.2. Application of TTF profiling to a cell line panel representing malignant (NSCLC and mesothelioma) and non-malignant (endothelial and stromal cells, normal bronchial epithelium) cell types.

1.3. Gene expression profiling of the cell line panel using Affymetrix microarrays.

1.4. Correlation of TTF and gene expression profiles from the cell line panel to determine gene expression signatures that correlate with activation of individual proteins (e.g. EGFR activation) and critical signaling pathways (e.g. RAS pathway activation).

Specific Aim 2: To determine the sensitivity of the cell line panel to the selected drug and therapeutic target *s*iRNA (DATS) screen.

2.1. Screening of the cell line panel for sensitivity to a panel of 20-25 targeted agents and standard chemotherapy agents.

2.2. Screening of the cell line panel using siRNA representing potential therapeutic targets, including molecules targeted by specific agents in Aim 2.1 (e.g. EGFR, IGFR-1, etc) and potential therapeutic targets for which drugs are not currently available (e.g., RTKs for which drugs are currently in development).

2.3. Comparison of *in vitro and in vivo* profiles (TTF and global) and drug sensitivity in selected NSCLC cell lines and xenografts grown from the same lines.

Specific Aim 3: Development of markers for predicting drug and targeted siRNA sensitivity *in vitro* based on TTF and molecular profiles, and identification of candidate therapeutic targets in chemotherapy-resistant lines.

Update

Over the past year, protein profiling of a large panel of NSCLC cell lines has been applied to the development of drug response signatures. Specifically, we have developed signatures for predicting sensitivity to pemetrexed, as well as a model for selecting whether a cell line is more likely to be sensitive to a taxane or an EGFR inhibitor. These results were presented in various national meetings, including the AACR Annual Meeting, and we are in the process of validating these findings in an independent set of NSCLC cell lines and in clinical samples from patients treated with these drugs.

Overview: NSCLC is a molecularly heterogeneous disease, with a variety of cell signaling pathways driving progression and therapeutic resistance. Although agents are available that target many of these critical pathways, there is currently no biologically-based method for selecting the best drug for a patient. Using reverse phase protein array (RPPA), a high-throughput technology that systematically measures key signaling proteins, we profiled 44 NSCLC cell lines for markers of sensitivity and resistance to 15 cytotoxic and targeted agents. RPPA is a quantitative, antibody-based assay that allows broad and simultaneous profiling of numerous therapeutically relevant targets from small amounts of protein, such as that obtained from routine biopsy. Unlike gene expression arrays, RPPAs directly measure protein levels and can discern specific post-translational modifications such as phosphorylation or cleavage. The ability to compare levels of phosphorylated versus non-phosphorylated proteins is particularly critical to determining the activity of signaling proteins such as tyrosine kinases.

In order to develop drug-response signatures, the drug concentration required for 50% growth inhibition (IC_{50}) was first determined for 44 cell lines using MTS assays. Then, RPPA was performed by printing serial dilutions of pre-treatment cell lysates on nitrocellulose-coated glass slides. Each slide was incubated with one of 59 validated, monospecific antibodies, and a single, representative logarithmic value for the signal intensity-serial dilution curve was determined for each sample. This represented the quantitative measure of a specific protein.

Subsets of sensitive and resistant cell lines were identified for each drug, despite most cell lines having never been exposed to any treatment either in the patient from which they were derived or *in vitro*. When subjected to unsupervised clustering, mechanistically-related drugs grouped together (such as taxanes, platinum agents, and epidermal growth factor receptor inhibitors), with similar patterns of protein expression characterizing sensitivity or resistance (Figure 1). For example, resistance to cisplatin and carboplatin was associated with increased expression of the cell adhesion molecules β-catenin and E-cadherin and with Rab25, a GTPase previously correlated with worse outcome in breast and ovarian cancer.

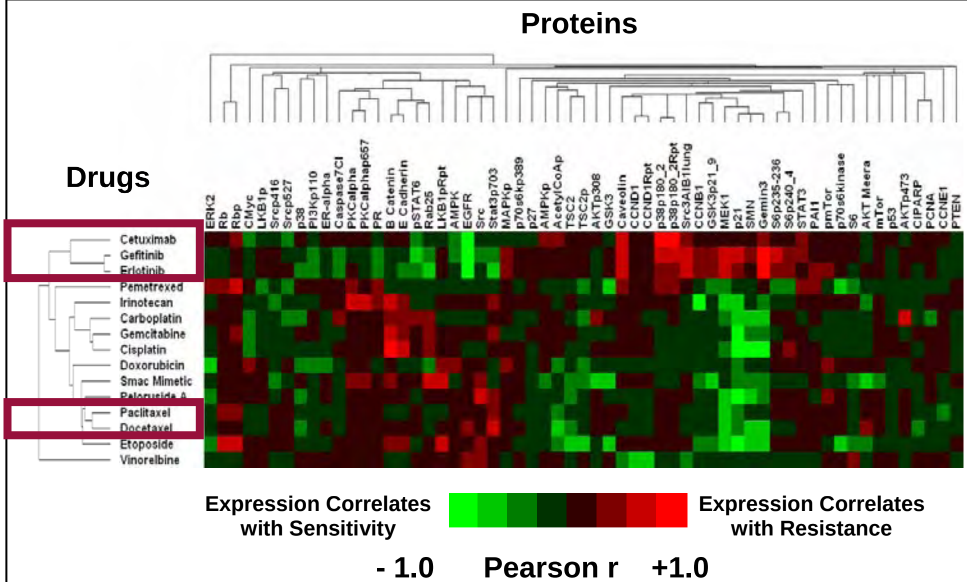

Figure 1. RPPA protein expression signatures cluster drugs according to mechanisms of action. Pearson correlation values are calculated between the expression vectors of each protein and the IC50 vectors of each drug, across all cell lines. These reflect association between level of protein expression and level of resistance to the drug. Each vertical segment represents a different protein's Pearson value with the intensity indicating the strength of the Pearson value (from -1.0 bright green (sensitivity) to 0 (black) to 1.0 bright red (resistance)). In hierarchical clustering analysis, drugs cluster according to their mechanism of action. For example, erlotinib and gefitinib have similar signatures and cluster most closely with cetuximab. Similarly, paclitaxel and docetaxel cluster together *(as indicated by red boxes).*

<u>Pemetrexed response signature</u>: Cell lines treated with pemetrexed showed the greatest variation in IC50's, with a 1000-fold difference between sensitivity and resistance across 42 cell lines. Pemetrexed resistance was strongly associated with a number of proteins, including increased phospho-Rb (pRb) and PKCalpha. However, no single marker was able to predict pemetrexed resistance by itself. Rather, response to pemetrexed was predicted by a multivariate model which evaluated 10 markers for their "presence" or "absence," as determined by unique cutoff values for each protein defined in the model (Figure 2). These results were presented at the AACR-NCI-EORTC International Conference and the IASCL Annual meeting this past year. Finally, for PKCalpha, one of the non-phosphorylated protein markers in the model, we demonstrated that high PKCalpha mRNA levels correlated with resistance and with protein levels (data not shown).

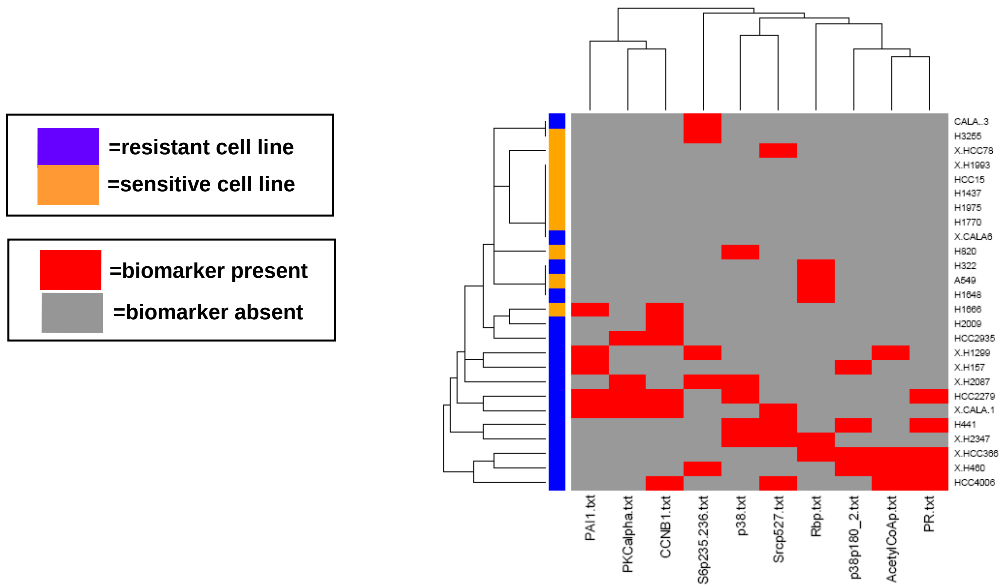

Figure 2. Pemetrexed response signature predicts resistance to pemetrexed. For each cell line, ten protein markers were determined to be either present *(red)* or absent *(gray)*. Two-way hierarchical clustering performed, resulting in 12 of the 16 resistant cell lines clustering together *(blue bar)* on the basis of having ≥2 markers present.

This 10-marker response signature will be validated in an independent set of cell lines and in pre-treatment samples from patients treated with single-agent pemetrexed. Because pemetrexed is commonly used as a single-agent in the setting of advanced NSCLC, we are hopeful that this signature can be clinically developed into a tool for identifying patients most likely to benefit from this drug, as well as identifying potential new therapeutic targets that might be combined with pemetrexed to overcome drug resistance.

5-Protein Signature for selecting EGFR TKIs versus Taxanes: RPPA proteomic profiling identified intracellular signaling pathways and proteins associated with sensitivity and resistance to the taxanes and EGFR-inhibitors in NSCLC. Moreover, markers of resistance to docetaxel were observed to be associated with sensitivity to erlotinib, and visa versa. Since both drugs are commonly used as single agents in the second-line setting, these observations were developed into a model of identifying whether a cell line was more likely to be sensitive to docetaxel versus erlotinib.

For each NSCLC cell line, the difference (delta) between Log($IC50_{docetaxel}$) and Log($IC50_{erlotinib}$) was calculated. Five markers correlated (p-value ≤0.05) with the degree of difference between docetaxel and erlotinib sensitivity. These results were presented at the AACR Annual meeting this year. Phospho-STAT3, EGFR, and progesterone receptor (PR) increased with greater erlotinib sensitivity and docetaxel resistance. Whereas, gemin3 and CCNB1 (cyclin B1) were increased in cell lines that were more sensitive to docetaxel and less sensitive to erlotinib (Figure 3).

As with pemetrexed, docetaxel and erlotinib are both drugs used as single-agents in advanced NSCLC. Therefore, we anticipate that this model, which predicts which class of drug is likely to have the greatest activity, may have important clinical applications for selecting therapy for an individual patient. We plan to test this retrospectively in patients treated with these agents.

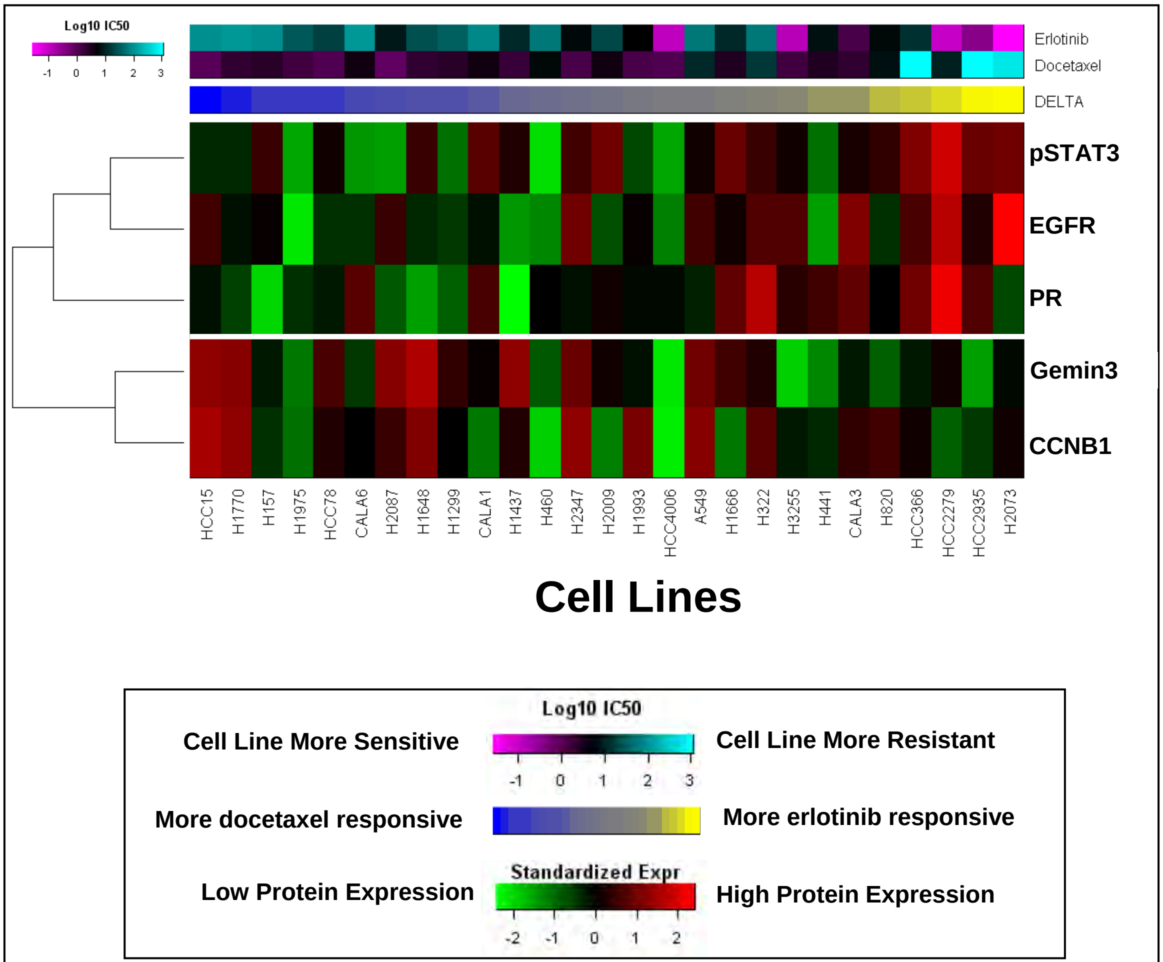

Figure 3. Five markers are inversely correlated with response to erlotinib versus docetaxel. For each cell line, the difference (delta) between Log($IC50_{docetaxel}$) and Log($IC50_{erlotinib}$) was calculated. Five markers correlated (p-value ≤0.05) with the degree of difference between docetaxel and erlotinib sensitivity. Phospho-STAT3, EGFR, and progesterone receptor (PR) increased with greater erlotinib sensitivity and docetaxel resistance. Whereas, gemin3 and CCNB1 (cyclin B1) were increased in cell lines that were more sensitive to docetaxel and less sensitive to erlotinib.

Key Research Accomplishments:

- Developed molecular signatures for predicting sensitivity to premetrexed.
- Developed a model for selection of sensitivity to taxanes vs EGFR inhibitors.

Reportable Outcomes:

Abstracts/Presentations

- Byers LA, Nanjundan M, Girard L, Coombes K, Xie Y, Peyton M, Ma Y, Zachariah S, Nikolinakos P, Cigarroa R, Mills G, Roth J, Minna J, Heymach J. "Reverse-phase protein array (RPPA) profiling of non-small cell lung cancer lines identifies tumor signatures for sensitivity and resistance to chemotherapy and targeted agents" [abstract]. In: Proceedings of the AACR-NCI-EORTC International Conference on Molecular Targets and Cancer Therapeutics; 2007 Oct 22-26; Washington, DC; San Francsisco (CA): AACR; Abstract B178, p 219, 2007.
- Byers, LA, et al. "Proteomic profiling of non-small cell lung cancer cell lines identifies tumor signatures of response to chemotherapy and targeted agents." IASCL 8th Annual Targeted Therapies of the Treatment of Lung Cancer Meeting, Santa Monica, CA, Feb 2008.

- Byers LA, Nanjundan M, Girard L, Coombes K, Xie Y, Peyton M, Zachariah S, Weber S, Siwak D, Nikolinakos P, Wistuba I, Roth J, Mills G, Minna J, Heymach J. "Reverse-phase protein array (RPPA) profiling of response to taxanes and epidermal growth factor receptor (EGFR) inhibitors identifies an inverse correlation between markers of sensitivity to docetaxel and erlotinib in non-small cell lung cancer lines". AACR Annual Meeting, San Diego, Abstract 3937, April 2008.
- Herynk MH, Xu L, Heymach JV. Sex differences in estrogen mediated growth and migration of NSCLC. Estrogen signaling promotes sex differences in the growth and migration of NSCLC. Impact of estrogen signaling on cell migration and proliferation of NSCLC cell lines. AACR Annual Meeting, San Diego, CA, Abstract 3034, April 2008.

Conclusions:
RPPA proteomic profiling identified intracellular signaling pathways and proteins associated with sensitivity and resistance to chemotherapies and targeted agents in NSCLC cell lines. These results suggest biologic mechanisms of therapeutic resistance. Our findings will be further investigated by correlating RPPA of tumor samples with clinical outcomes with the goal of developing predictive markers that can guide treatment selection and identify new targets in NSCLC.

Project 2. Tumor molecular profiles in patients with operable non-small cell lung cancer (NSCLC): impact on stage, prognosis, and relapse pattern

(Leaders: Drs. David Stewart, Jack Roth; Co-Leaders: Drs. Roy Herbst, Edward Kim, Katherine Pisters, Stephen Swisher)

Hypotheses:
We hypothesize that:
1. In tumors from patients with NSCLC, patterns of co-expression of molecules that modulate cell proliferation, survival, angiogenesis, invasion, metastasis and apoptosis will substantially influence tumor stage and size at the time of diagnosis, and will largely define patient prognosis.
2. Impact of adjuvant and neoadjuvant therapies on disease-free, progression-free, and overall survival will vary across prognostically distinct groups.
3. Specific molecular signatures in primary tumors will predict both metastatic patterns at relapse and molecular profiles of recurrent tumors, and this could help guide adjuvant strategies and therapeutic strategies at relapse.

Specific Aims:

Aim 1. To define characteristic TTF/gene expression profiles of prognostically distinct subpopulations of patients with resectable NSCLC, and to assess the extent to which these molecular profiles correlate with tumor stage and/or size.

The main goal of this aim is to use 150 archival NSCLC tumor samples from our tissue bank (with corresponding clinical data) and to prospectively collect tumor samples, blood samples and clinical data from 300 additional patients undergoing surgical resection of NSCLC. The tissue and blood samples will be used by Project 3 and the Pathology Core to generate comprehensive TTF/gene expression molecular profiles using methods developed in Project 1. We will construct Kaplan-Meier estimated survival curves for disease-free survival, progression-free survival and overall survival, and will use Cox proportional hazards models and recursive partitioning methods to identify important biomarkers and prognostically distinct subpopulations. We will also correlate TTF/gene expression molecular profiles with initial tumor size and stage. In addition, we will explore the feasibility of using nonlinear regression analyses of semilog plots of % disease-free survival, % progression-free survival and % overall survival vs time to facilitate identification of prognostically distinct subpopulations with characteristic TTF/gene expression molecular profiles.

Aim 2. To assess the impact of adjuvant and neoadjuvant chemotherapy on disease-free survival, progression-free survival, and overall survival in prognostically distinct subgroups, and to provide tumor, blood and clinical data to Project 3 for an assessment of factors contributing to resistance to chemotherapy and to Project 5 for assessment of profiling of EGFR and related molecules by new quantum dot technologies.

Of the 450 patients included in the project, we will assess 100 new prospectively recruited patients who will receive neoadjuvant therapy, 100 patients who will receive postoperative adjuvant therapy (including approximately 20 tumor bank patients and 80 new patients) and 250 patients who did not receive adjuvant or neoadjuvant therapy (including approximately 130 tumor bank patients and 120 new patients). We will collect patient clinical data on all 450 patients and will collect blood samples on the 300 new, prospectively recruited patients. Tumor and blood samples and clinical data will be provided to Project 3 for studies of therapeutic resistance and to Project 5 for assessment of profiling of epidermal growth factor receptor (EGFR) and related molecules by new quantum dot technologies, while in Project 2 we will assess impact of adjuvant and neoadjuvant therapy on outcome in each prognostic group.

Aim 3. To correlate TTF/gene expression molecular profiles in the primary tumor with metastatic patterns and with tumor molecular profiles at relapse.

For patients who relapse, we will define metastatic sites at relapse, obtain tumor tissues from selected patients who undergo biopsies to confirm relapse, and define TTF/gene expression molecular profiles in the patients' original primary tumor specimens that predict sites of later relapse (and in particular that predict relapse in brain). We will also assess whether tumor at relapse is enriched for particular molecular characteristics that may promote metastasis when compared to the primary tumor, and will assess the extent to which TTF/gene expression molecular profile at diagnosis may help guide choice of therapies at relapse.

Update

As presented in detail in Project 3 and the Pathology Core, we have identified approximately 736 archival tumor samples from our Tissue Bank that match eligibility criteria for inclusion in this trial, and we are now in the process of assessing in detail the quality of RNA, DNA and protein that is available from these specimens prior to making a final selection of the subset of 150 that will be used for full analysis under PROSPECT. In addition, tissue microarrays have already been constructed on 327 of these 736 samples and we are near completion of staining each of these for immunohistochemical (IHC) assessment of more than 100 relevant biomarkers. Bioinformatic assessment is already underway on the first 18 biomarkers that are linked to cellular senescence, autophagy, hypoxia/angiogenesis and selected membrane transporters (p53, p21, Ki67, COX2, DNA methyltransferase I, CTR1, DcR2, SHARP2, SURVIVIN, TUNNEL [apoptosis], Rb, p16 INK4a, p14ARF, TGFβ, ERCC1, HIF-1α, CAIX, VEGF).

Collection of prospective tumor samples is also going well. Of the 300 samples proposed over the course of the project, we have collected 135 between August 2007 and June 2008. Hence, we are on schedule with respect to tissue collection from prospectively accrued patients. With respect to prospective blood sample collections, our initial plan was to use our current serum banking and SPORE protocols for this collection but we subsequently decided to generate a separate protocol specifically for blood collection on PROSPECT to streamline the process and ensure collection rates. This protocol received final IRB and Department of Defense approval in March 2008 and is now the major vehicle for collecting blood samples for PROSPECT.

We have also made progress in our planned use of semilog plots to assess survival parameters, and have submitted a manuscript for publication. We had proposed that patient relapse and survival will follow first order kinetics and that inflection points would identify prognostically distinct subgroups which are defined by dichotomous (present vs absent) prognostic variables. We manually measured 172 published progression-free and overall survival curves, converted them to log-linear plots and used exponential decay nonlinear regression analysis to characterize the curves. We expected to identify multiple curve inflection points. Interestingly, 42% of the curves were uniphasic (no inflection points), 53% were biphasic (single inflection point) and only 5% were triphasic (2 inflection points). This leads us to hypothesize that most prognostic variables function as continuous variables rather than as dichotomous variables. If this is correct, then dichotomizing a variable into high vs low expression may succeed in identifying ones that are prognostically significant, but outcome of individual patients would probably be predicted better by models using continuous variable.

We also found that 54% of curves for studies in which patients received $\geq$ 2 chemotherapy agents for advanced NSCLC had major convexities, as illustrated in Figure 4, while convexities were not seen in any of the curves from studies involving a single agent or best supportive care. Based on this, we hypothesize that the practice of discontinuing chemotherapy for advanced disease after 4-6 cycles "synchronizes" patient death, and that assessment of characteristics of patients dying along the leading edge of the survival curve might identify those most likely to benefit from maintenance chemotherapy that is continued beyond this initial 4-6 cycles.

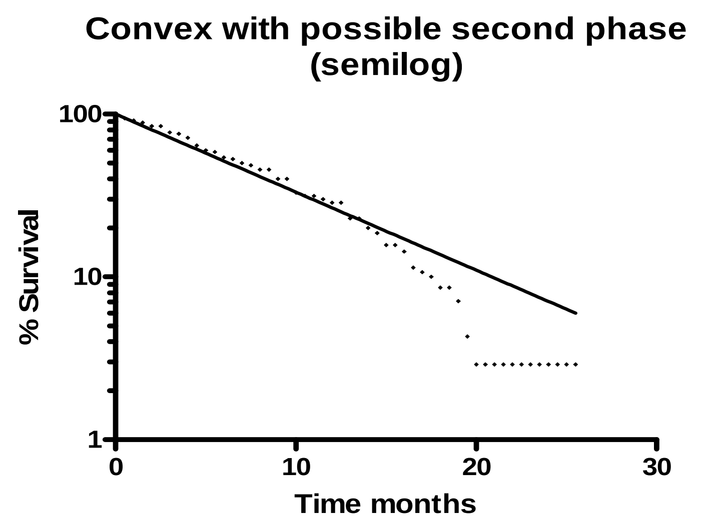

Figure 4. Example of semilog plot of % survival vs time showing a convex portion. The convexity suggests therapy details may be "synchronizing" patients relapse time to patient death.

We then took the 327 stage I-III NSCLC patients for whom tissue microarrays have been done using tumors from our tissue bank and performed similar survival analyses. If recurrence-free patients are censored at time of last follow-up or at death (if recurrence-free at death) or at development of a second primary tumor (if recurrence-free from their initial NSCLC at time of development of a second primary), we found that the recurrence-free curve could be fit by a 3-phase model, with 60.7% of patients achieving long-term recurrence-free status, 7.4% recurring rapidly, with a half-life to recurrence of 5.9 months, and 31.9% recurring more slowly, with a half-life to recurrence of 23.6 months (Figure 5). This suggests that more than 60% of the population are "true cures", while the relapsing patients constitute 2 distinct populations, one with rapid relapse and one with slow relapse. While this may at first seem contrary to reported survival data, we believe that this data indicates that the need for further dissection of the confounding factors such as COPD, heart disease, etc, that are common in this patient population. Tumor biomarkers might correlate with time to relapse of the tumor, but should not correlate with time to death from other causes. Many studies that report on biomarkers use "relapse-free survival", with patients being declared a "failure" if they either relapse or die and, hence, the potential impact of the biomarker on tumor biology is potentially diluted by the impact of death from other causes. In addition, patients with lung cancer who are cured of their lung cancer are at fairly high risk of developing other malignancies. Treating these patients as "failures" would tend to dilute the impact of biomarkers. Finally, data on a patient who has died is sometimes questionable and to whether or not s/he has not had a relapse. Consequently, we hypothesize

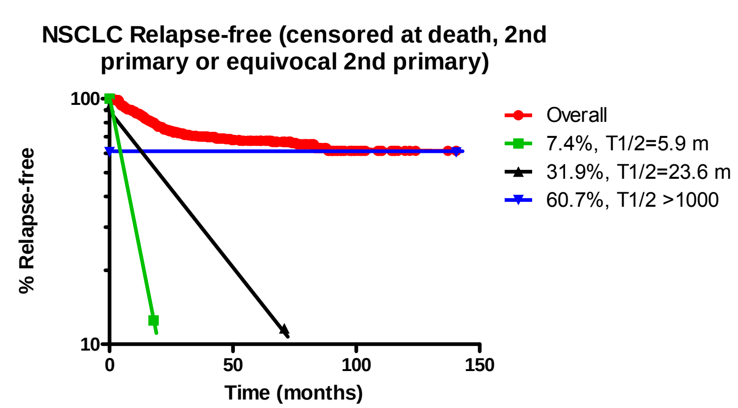

Figure 5. Semilog plot of time to patient relapse for 327 patients with resected NSCLC. Exponential decay nonlinear regression analysis suggested 3 distinct cured, slowly relapsing and rapidly relapsing subgroups. Patients were censored at last follow-up, death or development of a second primary if relapse-free at that time.

that one set of factors (e.g., those leading to apoptosis resistance, pro-angiogenic factors, etc.) will correlate with probability of developing metastases, while another set (e.g., growth factors influencing rate of tumor cell growth) will determine whether a patient is in the rapidly relapsing vs slowly relapsing group. These hypotheses will be tested as profiling data are generated on PROSPECT patients.

Of interest, when we plotted log % survival vs time (Figure 6), we obtained a uniphasic curve, with a half-life of 74 months and only about 30% of patients surviving at 12 years. Taken together with the relapse-free curve (Figure 5), this suggests that co-morbid conditions are playing a major role in death of patients in this patient population with only about half of the patients succumbing to lung cancer, and that correlation of biomarkers with time to relapse (with censoring at the time of relapse-free death or relapse-free development of a second primary cancer) will give a much better indication of the importance of a biomarker with respect to tumor cell biology than will correlation of the biomarker with either overall survival or with relapse-free survival (for which either relapse or death is an endpoint). The other somewhat unexpected conclusion from the analysis is that more than 12% of the surviving patients who are relapse-free at 4 years and 6% of surviving patients who are relapse-free at 6 years and 3% relapse-free at 8 years will still eventually develop relapses of their original lung cancer.

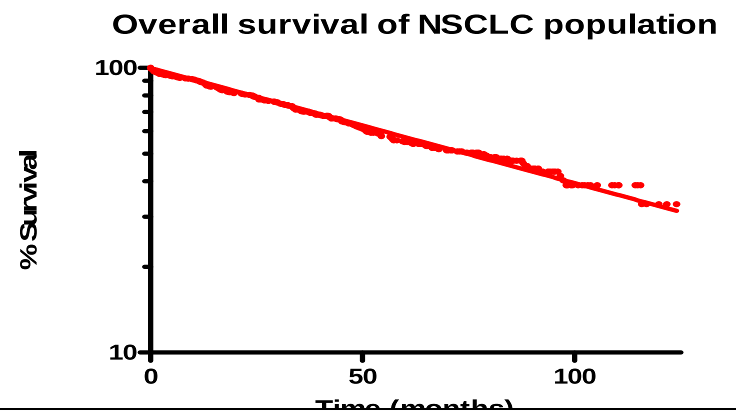

Figure 6. Semilog plot of overall survival time for the same population of 327 NSCLC patients portrayed in Fig. 5. Exponential decay nonlinear regression analysis failed to demonstrate prognostically distinct subgroups.

We expected to find several inflection points on the relapse-free survival curve, but with both our own patient population and with published curves, only found one or two inflection points. Our initial hypothesis that one important dichotomous variable will equal one inflection point on the curve may be incorrect, or our methods may have been too insensitive to detect inflection points. Conversely, if we are correct, it suggests that there are very few dichotomous factors that are important. Since there are many biological factors that are important, this further suggests that most of them are acting as continuous variables or as surrogates for continuous variables (e.g., gender being a surrogate for hormone levels), with probability of relapse being proportional to the expression of the variable rather than the variable dividing them into two distinct high risk vs low risk groups. If most biomarkers act as continuous variables and only one or two act as true dichotomous factors, which would behave differently than the others and actually be dichotomous? We will further pursue concrete answers to these questions with further analysis during PROSPECT.

With respect to Aim 2, 147 of the 736 patients for whom we have tissues in our tissue bank received neoadjuvant chemotherapy and an additional 131 received postoperative adjuvant therapy. Thirty-four patients have been entered on a neoadjuvant protocol and at least 18 of the prospectively collected tumor samples have come from patients receiving neoadjuvant chemotherapy. No analyses yet have assessed interactions between molecular characteristics and impact of neoadjuvant or adjuvant therapy.

With respect to Aim 3, we are currently following the patients and collecting information on sites of relapse. Because we are still very early in the study, only limited data are available to date.

Key Research Accomplishments:

- Identified tumors from more than 700 patients in our Tissue Bank from which we will be able to select 150 for PROSPECT
- Constructed tissue microarrays on 327 tumors from the Tissue Bank, and immunohistochemical staining for more than 100 different biomarkers is nearing completion
- Bioinformatic assessment of the first 18 biomarkers has been initiated

- Collection of prospective tumor samples from patients with and without neoadjuvant chemotherapy is on schedule
- Performed exponential decay nonlinear regression analysis on 172 published survival curves and on the 327 patients for whom we have generated tissue microarrays; this exercise has led to the generation of additional hypotheses to be tested as biomarker data mature

Reportable Outcomes:

Publications (including In Press and submitted):

- Stewart, DJ. Non-small cell lung cancer patient survival when assessed as a first order nonlinear process:effect of therapy and stage. Submitted for publication.

Conclusions:

We are on schedule for prospective tissue collection and for identification of archived specimens from our tissue bank. We are also on schedule with respect to processing of archived specimens. We have gained preliminary experience with exponential decay nonlinear regression analyses of patient survival curves and this has led to additional hypotheses.

Project 3: Molecular Profiling of Non-Small Cell Lung Cancer Tissue Specimens and Serum and Plasma Samples: Correlation with Patient Response and Tumor Resistance to Chemotherapy

(Leader: Dr. Ignacio Wistuba; Co-Leaders: Li Mao, Lin Ji, John Minna)

Hypothesis:

In Project 3, we hypothesize that systematic molecular profiling of surgically resected non-small cell lung cancer (NSCLC) tissue specimens using therapeutic target-focused (TTF) and mRNA approaches, along with serum phosphopeptide screening and plasma DNA analysis, will lead to the following results:

1. The validation in patients' tissue specimens of molecular signatures obtained from NSCLC cell lines that are associated with *in vitro* and *in vivo* (xenograft) resistance of NSCLC cell lines to chemotherapeutic and targeted agents.
2. The identification of molecular profiling signatures associated with NSCLC sensitivity or resistance to chemotherapeutic agents that can identify NSCLC patients most likely to respond to a given targeted therapeutic agent.
3. The development and validation of serum phosphopeptide profiles and plasma DNA markers associated with NSCLC patient response and tumor resistance to chemotherapeutic agents.

Objectives:

The greatest obstacle to creating effective treatments for lung cancer is the development of resistance to both chemotherapeutic and targeted agents. In this highly integrated and translational program project, we tackle one of the most clinically significant problems in lung cancer: the prediction of patient response to therapy, especially in the context of tumor resistance to current standard chemotherapies. The main objectives of this project are as follows.

a) Profile surgically resected tumor tissue specimens obtained from NSCLC patients to validate molecular signatures found in the TTF and mRNA profiles developed in Project 1. These profiles will be compared with molecular signatures obtained from NSCLC cell lines that are associated with *in vitro* and *in vivo* (xenograft) resistance to chemotherapeutic and targeted agents.
b) By comparing NSCLC tumor specimens (collected in Project 2) from patients who have received preoperative chemotherapy and from those who have not, validate TTF and mRNA signatures that are found in Project 1 to be associated with resistance to therapy and with the activation of resistance-associated molecular pathways or that are found in Project 1 to be potentially exploitable as new therapeutic targets.

c) Identify serum and plasma biomarkers as surrogate markers to predict the response of NSCLC patients to neoadjuvant chemotherapy and to predict patient outcome.
d) Provide tissue- and serum-based molecular profile signatures or markers to Project 2 that can predict the clinical outcome of NSCLC patients who had undergone surgical resection with curative intent, with or without neoadjuvant therapy.

This interdisciplinary research proposal for profiling cell lines, tumor tissue and serum samples from NSCLC patients requires extensive histopathological, molecular and immunohistochemical studies, which will be coordinated and/or performed by the Pathology Core (see Pathology Core's report).

Specific Aims:

Aim 1: To validate, in retrospectively collected NSCLC tumor tissue specimens, the TTF and mRNA profiles predictive of the *in vitro* and *in vivo* (xenograft) resistance of NSCLC cell lines to chemotherapeutic and targeted agents.

<u>Summary of proposal</u>: We will select 150 surgically-resected NSCLC tumor specimens from The University of Texas Lung SPORE (UT-SPORE) Tissue Bank for TTF and mRNA profiling. Using those 150 frozen archival NSCLC tumor tissues, we will perform reverse-phase protein array (RPPA), multiplex bead-based protein analysis (MBA) and Affymetrix U133 Plus 2.0 array to validate the molecular signatures developed in Project 1. Then, we will compare the profile signatures obtained from the NSCLC tumor specimens with the signatures obtained from NSCLC cell lines in Project 1 that predict the *in vitro* and *in vivo* resistance to chemotherapeutic and targeted agents. Finally, using formalin-fixed and paraffin-embedded tissue specimens, we will validate the expression of proteins abnormally represented in the molecular profiling analyses of NSCLC tumor specimens by using tissue microarrays (TMAs) and semiquantitative immunohistochemical (IHC) methods.

<u>Update</u>
During the first year, we have mainly focused on the identification, characterization, and processing of tissue specimens from surgically resected NSCLC specimens to achieve the goals of Aim 1. Our progress is as follows:

1) <u>Selection of retrospectively collected cases</u>: From the 1,150 NSCLC and 93 malignant pleural mesothilioma (MPM) cases with frozen tissue banked in the Thoracic Malignancy Tissue Bank, we selected 736 NSCLC and 80 MPM for tissue processing for DNA, RNA (mRNA and microRNA) and protein extractions.

2) <u>Collection of clinicopathological data for NSCLC cases in the MDACC frozen tissue bank.</u> We have completed the collection of the clinicopathological data on 736 lung NSCLC cases (Table 1), including detailed pathology information of tumor specimens and patients' demographic, clinical characteristics, adjuvant treatments, outcome (recurrence and survival), and treatment at recurrence. In our original submission, we presented data on response to treatment at recurrence in 30 patients. Currently, we are in the process of completing the assessment of response to therapy at recurrence in all these patients. Of interest, 147 (20%) and 131 (18%) out of 736 NSCLC cases have received neo-adjuvant (pre-operative) and adjuvant (post-operative) chemotherapy, respectively.

3) <u>Histopathological characterization of frozen normal and tumor tissue specimens used for extractions</u>: Each tumor H&E-stained section has been examined by experienced lung cancer pathologists (Dr. Alejandro Corvalan and Dr. Ignacio Wistuba) to assess the percentage of tumor vs. adjacent normal tissues, and most importantly, the percentage of malignant cells vs. tumor non-malignant stromal (inflammatory, vascular and fibroblasts) cells and normal cells present in the adjacent normal tissue. In addition, tumor cell viability has been addressed by examining the presence of necrosis and hemorrhage. In addition, we have performed digitalization of 89 of H&E-stained section for future comparison of histological analysis.

Table 1. Summary of clinicopathologic features of 736 surgically resected NSCLC with follow-up and clinical information on treatment available for profiling analysis.

Histology	Adenocarcinoma	448 (61%)
	Squamous cell carcinoma	288 (39%)
Stage (pathological)	I	395 (54%)
	II	130 (18%)
	III	187 (25%)
	IV	21 (3%)
Disease Free Survival	17.8 months (range 4- 42)	
Overall Survival	32.9 months (range 15-52 months)	
Neo-adjuvant (Pre-operative) Chemotherapy		147 (20%)
Adjuvant (Post-operative) Chemotherapy by Stage	I	57 (44%)
	II	34 (26%)
	III	37(28%)
	IV	3 (2%)
	Total	131 (100%)
Type of Adjuvant (Post-operative) Chemotherapy	Carboplatin/Paclitaxel	57 (44%)
	Carboplatin/Docetaxel	16 (12%)
	Cisplatin/Docetaxel	16 (12%)
	Carboplatin/Pemtrexed	11 (8%)
	Carboplatin/Gemcitabine	16 (12%)
	Other	15 (12%)
Recurrence by Stage	I	104 (38%)
	II	60 (22%)
	III	93 (33%)
	IV	18 (7%)
	Total	275 (100%)

4) Extraction of DNA, RNA and protein of NSCLC frozen tissue specimens. We plan to extract DNA, RNA, and protein from all 736 NSCLC tumor and normal specimens selected from our tissue bank. From these, we will select the 150 resected NSCLC retrospectively collected we propose to profile in Aim 1 of our project. Then, we will add 300 cases collected prospectively. Thus far, we have extracted DNA and RNA from 387 (363 retrospectively and 24 prospectively collected cases) NSCLC specimens, including paired normal and tumor tissue samples. In addition, DNA and RNA have been extracted from from 80 MPMs. The extraction method consists of histology evaluation of tumor components using 5 µm thick haematoxylin-eosin (H&E)-stained histology sections obtained at four levels of the tissue specimen that are alternated by two sets of thirty 20 µm thick sections obtained for RNA and protein extractions ("sandwich" technique) which was established by the pathology core (Figure 7). All the processing to obtain these histology sections has been performed using RNase free conditions. After sectioning, all samples have been stored in an -30°C freezer until the extractions are performed.

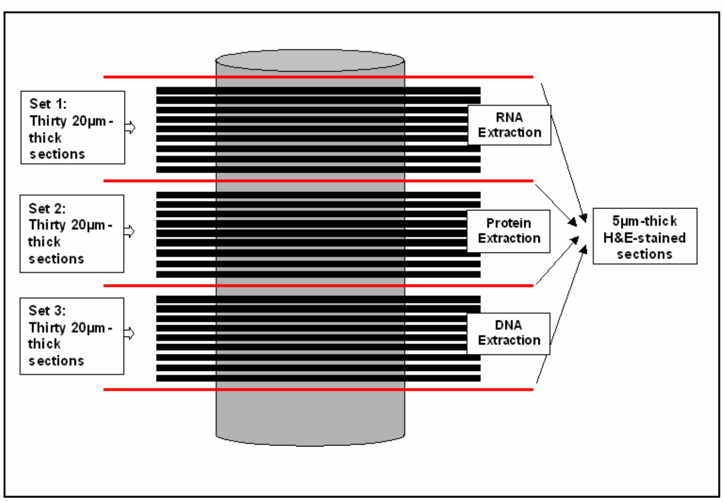

Figure 7. Method for tissue processing for DNA, RNA, and protein extractions.

The 387 (229 adenocarcinomas and 158 squamous cell carcinomas) cases from which DNA and RNA have been extracted represent 53% of 736 NSCLC available in the Thoracic Malignancy Tissue Bank. Paired normal and tumor sample were found in 361 (93.5%) of these cases. By applying a cutoff of >70% for amount of tumor in the specimen and >50% of the cells being tumor cells, 207 cases (54%) are eligible for molecular (DNA or RNA) studies (125 adenocarcinomas and 82 squamous cell carcinomas). A representative example of an eligible case is given in Figure 8.

These 387 cases represent 52.6% of 736 NSCLC available in the Thoracic Malignancy Tissue Bank. Paired normal and tumor sample were found in 361 (93.5%) of these cases. Detailed pathology verification of tumor tissue content and quality by H&E-stained section has been examined by an experienced lung cancer pathologist.

Figure 8. Representative example of tumor H&E stained section examined to assess the percentage of tumor and the percentage of malignant cells vs tumor non-malignant stromal (inflammatory, vascular, and fibroblast) cells and normal cells.

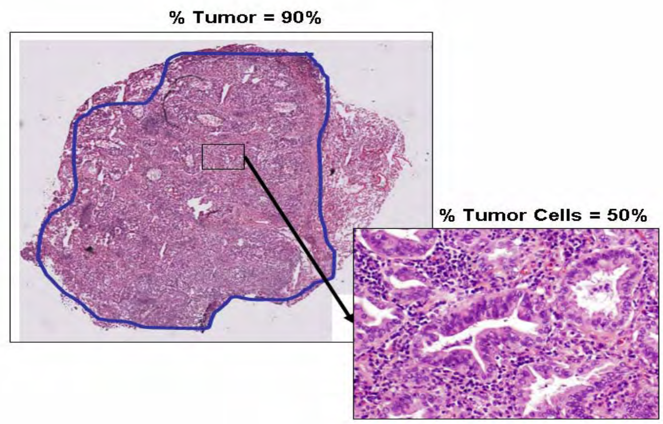

5) DNA and RNA concentration and quality assessment: For each normal and tumor DNA and RNA sample, both concentration and quality of the samples are being assessed. A summary of the characteristics of the DNA and RNA extracted from 387 paired cases is showed in Table 2.

Table 2. A summary of the characteristics of the DNA and RNA extracted from 387 NSCLC cases.

	DNA				RNA			
Measurement	Tumor		Normal		Tumor		Normal	
	Average	SD	Average	SD	Average	SD	Average	SD
Micrograms	112.39	408.23	130.47	460.71	100.05	109.19	57.33	62.30
Concentration (ng/ul)	380.29	879.68	387.62	943.38	817.01	832.08	527.77	556.62
Ratio 260/280	1.88	0.94	1.98	0.96	1.98	0.28	2.01	0.60
Ratio 260/230	0.50	6.80	5.84	213.77	1.47	0.66	1.45	0.83
RNA Integrity # (RIN)	NA	NA	NA	NA	5.11	2.63	4.66	2.64

A large variability in DNA and RNA is noted according to amount (micrograms) obtained. Quality of RNA, according to RNA integrity number (RIN), defined as an estimation of the integrity of total RNA samples by the entire electrophoreses trace of the RNA sample including degradation products is 5.11.

6) Profiling mRNA (Affymetrix) and protein (RPPA): We will begin these experiments once the all the extractions and quality assessments are completed (August 2008) and eligible RNA samples are matched with the clinical and pathological characteristics of the cases.

Profiling Strategy. We plan to select 200 stages I/II NSCLCs (adenocarcinoma and squamous cell carcinoma) divided into two groups with 100 NSCLCs on each group: a) cases that did not receive adjuvant (post-operative) chemotherapy to study the prognostic value of the molecular signatures; and, b) cases that received adjuvant (post-operative) platinum/taxol therapy to study the predictive value of several molecular signatures. When available, molecular signatures optimized in formalin-fixed paraffin embedded (FFPE) tissue will be also examined. The squamous cell carcinomas profiled in this effort will overlap with the cases submitted by M. D. Anderson to NCI's The Cancer Genome Atlas (TCGA) project. Summary of our profiling plan for both frozen and FFPE specimens is outlined in Table 3.

Table 3. Summary of the plan and status of our molecular profiling analysis in prospectively collected stages I/II NSCLC.

Sample	Tissue Set	Number	Analysis	Platform/ Lab	Company	Status
DNA	Frozen	200	SNP array	Illumina	TBD	Pending the identification of partner
	Frozen	200	Methylome	TBD	TBD	Pending the identification of partner
	Frozen	200	aCGH	Myriad Company	Myriad	Scientific agreement ready
	Frozen	200	Gene mutation	Myriad	Myriad	Scientific agreement ready
mRNA	Frozen	200	Gene expression	Affymetrix	--	Pending completion of DNA/RNA extraction
	FFPE	200	Gene expression	Affymetrix	Response Genetics	Sample analysis in progress
	Frozen	200	Gene expression	Illumina	--	Pending completion of DNA/RNA extraction
miRNA	FFPE	200	miRNA profiling	Rosetta Genetcis	Rosetta Genetics	Pending shipping of samples
Proteins	Frozen	200	RPPA	MDACC Kleberg	--	Pending completion of protein extraction
	FFPE	200	TMA-IHC	Pathology Core	--	Pending preparation of TMAs

Aim 2: To develop TTF and mRNA signatures of NSCLC resistance to chemotherapy, and identify chemoresistance-associated targets/pathways as new therapeutic targets.

Summary of proposal: Whereas Aim 1 focuses on the identification in archived tumor specimens of TTF and mRNA molecular profiles detected in NSCLC cell lines, the main focus of Aim 2 is to determine whether the molecular signatures in the tumor specimens correlate with patient response to neoadjuvant chemotherapy. From the clinical trial in Project 2, we will use specimens from 100 NSCLC patients who received neoadjuvant therapy and had surgical resection with curative intent (cases) and from 200 NSCLC patients who had surgical resection but did not receive neoadjuvant therapy (controls) to perform RPPA, MBA, and Affymetrix U133 Plus 2.0 array analyses. Then, we will compare the TTF and mRNA profile signatures obtained from these NSCLC tumor specimens with signatures obtained in Project 1 to predict the *in vitro* and *in vivo* resistance of NSCLC cell lines to therapy. Those data will be provided to Project 2 for correlation with clinical characteristics, including prognosis and metastasis. Finally, using formalin-fixed and paraffin-embedded tissue specimens, we will validate the expression of proteins abnormally represented in the molecular profiling analyses in NSCLC tumor specimens from all patients enrolled in Project 2 by using TMAs and semiquantitative IHC methods.

Update

During the first year, we have mainly focused on the identification, characterization, and processing of tissue specimens from surgically resected NSCLC specimens from patients that have received neoadjuvant chemotherapy. Our progress is as follows:

1) Selection of retrospectively collected cases: From the 736 NSCLC cases, we have identified 147 (20%) patients who have received neoadjuvant chemotherapy (Table 1). Our goal was to obtain 100 cases from the treated group and 200 from the.non-treated group.
2) Selection of prospectively collected cases: Since the activation of the PROSPECT laboratory protocol on August 2007, the Pathology Core has collected fresh and formalin-fixed tissue specimens from 135 NSCLC and 9 MPM surgically resected cases. From the 135 NSCLC cases, at least 18 cases have received neoadjuvant chemotherapy.
3) Histopathological characterization of frozen tissues and extractions of DNA, RNA and protein: This will be completed by August 2008.

4) Profiling mRNA (Affymetrix) and protein (RPPA): These experiments will begin once all the extractions are completed and will be performed at the same time as the samples from Aim 1. Based on the histopathology characteristics of chemotherapy-treated tumors (percentage of necrosis and fibrosis), the use of microdissection technique will be considered.
5) Additional tissue sets for profiling studies. We have signed a collaborative agreement with the Intergroupe Francophone de Cancérologie Thoracique (IFCT) to obtain up to 250 frozen lung tumor tissues from patients enrolled in IFCT-0002 clinical trial (a open-labelled, multicentric, randomized phase III study) which was designed to define the best timing of neoadjuvant chemotherapies. The samples will be used to identify a gene expression signature of resistance to platinum-based chemotherapies. We will evaluate the utility of this signature for chemo-response prediction. Selected genes will be validated in both clinical samples and through in vitro biological assays. As secondary objectives, (1) we will evaluate the impact of platinum-based chemotherapies on gene expression in these tumors to identify key molecules as novel therapeutic targets; (2) we will identify a prognostic signatures for those with poor clinical outcomes in the treatment setting; and (3) we will use reverse-protein microarrays to screen 100 signalling proteins/protein modifications to determine to identify markers with potential predictive or prognostic implications.

Aim 3: To identify surrogate serum phosphopeptide profiles and plasma DNA markers associated with NSCLC tumor resistance and patient response to neoadjuvant chemotherapy.

We will identify serum samples from the UT-SPORE Tissue Bank that match the NSCLC tumor resection specimens examined in Aim 1. We will use these serum samples for phosphopeptide profiling and peptide mapping by ProteinChip array-based surface-enhanced laser-desorption-ionization (SELDI) mass spectrometry (MS) and laser desorption/ionization (LDI) mass spectrometry (MS)/MS to compare serum phosphopeptides with TTF and mRNA profiles. The phosphopeptide MS profiles from retrospective specimens will later be used as references and controls for the prospective serum proteomic analysis. As in Aim 2, we will use serum samples collected prospectively in Project 2 from 100 NSCLC cases undergoing neoadjuvant chemotherapy and 200 NSCLC controls undergoing surgery without neoadjuvant chemotherapy, and, when relevant, at the time of relapse. Using these serum specimens, we will perform phosphopeptide profiling on ProteinChip arrays by SELDI-MS to measure the temporal changes in serum phosphopeptides before and after the therapeutic intervention. We will use LDI-QSTAR-MS/MS and liquid chromatography (LC)-MS/MS to identify specific serum phosphopeptides that are determined by SELDI-MS to be relevant to targeted therapeutic response and acquired resistance in lung cancer patients. In addition, we will compare serum phosphopeptide profiles with TTF (RPPA and MBA) profiles, mRNA profiles, and TMAs and IHC analysis developed in Project 1 and in Aims 1 and 2 of this project. This comparison will identify TTF serologic molecular signatures and elucidate the biologic pathways potentially associated with patient response and tumor resistance to targeted therapeutic agents. Finally, in collaboration with Project 2 we will perform correlation analysis of these NSCLC serum phosphopeptide profile signatures with patients' clinical characteristics to predict lung cancer, cancer progression, cancer stages, and overall survival rate; to characterize serum phosphopeptide proteomic patterns and signatures in correlation to tumor recurrence, clinical response to adjuvant chemotherapeutic and targeted agents, and development of resistance; and to identify serum phosphopeptide markers as surrogate predictors of patient outcome.

Moreover, in Aim 3 we will quantify total circulating plasma DNA and methylation-specific DNA in all 300 patients with NSCLC enrolled in the Project 2 clinical trial. The circulating DNA levels will be correlated with patients' clinicopathologic characteristics. Any changes in these levels during chemotherapy and after surgery will be correlated with patient response to neoadjuvant therapy and patient outcome after surgery. The correlation between circulating methylated DNA levels and tumor DNA methylation will also be examined in a selected panel of patients.

Update

We have identified a phosphorylated peptide of OMR in human lung cancer serum and found that the phosphorylated OMR is significantly upregulated ($p = 0.0271$) in lung cancer serum compared to normal serum samples and upregulated expression and phosphorylation of OMR peptide are also detected in human NSCLC cell lines compared to those of normal lung fibroblast and bronchial epithelial cells. We also found that the phosphorylated OMP protein functions as a ligand of and interacts with human nicotinic acetylcholine receptor1 (AChR), an archetypal member of the cysteine loop receptor superfamily and a newly identified human lung cancer susceptibility gene. We will validate this exciting finding of phosphorylated OMR peptide as a serum biomarker for lung cancer detection and prediction in matched human lung cancer serum samples in above selected and collected cases.

In addition, we have collected plasma samples from 30 patients treated with neoadjuvant (pre-operative) chemotherapy and nearly 120 patients without neoadjuvant treatment. These samples will be used for DNA extraction and methylation analysis.

Key Research Accomplishments:

- Collection of relevant clinical and pathological information from of 736 NSCLCs with frozen tissue in the Pathology Core tissue bank, including 147 cases treated with neoadjuvant (pre-operative) and 131 cases with adjuvant (post-operative) chemotherapy.
- Establishment of a methodology for DNA and RNA extraction for a large number of frozen tissue specimens. We have extracted DNA and RNA from paired normal and tumor tissue 387 (53%) out of 736 NSCLC available.
- Establishment of a profiling strategy for NSCLCs.

Reportable Outcomes:
None.

Conclusions:
During the first year, we have identified and collected detailed relevant clinical and pathological information from NSCLC (N=736; Aim 1) banked in our Pathology Core bank, including 147 NSCLCs treated with neo-adjuvant chemotherapy (Aim 2). The goal for the retrospectively collected NSCLC was 150 cases, so we have exceeded our goal. In addition, we are about to complete DNA and RNA extraction from all those cases. Profiling mRNA analysis for a large number of retrospectively collected NSCLC without adjuvant therapy, with neoadjuvant (pre-operative) and with adjuvant (post-operative) chemotherapy will be performed during second year of PROSPECT grant.

Project 4: Target Modulation Following Induction Treatment With Dasatinib in Patients With Malignant Pleural Mesothelioma (MPM) and Identification of New Therapeutic Targets/Strategies for MPM

(Leaders: Drs. Anne Tsao, Dave Rice)

Hypothesis:
We hypothesize that dasatinib, a broad spectrum ATP-competitive inhibitor for oncogenic tyrosine kinases (BCR-ABL, SRC, c-Kit, PDGFR, and ephrin receptor kinases), may be a new therapeutic agent in malignant pleural mesothelioma (MPM) and that conducting therapeutic target-focused (TTF) molecular and gene profiling (Affymetrix arrays) will lead to development of other novel therapies for MPM.

Specific aims:

Aim 1: Conduct a phase I clinical trial with the primary endpoint of biomarker modulation using dasatinib as induction therapy in patients with resectable MPM.

1a. Determine the effects of dasatinib induction therapy on selected tumor biomarkers (activated Src, PDGFR, VEGFR) pre- and post-induction therapy.

1b. Determine the modulatory effects of dasatinib on selected biomarkers of survival and apoptosis (PI3K/AKT, bcl-xL, caspases), proliferation (IGFR, Ki-67), angiogenesis (IL-8, bFGF, TNF-α), epithelial-mesenchymal transition (TNF-β, E-cadherin, c-Kit/Slug) and invasion/migration (Ephrin, MMP) in tumor specimens pre- and post- induction therapy.

1c. Determine the effects of induction dasatinib therapy on tumor mean vessel density, cell apoptosis, and the proliferation index.

1d. Determine the modulatory effects of dasatinib on serum, platelet, and pleural effusion markers of survival (PI3K/AKT, bcl-xL, caspases), proliferation (IGFR, Src), angiogenesis (soluble VEGFR, VEGF, PDGF, IL-8, bFGF, TNF-α), and invasion/migration (Ephrin, MMP).

1e. Determine the drug concentration of dasatinib in tumor and serum.

1f. Assess the effects of dasatinib and cytoreductive surgery on the serum mesothelin-related peptide (SMRP) level.

1g. Assess the safety and toxicity profile of induction dasatinib in patients with resectable MPM.

Aim 2: Conduct radiographic correlates of tumor response and clinical outcome with positron-emission technology-computer tomography (PET-CT).

Aim 3: Explore and develop new therapeutic targets and treatment strategies for MPM in tumor specimens collected from Specific Aim1 and in MPM cell lines.

3a. Determine key signaling pathways involved in tumor resistance or sensitivity to dasatinib using therapeutic target-focused (TTF) molecular and global gene expression profiling on MPM tumor specimens pre- and post- induction dasatinib therapy.

3b. Determine the sensitivity of a panel of MPM cell lines to targeted agents tested in Project 1 via TTF profiling and DATs (drug and therapeutic target siRNA).

Update

In the last year, we have focused on establishing the infrastructure for Project 4, completed the regulatory procedures to activate Protocol 2006-0935, and established the laboratory and clinical personnel to conduct the translational studies on the study. Protocol 2006-0935 is a phase I study of dasatinib induction therapy in patients with resectable malignant pleural mesothelioma. The primary endpoint is biomarker modulation of Src Tyr^{419} in tumor tissue. Translational correlates are built into the study protocol to evaluate serum/plasma/platelets (at baseline, weekly x4,and at time of final surgery) and also pleural effusion collections at 2 time points (during the surgical staging and at the time of definitive surgery). The tissue collection occurs at two time points: during the extended surgical staging (ESS) and then 4 weeks later at time of final surgery (either a pleurectomy/decortication or extrapleural pneumonectomy).

The trial was activated and the study opened for enrollment on 3-29-08. Since opening the trial, we have approached 13 patients for enrollment onto the trial. Only three patients made it through the eligibility criteria and consented to proceed with the initial surgery (ESS). Two patients have completed the initial staging surgery (ESS) and one of these patients was found to have metastatic microscopic abdominal disease and could not participate on the trial. Once patient has made it successfully thru the ESS and will start the dasatinib therapy this week. The third patient has his initial staging surgery scheduled on June 24. We also plan on seeing 2 additional potential candidates this week in the clinic. As this is a rare tumor type, we are pleased at the number of patients that have considered going onto this study in the last 2.5 months (5.2 patients per month approached with 2 patients per month consenting). We anticipate that enrollment of the required number of patients (24) will be achieved within the next 2 years (requiring 1 patient per month to achieve goal). We have also instituted programs, as described below, to aid in increasing awareness of this trial to hopefully attract additional patients.

In support of our program, we have created the Mesothelioma Focus Group (MFG) which meets every month to discuss enrollment on the mesothelioma induction trial. Administrative support for this group is provided by the Department of Thoracic/Head and Neck Medical Oncology (Bich Tran and Brenda Robinson). This project is truly multidisciplinary. The research team includes Drs. Swisher, Roth, Mehran, and Rice from the Department of Thoracic Surgery; Drs. Komaki, Liao, Chang, and McAleer from Radiation Oncology; Drs. Tsao, Lippman, Papadimitrakopoulou, and Heymach from the Department of Thoracic/Head and Neck Medical Oncology; Drs. Jimenez and Eapen from the Department of Pulmonary Medicine; Dr. Wistuba from the

Department of Pathology, and Dr. Hai Tran, also from the Department of Thoracic/Head and Neck Medical Oncology but whose specialty is Pharmacology. Additional research support team members include Dr. Milind Suraokar (Post-doc fellow), Adam Cantu (Research Assistant), Dandan He (Research Assistant), James Gil (Research RN), Christine Alden (Research RN), Dana Bethancort (Pulmonary Research RN), Natasha Pappas (LVN), and Patricia Hutchinson (serum collection LVN).

The clinical research team to has a concerted effort to facilitate patient enrollment onto the study: Pharmacy has set up a mechanism for monitoring and distribution of the study drug; the clinical research RNs are trained to educate patients on the study details; informed consent and information sheet has been created; a registration algorithm for patients to be enrolled has been established; the Thoracic New Patient Business office will notify the Project Leader (Tsao) and clinical research RNs (James Gil, Christine Alden) when a new mesothelioma patient is coming to MDACC; and the Thoracic Surgery and Thoracic Medical Oncology Departments will see any potentially resectable mesothelioma patients within the week if a patient is a potential candidate for Protocol 2006-0935.

In addition, we are coordinating an advertisement program to increase patient enrollment onto the study. The Mesothelioma Action Research Foundation is the largest mesothelioma patient advocacy group and hosts a yearly conference. Dr. Tsao will be a keynote speaker at this meeting and will be highlighting Protocol 2006-0935 to the mesothelioma patients. A Mesothelioma Brochure is being created to highlight the clinical trials our program is offering. This will be mailed out to local oncologists in Texas to raise awareness. Online marketing on the MDACC website is underway to increase awareness of the clinical study.

Finally, in preparation for studies in Aim 3, we have identified 93 patients for whom we have mesothelioma tissues in our tissue bank, and are currently processing tissues for 80 of these. We also have 4 mesothelioma cell lines for *in vitro* studies.

Key Research Accomplishments:

- Established the administrative and clinical research team and the Mesothelioma Focus Group (MFG) in support of the clinical trial and to facilitate patient enrollment onto the study.
- Obtained IRB approval and activated Protocol 2006-0935.
- Developed the clinical procedures in the Surgical OR for the tissue, serum/plasma, pleural effusion, platelet collection on Protocol 2006-0935.
- Mechanism set-up by Pharmacy for monitoring and distribution of the study drug.
- Trained clinical research RNs to educate patients on the study details.
- Creation of Informed consent and information sheet.
- Established registration algorithm for enrollment of patients.
- Created procedure for notification by Thoracic New Patient Business office when a new mesothelioma patient is coming to MDACC.
- Prioritization of resectable mesothelioma patients who are potential candidates for Protocol 2006-0935 by Thoracic Surgery and Thoracic Medical Oncology Department.
- Coordination of an advertisement program to increase patient enrollment onto the study.
- Established the laboratory Infrastructure to manage the translational correlates on the clinical trial.
- Identification of retrospective specimens and cell lines for research in Aim 3.

Reportable Outcomes:
None.

Conclusions:
Work is on schedule. The major effort to date has been in initiating the clinical trial and setting-up the infrastructure needed. Now that this is active, we expect that accrual will be on schedule.

Project 5: Development of a Novel Multi-Biomarker System Using Quantum Dot Technology for Assessments of Prognosis of NSCLC and Prediction of Outcome of EGFR-Targeted Therapy

(Leader: Dr. Zhuo Georgia Chen; Co-Leaders: Drs. Fadlo Khuri, Dong Shin, Ruth O'Regan, Shi-Yong Sun)

Quantum dots (QDs) provide sharper fluorescent signals than organic dyes and can detect multi-biomarkers simultaneously in the same material, allowing quantification and correlation of molecular signature with cellular response to targeted therapies.

Hypothesis:

A multi-biomarker system using quantum dot (QD) technology will enhance accuracy in assessment of prognosis of non-small cell lung cancer (NSCLC) and prediction of outcome of epidermal growth factor receptor (EGFR)-targeted therapy.

Specific Aims:

Specific Aim 1. **Development of QD-Abs and imaging systems for detection and quantification of multi-biomarkers (MBM) using lung cancer cell lines.**

Update

NSCLC is by far the most devastating cause of cancer-related death in the United States, resulting in approximately 156,000 deaths each year and approximately 1.3 million deaths worldwide annually. Much of the work in the last two decades has focused on identifying critical proteins such as EGFR in lung cancer progression. The EGFR tyrosine kinase inhibitor (TKI) erlotinib has recently been approved for lung cancer treatment by the U.S. Food and Drug Administration (FDA) due to its unique antitumor effect. However, response rate to EGFR TKIs in the broad lung cancer population is limited, with the most profound responses occurring in individuals harboring EGFR-TK mutations. Even these patients eventually acquire resistance. There is, therefore, an urgent need for understanding the mechanism of EGFR-TKI resistance and for pre-selection of the patients who may get the most benefit from EGFR-TKIs prior to the initiation of treatment with these agents. Simultaneous detection and quantification of multi-biomarkers using clinical specimens may be an optimum way for both selection of appropriate targeted therapies for the patients and for assessing overall prognosis, but this is difficult to achieve by conventional immunohistochemical (IHC) methods which can neither provide accurately quantifiable signal with high resolution nor detect multi-biomarkers in the same sample. We believe that QD-based nanotechnology may prove useful in this regard.

The current study developed and validated a quantification strategy for QD-based immunostained signals and sub-cellular distributions of the tested proteins. Three biomarkers were initially examined using secondary antibody conjugated QDs as illustrated in Figure 9. The advantages of using the secondary antibody conjugated QD are that they are less expensive and less complicated than using primary antibody conjugated QDs. Since QD linked secondary antibodies raised from several species are commercially available (Invitrogen, Palo Alto, CA), they can be chosen to label several primary antibodies individually. Therefore, conjugation and purification when conjugated directly to each of QD-primary antibodies can be avoided.

Primary antibody:

E-cad (mouse)

EGFR (rabbit)

β-catenin (goat)

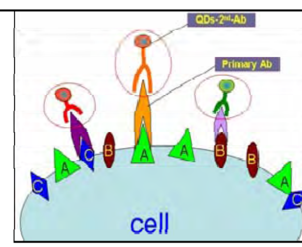

QDs-second-antibody:

QDs 565 goat F(ab')2 anti-mouse antibody,

QDs 605 goat F(ab')2 anti-rabbit antibody,

QDs 655 rabbit F(ab')2 anti-goat antibody.

Staining process :

1st Ab (cocktail) ⟹ QDs 2nd Ab (cocktail)

Figure 9. The cocktail method with QDs-2nd-Ab. Three biomarkers were initially tested to establish the cocktail method for QD-based immunocytochemical and immunohistochemical analyses.

Using this strategy, expression and cellular localization of EGFR and E-cadherin (E-cad) were compared between EGFR-tyrosine kinase inhibitor (TKI) sensitive and insensitive NSCLC and squamous cell carcinoma of the head and neck cancer (SCCHN) cell lines. Note that all SCCHN work was supported through other mechanisms but is included here to present a clearer understanding of the context of the results because of the expression of EGFR and the response to its inhibitors in SCCHN patients. Substantial differences in EGFR and E-cad expression and localization were identified among these cell lines both at the basal level and in response to EGF and EGFR-TKI, providing one of the mechanisms for cellular resistance to EGFR-targeted therapy and a basis for predicting response to EGFR-targeted therapy. Our major findings are described below.

EGFR-TKI Sensitive Cells are Different from EGFR-TKI Insensitive Cells in Expression of EGFR and E-cad. To further understand EGFR-TKI resistance, we tested the following lung and head and neck cancer cell lines: (i) four lung cancer cell lines, including two EGFR-TKI sensitive (H292, H322) and two EGFR-insensitive (H1703, and H460) cell lines; (ii) an EGFR-TKI resistant cancer cell line 686LN-R30 selected under a constant pressure of administering gefitinib to its EGFR-sensitive parental cell line 686LN; (iii) a highly metastatic head and neck cancer cell line 686LN-M4e selected *in vivo* from the same parental cell line as 686LN-R30; and (iv) SCCHN cell lines UPCI-37A and -37B, in which PCI-37A was from a primary tumor, while PCI-37B was from lymph node metastases of the same patient as PCI-37A.

Cell growth inhibition by EGFR-TKI erlotinib was first examined in nine of these cell lines. It was determined that that IC_{50}s of erlotinib in the EGFR-TKI insensitive cell lines (H1703, 686LN-R30, and 686LN-M4) are about 10 times higher than those in the sensitive cell lines (H292 and 686LN) (Figure 10A). A similar difference in IC_{50} of erlotinib between EGFR-TKI sensitive cells, H322 and UPCI-37A, and insensitive cells, H460 and UPCI-37B, has been reported by us and others previously.

Fig. 10B demonstrates alterations of E-cad, p-EGFR, and total EGFR expression levels in the presence or absence of erlotinib by immunoblotting. The data indicated that though almost no growth inhibition was observed in the EGFR-TKI insensitive cell lines H1703, 686LN-M4e, 686LN-R30, and 37B by treatment with erlotinib at 0.5 μM, p-EGFR was reduced by erlotinib at this concentration in these cells. Thus, reduction of activated EGFR did not correlate with growth inhibition by erlotinib in the EGFR-TKI insensitive cell lines. Furthermore, the EGFR-TKI insensitive cell lines had lower total levels of EGFR and E-cad than EGFR-TKI sensitive cell lines.

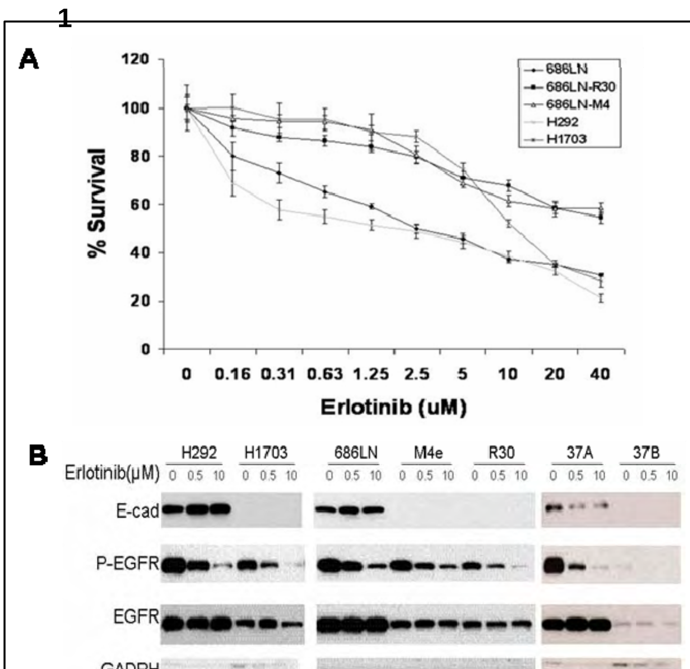

Figure 10. Response of the cancer cells to the EGFR-TKI erlotinib. Effect of erlotinib on (A) growth of NSCLC and SCCHN and (B) expression of E-cadherin (E-cad) and EGFR.

Since immunoblotting can only show the total level of each protein, QD-Immunocytochemistry (ICC) combining its interrelated imaging and quantifying system was used to obtain the quantified co-localization of the related proteins in the same sample and at the same time point. Figure 11 shows membrane and cytoplasmic distribution of E-cad and EGFR in EGFR-TKI sensitive and insensitive cells. Results of the quantification show that the mean of average membrane signal of E-cad in 5 EGFR-TKI sensitive cell lines is 0.512±0.110 a.u., while that in four EGFR-TKI insensitive cells is only 0.307±0.055 a.u. ($P<0.008$). The mean average membrane signal of EGFR in EGFR-TKI sensitive cell lines is 1.413±0.448 a.u. compared to 0.443±0.076 a.u. in EGFR-TKI insensitive cells ($P< 0.002$). The QD-based quantification also confirmed that not only membrane but also total protein levels of both EGFR and E-cad were lower in EGFR-TKI-insensitive cell lines than those in the sensitive cell lines (data not shown).

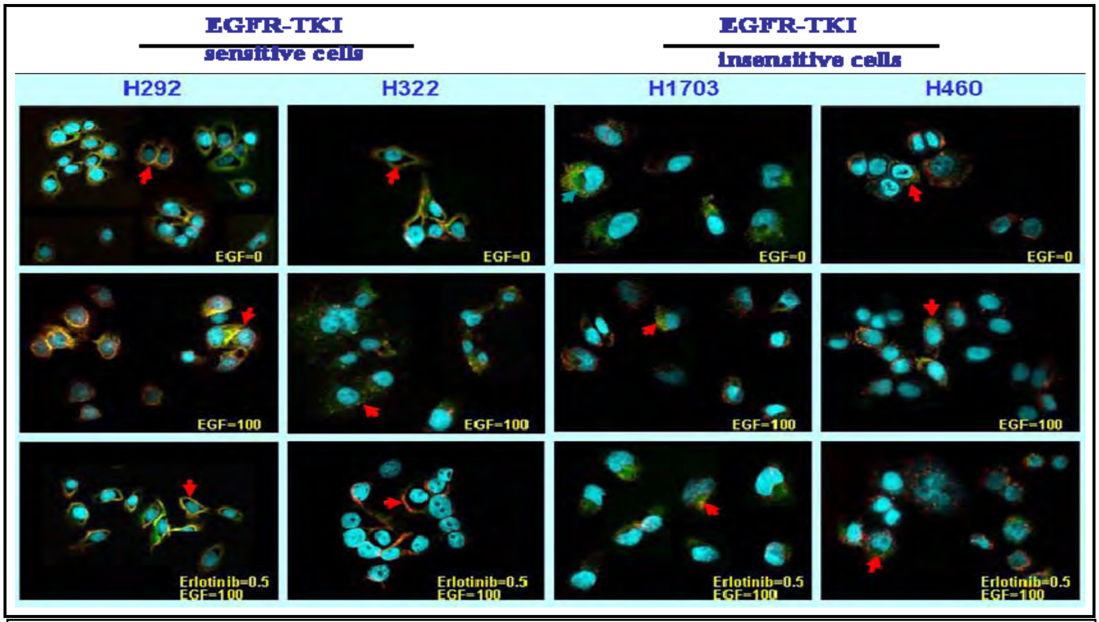

Figure 11. Merged image of E-cad (QD565, green) and EFGR (QD605, red) using an Olympus microscope 1x71 with CRi spectral imaging and quantifying system.

EGFR-TKI Sensitive Cells are more responsible for EGF-induced EGFR Internalization than EGFR-TKI Insensitive Cells. Localization of EGFR and E-cad was tracked and quantified by different QDs signals simultaneously after induction with EGF. Both EGFR and E-cad internalized from the cell membrane to the cytoplasm in EGFR-TKI sensitive cell lines. In contrast, in EGFR-TKI insensitive cells, these dynamic changes were not observed (Figure 11). Quantification showed that the capability of EGF induced EGFR and E-cad internalization in EGFR-TKI sensitive cells is much stronger than that in EGFR-TKI insensitive cells. In detail, the percentage of EGFR relative internalization in the EGFR-TKI sensitive cells was 1.39 to 2.21-fold greater than that in the insensitive cells, and the E-cad internalization in the EGFR-TKI sensitive cells was 1.64 to 1.99-fold greater than that in the insensitive cells (Figure 12). The EGFR internalization induced by EGF was confirmed with traditional FACS, which showed that the percentage of relative internalization is 72.97% to 97.99% in EGFR-TKI sensitive cells compared to only 42.82% to 58.59% in EGFR-TKI insensitive cells. These results are similar to the analysis by QDs-based immunostains.

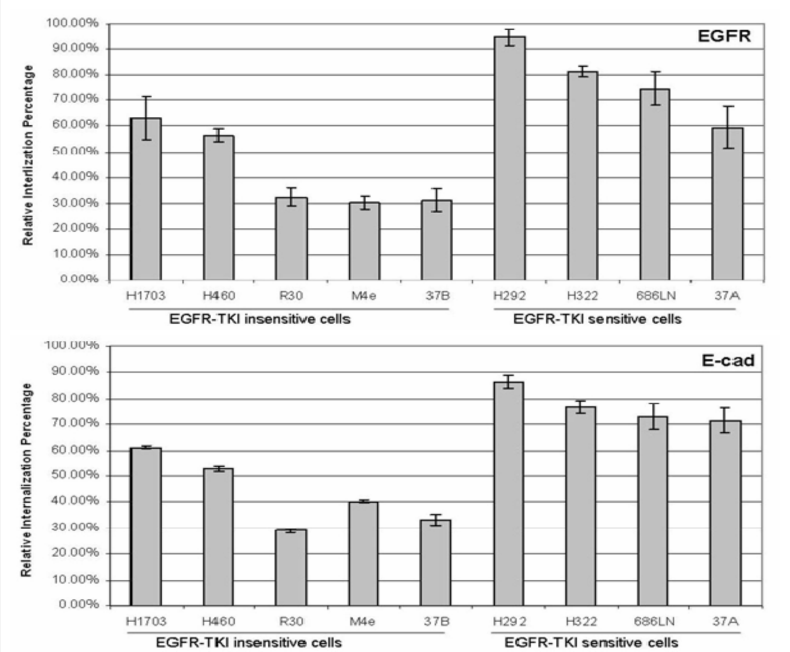

Figure 12. Comparison of relative internalization of E-cad and EGFR induced by EGF between EGFR-TKI sensitive and insensitive cell lines.

Erlotinib Inhibits EGF-induced EGFR Internalization in EGFR-TKI Sensitive Cells with a Minimal Effect on EGFR-TKI Insensitive Cells. QD quantification showed that erlotinib at 0.5 μM inhibited EGF-induced EGFR internalization 30.90% to 63.59% in the EGFR-TKI sensitive cells as compared with the untreated control, whereas the inhibition was only 5.28% to 11.47% in the EGFR-TKI insensitive cells (Fig. 13). Erlotinib at 0.5 μM has also a significant inhibitory effect on E-cad internalization in EGFR-TKI sensitive cells.

Quantified immunostaining showed that the inhibition of EGF-induced E-cad internalization was 30.0% to 46.6% in the EGFR-TKI sensitive cells compared to 3.52% to 9.60% in EGFR-TKI insensitive cells (Figure 13). FACS analyses also confirm these observations and showed that inhibition of EGFR internalization by erlotinib was dose-dependent in both EGFR-TKI sensitive and insensitive cell lines (data not shown, but the inhibition is much stronger in EGFR-TKI sensitive cells than in the insensitive cells.

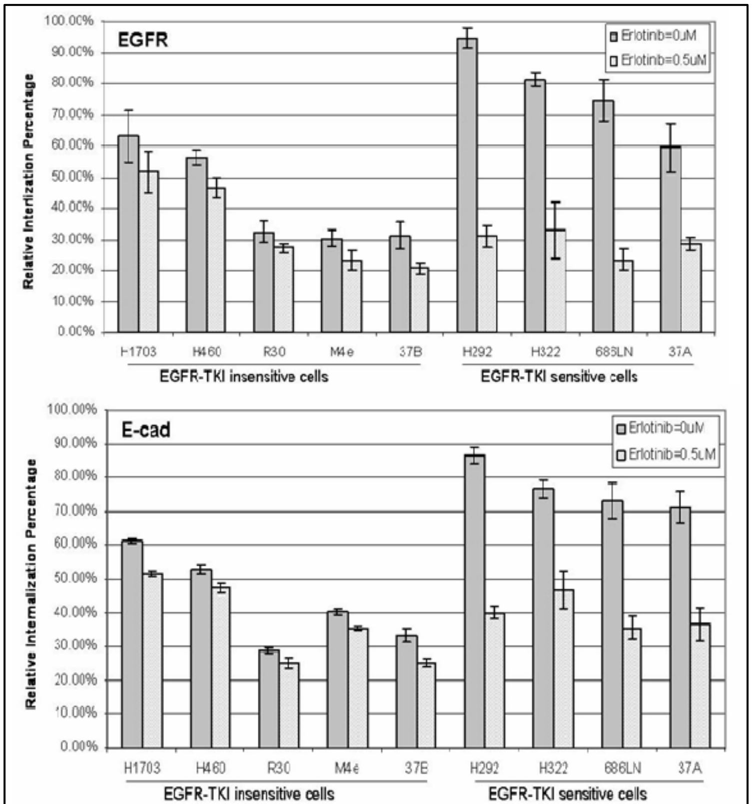

Figure 13. Comparison of EGFR and E-cad internalization induced by EGF under treatment with erlotinib between EGFR-TKI sensitive and insensitive lung cancer cell lines.

Specific Aim 2. Verification of QD-Abs for detection and quantification of MBM by comparison with conventional IHC using paraffin-embedded tissues and evaluation of their prognostic value in NSCLC.

Update

In addition to the cell lines studied, we have established and optimized the conditions for immunohistochemical analysis using formalin fixed and paraffin embedded (FFPE) tumor tissues. Three methods were compared: (1) the cocktail method, (2) step-by-step method with QDs-streptavidin, and (3) mixed method with QDs-2nd Ab plus QDs-streptavidin. Figure 14 illustrated a comparison between the cocktail method by QDs-2nd Ab and step-by-step method with QDs-streptavidin. Among these QD-based immunostaining methods for FFPE tissues, the cocktail method provides more evenly distributed signals for all three immunostained biomarkers and is considered a better method than the others.

We collected about 100 NSCLC tissues with matched normal tissues as the control. These specimens are being currently confirmed by a pathologist and will be ready for analysis.

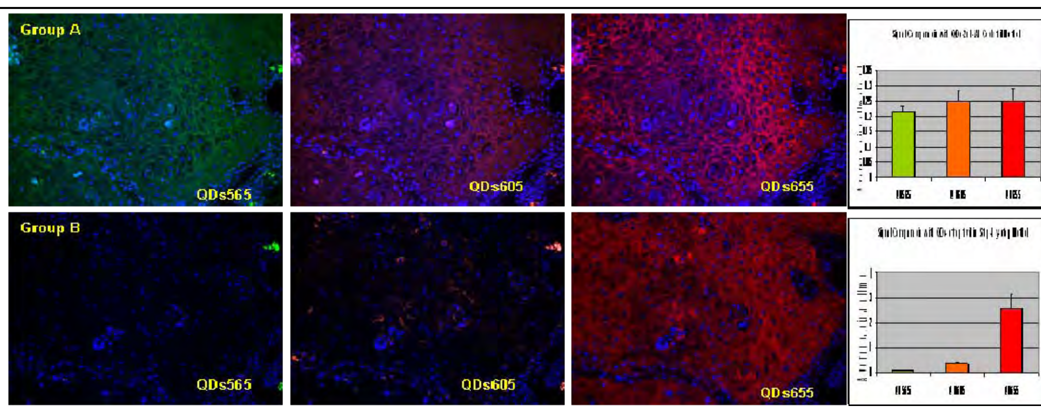

Figure 14. Comparison of different QD methods for immunostaining of FFPE tissues. Three methods – cocktailed staining with QD direct conjugation with primary antibody, cocktailed staining with QD conjugated to secondary antibody, and stepwise staining with QD conjugated to streptavidin – were used to stain and quantify EGFR, E-cad, and b-catenin in FFPE tissues. Our results suggested that the cocktailed staining with QD conjugated to secondary antibody (Group A) showed more evenly distributed signals than the stepwise staining with QD conjugated to streptavidin (Group B). QD direct conjugation with primary antibodies costs too much, so this method was abandoned in our study.

Specific Aim 3. Correlation of the MBM detected by QD-Abs with outcomes of chemotherapies and EGFR- targeted therapy using resectable NSCLC tissues.

Update
This study was proposed for year 3 and 4. Thus, we have not started working on this Aim yet. Currently, there is no change for this Specific Aim.

Key Research Accomplishments:
- Optimized QD-staining conditions for multiplexing three biomarkers, EGFR, E-cadherin, and β-catenin in both cell lines and FFPE tissues;
- Developed a quantification method for QD signals using the CRi Nuance spectral system;
- Identified substantial differences between EGFR-TKI sensitive and insensitive NSCLC cells in response to EGF and/or erlotinib.

Reportable Outcomes:
Presentations:
- Donghai Huang, Ling Su, Xianghong Peng, Hongzheng Zhang, Fadlo R. Khuri, Dong M. Shin, Zhuo (Georgia) Chen. Using Quantum Dots to Examine Dynamic Relocalization of EGFR, E-Cadherin, and β-Catenin in Lung Cancer Cells upon Treatment with EGFR-TKI. American Association for Cancer Research annual meeting, 2008

Abstracts:
- Huang D-H, Su L, Peng X-H, Zhang H, Khuri F, Shin DM, Chen Z(G). Using quantum dots to examine dynamic relocalization of EGFR, E-cadherin, and β-catenin in lung cancer cells upon treatment with EGFR-TKI. AACR Annual Meeting, San Diego, Abstract 3737, April 2008.

Conclusions:
We have established both staining and quantification methods for using QD-based immunocytochemical and immunohistochemical analyses. Using this strategy, expression and cellular localization of EGFR and E-cad were compared between EGF-TKI sensitive and insensitive NSCLC and SCCHN cancer cell lines. Substantial differences in EGFR and E-cad expression and localization were identified among these cell lines both at the basal level and in response to EGF and EGFR-TKI, Our observations suggest quantification of membrane expression of EGFR and E-cad may serve as biomarkers in predicting efficacy of EGFR-targeted therapy at least for one population of NSCLC and SCCHN patients. Our findings provide new biomarkers and QD methodology in predicting sensitivity to EGFR-targeting therapy which can be applied to tumor tissue specimens for clinical application. Furthermore, clarifying substantial differences between EGFR-TKI sensitive and insensitive cancer cells will help understand the mechanism of EGFR-targeted resistance and will facilitate development of new targeted therapies.

Pathology Core

(Director: Dr. Ignacio Wistuba)

The Pathology Core is an essential component of the PROSPECT program. The Pathology Core plays an important role by collecting, processing and distributing tissue and serum specimens obtained from Clinical Trials on NSCLC (Project 2) and malignant pleural mesothelioma (MPM; Project 4) for molecular profiles and biomarker analysis.

Our objectives (functions) are as follows:

1. Develop and maintain a repository of tissue and serum specimens from patients with non-small cell lung carcinoma (NSCLC) and malignant pleural mesothelioma (MPM).

2. Process NSCLC cell lines and tissue specimens for histopathologic and molecular analyses.
3. Perform and evaluate immunohistochemical (IHC) analysis in human tumor tissue specimens and mouse xenograft tissues.

Objective 1. Develop and maintain repository of tissue and serum specimens from patients with lung cancer and malignant pleural mesothelioma (MPM).

a) Selection of lung cancer and mesothelioma specimens available in Thoracic Malignancy Tissue Bank. This tissue bank has been in place in our institution for the last 11 years, and over 16,000 aliquots of blood and frozen lung normal and tumor tissues have been banked. As potential cases for PROSPECT projects 2 and 3, we have identified 1,150 non-small cell lung cancer (NSCLC) tumor specimens, including the major histology types (Table 4). In those specimens, we have frozen tumor tissue available from patients who have consented to their tissue to be banked and used for research purposes. Corresponding non-malignant peripheral lung and bronchial frozen tissue is available in over 90% and nearly 30% of the tumors, respectively. Quality control has been performed on most specimens. The corresponding archival paraffin blocks and slides, as well as clinicopathological information, are available in all cases. In addition, this tissue bank stores archival paraffin blocks and slides from all available surgically resected lung cancers in our institution for the period of 1982 to 2005. More than 3,733 cases have been identified and specimens banked. All the cases retrieved are under histopathological review and classified according to the 2004 WHO Pathology Classification for lung cancer. Detailed histopathological analysis has been performed in nearly 1,500 cases to date.

Table 5. Summary of frozen NSCLC specimens in Thoracic Malignancy Tissue Bank.

Tumor Type	N of Cases (Tumor and Normal Tissue)
Lung Cancer	1150
Adenocarcinoma	630
Squamous Cell Carcinoma	379
Large Cell Carcinoma	29
Other NSCLC	112
Mesothelioma	93

From the Thoracic Malignancy Tissue Bank, we have identified 93 MPMs with frozen tumor tissue available for PROSPECT Project 4. Formalin-fixed and paraffin-embedded tissues from 91 MPMs have been collected, and clinical and pathological information have been obtained in all cases.

In addition, the Thoracic Malignancy Tissue Bank has banked frozen mononuclear blood cells and serum samples from 339 NSCLC and 28 MPM patients (Table 6). These blood specimens have been collected at time of tumors surgical resection. Of interest, for NSCLC 147 (20%) out of 736 cases have received neoadjuvant chemotherapy.

Table 6. Summary of frozen peripheral mononuclear blood cells (PMBC) and serum samples in the Thoracic Malignancy Tissue Bank.

Tumor Type	N of Cases (Serum and PMBC)
Lung Cancer	339
Adenocarcinoma	184
Squamous Cell Carcinoma	114
Large Cell Carcinoma	8
Other NSCLC	33
Mesothelioma	28

b) <u>Prospective collection and banking of lung cancer and mesothelioma specimens for PROSPECT projects</u>. Since the activation of the PROSPECT laboratory project on August 2007, the Pathology Core has collected fresh and formalin-fixed tissue specimens from 135 NSCLC and 9 MPM surgically resected cases (Table 7). From those, snap frozen normal and tumor tissue have been collected in all cases (N=397 samples). In addition, we have obtained and banked tumor specimens (N=142 samples) in RNAlater® (Ambion, Austin, TX), 12% dimethyl sulfoxide (DMSO)-preserved samples (51 samples) and OCT-embedded for frozen sectioning (N=96 samples). From the 135 NSCLC cases, at least 18 patients have received neoadjuvant chemotherapy.

Table 7. Summary of prospectively collected tumor tissue specimens from NSCLC and MPM cases.

Tumor Type	Tissue (Tumor and Normal) N of Cases	Serum /PMBC N of Cases
Lung Cancer	135	59
Adenocarcinoma	65	33
Squamous Cell Carcinoma	32	13
Large Cell Carcinoma	1	1
Other NSCLC	37	5
Mesothelioma	9	5
No tumor present	4	2

Thoracic Malignancy Tissue Bank Database. To better handle tissue and blood specimens, our institution has developed a web based tissue banking system, named TissueStation (Figure 15). This is a software application built around the principles of integration with our suite of clinical systems, primarily in the J2EE environment and/or a combination of Perl/PHP/Java technologies. Also, we have in place a Microstrategy Report Services, Oracle-based, which allows to run reports and retrieve data from the TissueStation database. Both applications (TissueStation and Microstrategy) have been instrumental for the selection and processing of tissue specimens for PROSPECT projects.

Figure 15. Screen shots of the Tissue Station developed for the Thoracic Malignancies Tissue Bank.

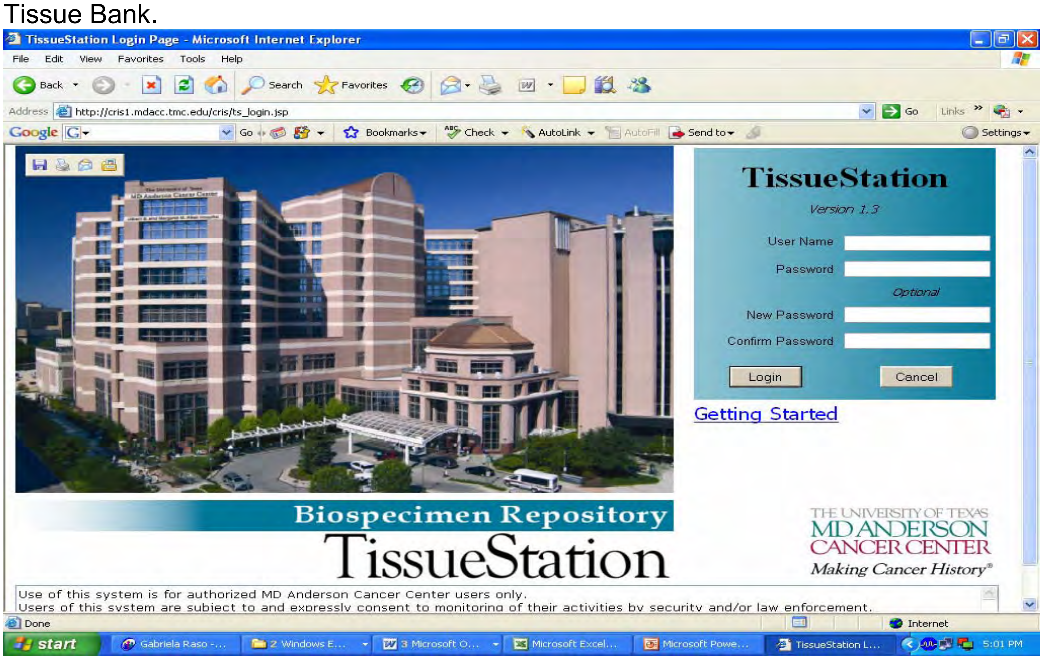

These systems follow UT-MD Anderson information security and compliance requirements with a comprehensive information security program that includes an ongoing risk assessment, disaster recovery planning, as well as incident prevention and management. Supporting incident prevention and management efforts are a variety of security tools, including desktop and server anti-virus, intrusion detection and prevention systems, multiple firewalls, etc. Additionally, an identity management program, currently based on Shibboleth and Novell eDirectory, is in place to further address these issues.

The TissueStation web database system allows us to make collection requests a day in advance to the surgery, enter sample and specimen information, consent information, location and freezer inventory, annotated histopathology information among other features. It also generates a de-identified number for each sample and 3D barcode system which are printed on special labels customized for cryovials.

Objective 2. Process NSCLC cell lines and tissue specimens for histopathological and molecular analyses.

a) Tissue Specimens: From the 1,150 NSCLC and 93 MPM cases with frozen tissue banked in the Thoracic Malignancy Tissue Bank, we selected 736 NSCLCs and all MPMs for tissue processing for DNA, RNA (mRNA and microRNA) and protein extractions. For these specimens, detailed clinical and pathological data have been obtained including demographic, smoking history, clinical and pathological staging, treatments (surgical; neo- and/or adjuvant), follow-up for recurrence and survival, recurrence pattern, and treatment at recurrence (Table 8). We are currently evaluating how to assess response to treatment at time of recurrence by CT analysis.

Table 8. Summary of main clinicopathologic features of 736 surgically resected NSCLC specimens with follow-up and clinical information on treatment available for profiling analysis of Project 3.

Features		Number
Histology	Adenocarcinoma	448 (61%)
	Squamous cell carcinoma	288 (39%)
Stage (pathological)	I	395 (54%)
	II	130 (18%)
	III	187 (25%)
	IV	21 (3%)

Histopathological processing for DNA/RNA/protein extractions. Our method of extraction consist of histology evaluation of tumor components using 5 μm thick haematoxylin-eosin (H&E)-stained histology sections obtained at four levels of the frozen tissue specimen that are alternated by two sets of thirty 20 μm thick sections obtained for RNA and protein extractions. The histopathological analysis of the frozen tissue specimens includes, among other factors, percentage of tumor, percentage of malignant cells, intensity of inflammation, and percentages of necrosis and fibrosis. We have processed and performed quality control in 387 NSCLC cases (363 out of 736 retrospectively collected, and 24 prospectively collected cases) and 80 MPM cases. Of those, digital images of histology have been obtained and filed for future reference is 89 cases (Figure 16).

b) Cell Lines. In collaboration with Drs. John Heymach (M. D. Anderson Cancer Center) and John Minna (UT-Southwestern Medical Center, Dallas) we have established a repository of NSCLC (n=60) and MPM (n=6) cell lines which are available for PROSPECT projects. In the Pathology Core, we have developed formalin-fixed and paraffin-embedded pellets which are being used for immunohistochemistry and fluorescent *in situ* hybridization (FISH) optimizations.

Figure 16. Pictures showing digital images of histology of frozen tumor and normal tissue used for DNA, RNA and protein extractions. *a*, file with multiple cases. *b*, low magnification of a representative NSCLC case.

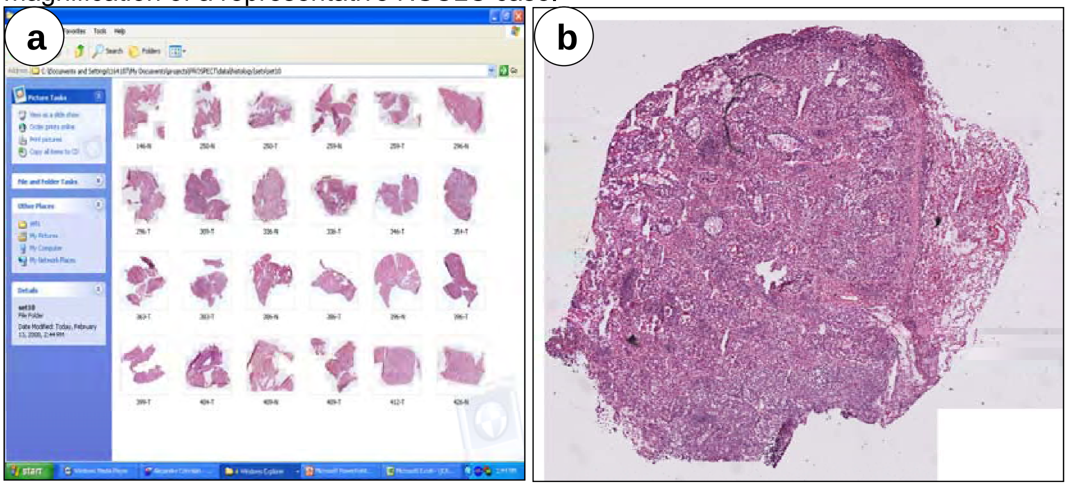

Objective 3. Perform and evaluate immunohistochemical (IHC) analysis in human tumor tissue specimens and mouse xenograft tumor specimens.

We have not performed any IHC analysis for markers discovered by our PROSPECT projects yet. However, our IHC Lab continues optimizing new antibodies which are examined in NSCLC and MPM cell lines pellets and tumor specimens for different projects. The list of antibodies includes nearly 140 markers. In addition, the histopathological examination of tissue specimens of cases selected from the retrospective tissue bank (Table 8) will allow us to construct the tissue microarrays (TMA) containing all these cases during the second year of the PROSPECT grant.

Key Research Accomplishments:

- Identification of 736 NSCLC and 93 MPM cases with frozen tissues from the Thoracic Malignancy Tissue Bank and completed collection of detailed annotated clinico-pathologic data.
- Establishment of the tissue histology processing methods that allows direct examination of frozen tissue used for DNA/RNA and protein extractions; 433 out of 736 cases have been processed using these procedures.
- Prospective collection of frozen tissue specimens from 135 NSCLC and 9 MPM cases, including 18 NSCLC cases treated with neo-adjuvant chemotherapy.
- In close collaboration with PROSPECT Project 1, establishment of NSCLC and MPM cell lines repository at the M. D. Anderson Cancer Center.

Reportable Outcomes:
Establishment of NSCLC and MPM cell lines repository at the M. D. Anderson Cancer Center.

Conclusions:
During the first year, the PROSPECT Pathology Core has achieved and exceeded its goals for the first year by identifying and processing a large number of frozen tissue specimens from NSCLC (N=736) and MPM (n=93) for DNA/RNA and protein extractions, including 153 NSCLC cases treated with neo-adjuvant chemotherapy. The goal for the retrospectively collected NSCLC was 150 cases. In addition, the prospective collection and processing of tissues (NSCLC=135) during the first year is an indication that the goal of 350 prospective NSCLC cases in four years will be achieved. The repository of NSCLC and MPM cell lines is in place.

Core C: Biostatistics/Bioinformatics Core:

(Director: Dr. J. Jack Lee; Co-Director: Kevin Coombes)

In close collaboration with the Pathology Core and each of the five main projects, the Biostatistics and Data Management Core (BDMC) for the Department of Defense (DoD) PROSPECT lung cancer research program is a comprehensive, multi-lateral resource for designing clinical and basic science experiments; developing and applying innovative statistical methodology, data acquisition and management, and statistical analysis; and publishing translational research generated by this research proposal. We deliver planned and tailored statistical analyses for rapid communication of project results among project investigators, and by collaborating with all project investigators to facilitate the timely publication of scientific results.

The main objectives of the Biostatistics and Data Management Core are:
1. Provide the statistical design, sample size, and power calculations for each project.
2. Develop a secure, internet-driven, web-based database application to integrate data generated by the five proposed projects and the Pathology Core of the PROSPECT research project.
3. Develop a comprehensive, web-based database management system for tissue specimen tracking and distribution and for a central repository of all biomarker data.
4. Provide all statistical data analyses, including descriptive analysis, hypothesis testing, estimation, and modeling of prospectively generated data.
5. Provide prospective collection, entry, quality control, and integration of data for the basic science, pre-clinical, and clinical studies in the PROSPECT grant.
6. Provide study monitoring and conduct of the neoadjvant clinical trial that ensures patient safety by timely reporting of toxicity and interim analysis results to various institutional review boards (IRBs), the UTMDACC data monitoring committee, the DoD, and other regulatory agencies.
7. Generate statistical reports for all projects.
8. Collaborate with all project investigators and assist them in publishing scientific results.
9. Develop and adapt innovative statistical and genomic methods pertinent to biomarker-integrated translational lung cancer studies.

Update

In the first funding year, the BDMC worked with all project investigators in providing biostatistics and data management support. The accomplishments are summarized below.

(A) Biostatistics

We have worked with clinical investigators in providing the biostatistical support in the development and revision of PROSPECT protocols. We provide statistical report in our monthly project meetings to update the accrual, randomization, demographic data, etc.

(B) Data Management

PROSPECT Database Development

The PROSPECT database development takes advantage of the revitalization effort from the VITAL program because similar databases were developed in both projects. To tailor for the PROSPECT specific needs, database extensions were made to allow the collection and management of data from multiple studies including the neoadjuvant studies, adjuvant studies, and regular chemotherapy studies. In addition, the PROSPECT database was developed to extend the reVITALization database in VITAL to provide additional clinical, pathological, and biomarker data repositories and tissue tracking.

The SQL Server 2005 database and ASP.NET web application is implemented with VB.net language. Queries and SQL 2005 reports are provided. Secure Socket Layer (SSL) and secured database password are used to keep data transaction protected and confidential. The tissue data includes clinical and pathological data.

1) The database's clinical module contains the following web forms:
- Patient Information
- Social History (Alcohol and Smoking history)
- Medical History
- Other Malignancy
- Treatments (Surgery, Chemotherapy, Radiotherapy and Other Treatments)
- Clinical Staging
- Follow up

2) The pathological module contains the following web forms:
- Primary and Metastasis data (Diagnosis and Surgery Specimens)
- Histology
- Staging and Tumor Information: Cancer staging (TNM classification) is automatically determined by the system based on the tumor information provided.
- Tissue Bank (Frozen Tissue and Paraffin)

3) Reports: Several Excel reports are provided for clinical and pathological module.
1. Clinical Report
2. Pathological Report
3. Patient Report
4. Accession Report
5. General Information Report
6. Other Malignancy Report
7. Surgery Report
8. Chemotherapy Report
9. Radiotherapy Report
10. Other Treatment Report
11. Staging Report
12. Follow up Report
13. Histology Diagnosis Report

4) Dictionaries: The database gives control for the users to update dictionaries; however, dictionary deletion is prohibited.

Key Research Accomplishments:
- Developed a secured, web-based database application to assist the study conduct.

Reportable Outcomes:
A web-based database application is developed and deployed at:
https://insidebiostat/DMI_PROSPECT/Common/Login.aspx

Conclusions:
In collaboration with clinical investigators, research nurses, Biomarker Core, and basic scientists, the Biostatistics and Data Management Core has continued to deliver the biostatistics and data management support as proposed.

Appendices:
Appendix B: PROSPECT Database Screenshots

KEY RESEARCH ACCOMPLISHMENTS

PROJECT 1

- Developed molecular signatures for predicting sensitivity to premetrexed.
- Developed a model for selection of sensitivity to taxanes vs EGFR inhibitors.

PROJECT 2

- Identified tumors from more than 700 patients in our Tissue Bank from which we will be able to select 150 for PROSPECT
- Constructed tissue microarrays on 327 tumors from the Tissue Bank, and immunohistochemical staining for more than 100 different biomarkers is nearing completion
- Bioinformatic assessment of the first 18 biomarkers has been initiated
- Collection of prospective tumor samples from patients with and without neoadjuvant chemotherapy is on schedule
- Performed exponential decay nonlinear regression analysis on 172 published survival curves and on the 327 patients for whom we have generated tissue microarrays; this exercise has led to the generation of additional hypotheses to be tested as biomarker data mature

PROJECT 3

- Collection of relevant clinical and pathological information from of 736 NSCLCs with frozen tissue in the Pathology Core tissue bank, including 147 cases treated with neoadjuvant (pre-operative) and 131 case with adjuvant (post-operative) chemotherapy.
- Establishment of a methodology for DNA and RNA extraction for a large number of frozen tissue specimens. We have extracted DNA and RNA from paired normal and tumor tissue 387 (53%) out of 736 NSCLC available.
- Establishment of a profiling strategy for NSCLCs.

PROJECT 4

- Established the administrative and clinical research team and the Mesothelioma Focus Group (MFG) in support of the clinical trial and to facilitate patient enrollment onto the study.
- Obtained IRB approval and activated Protocol 2006-0935.
- Developed the clinical procedures in the Surgical OR for the tissue, serum/plasma, pleural effusion, platelet collection on Protocol 2006-0935.
- Mechanism set-up by Pharmacy for monitoring and distribution of the study drug.
- Trained clinical research RNs to educate patients on the study details.
- Creation of Informed consent and information sheet.
- Established registration algorithm for enrollment of patients.
- Created procedure for notification by Thoracic New Patient Business office when a new mesothelioma patient is coming to MDACC.
- Prioritization of resectable mesothelioma patients who are potential candidates for Protocol 2006-0935 by Thoracic Surgery and Thoracic Medical Oncology Department.
- Coordination of an advertisement program to increase patient enrollment onto the study.
- Established the laboratory Infrastructure to manage the translational correlates on the clinical trial.
- Identification of retrospective specimens and cell lines for research in Aim 3.

PROJECT 5

- Optimized QD-staining conditions for multiplexing three biomarkers, EGFR, E-cadherin, and β-catenin in both cell lines and FFPE tissues;
- Developed a quantification method for QD signals using the CRi Nuance spectral system;
- Identified substantial differences between EGFR-TKI sensitive and insensitive NSCLC cells in response to EGF and/or erlotinib.

PATHOLOGY CORE

- Identification of 736 NSCLC and 93 MPM cases with frozen tissues from the Thoracic Malignancy Tissue Bank and completed collection of detailed annotated clinico-pathologic data.
- Establishment of the tissue histology processing methods that allows direct examination of frozen tissue used for DNA/RNA and protein extractions; 433 out of 736 cases have been processed using these procedures.
- Prospective collection of frozen tissue specimens from 135 NSCLC and 9 MPM cases, including 18 NSCLC cases treated with neo-adjuvant chemotherapy.
- In close collaboration with PROSPECT Project 1, establishment of NSCLC and MPM cell lines repository at the M. D. Anderson Cancer Center.

BIOSTATISTICS AND DATA MANAGEMENT CORE

- Developed a secured, web-based database application to assist the study conduct.

REPORTABLE OUTCOMES

Abstracts/Presentations

- Byers LA, Nanjundan M, Girard L, Coombes K, Xie Y, Peyton M, Ma Y, Zachariah S, Nikolinakos P, Cigarroa R, Mills G, Roth J, Minna J, Heymach J. "Reverse-phase protein array (RPPA) profiling of non-small cell lung cancer lines identifies tumor signatures for sensitivity and resistance to chemotherapy and targeted agents" [abstract]. In: Proceedings of the AACR-NCI-EORTC International Conference on Molecular Targets and Cancer Therapeutics; 2007 Oct 22-26; Washington, DC; San Francsisco (CA): AACR; Abstract B178, p 219, 2007.
- Byers, LA, et al. "Proteomic profiling of non-small cell lung cancer cell lines identifies tumor signatures of response to chemotherapy and targeted agents." IASCL 8th Annual Targeted Therapies of the Treatment of Lung Cancer Meeting, Santa Monica, CA, Feb 2008.
- Byers LA, Nanjundan M, Girard L, Coombes K, Xie Y, Peyton M, Zachariah S, Weber S, Siwak D, Nikolinakos P, Wistuba I, Roth J, Mills G, Minna J, Heymach J. "Reverse-phase protein array (RPPA) profiling of response to taxanes and epidermal growth factor receptor (EGFR) inhibitors identifies an inverse correlation between markers of sensitivity to docetaxel and erlotinib in non-small cell lung cancer lines". AACR Annual Meeting, San Diego, Abstract 3937, April 2008.
- Herynk MH, Xu L, Heymach JV. Sex differences in estrogen mediated growth and migration of NSCLC. Estrogen signaling promotes sex differences in the growth and migration of NSCLC. Impact of estrogen signaling on cell migration and proliferation of NSCLC cell lines. AACR Annual Meeting, San Diego, CA, Abstract 3034, April 2008.
- Huang D-H, Su L, Peng X-H, Zhang H, Khuri F, Shin DM, Chen Z(G). Using quantum dots to examine dynamic relocalization of EGFR, E-cadherin, and β-catenin in lung cancer cells upon treatment with EGFR-TKI. AACR Annual Meeting, San Diego, Abstract 3737, April 2008.

Publications (including In Press and submitted):

- Stewart, DJ. Non-small cell lung cancer patient survival when assessed as a first order nonlinear process:effect of therapy and stage. Submitted for publication.

Other:

- Establishment of NSCLC and MPM cell lines repository at the M. D. Anderson Cancer Center.
- A web-based database application is developed and deployed at: https://insidebiostat/DMI_PROSPECT/Common/Login.aspx

CONCLUSIONS

PROJECT 1

RPPA proteomic profiling identified intracellular signaling pathways and proteins associated with sensitivity and resistance to chemotherapies and targeted agents in NSCLC cell lines. These results suggest biologic mechanisms of therapeutic resistance. Our findings will be further investigated by correlating RPPA of tumor samples with clinical outcomes with the goal of developing predictive markers that can guide treatment selection and identify new targets in NSCLC.

PROJECT 2

We are on schedule for prospective tissue collection and for identification of archived specimens from our tissue bank. We are also on schedule with respect to processing of archived specimens. We have gained preliminary experience with exponential decay nonlinear regression analyses of patient survival curves and this has led to additional hypotheses.

PROJECT 3

During the first year, we have identified and collected detailed relevant clinical and pathological information from NSCLC (N=736; Aim 1) banked in our Pathology Core bank, including 147 NSCLCs treated with neo-adjuvant chemotherapy (Aim 2). The goal for the retrospectively collected NSCLC was 150 cases, so we have exceeded our goal. In addition, we are about to complete DNA and RNA extraction from all those cases. Profiling mRNA analysis for a large number of retrospectively collected NSCLC without adjuvant therapy, with neoadjuvant (pre-operative) and with adjuvant (post-operative) chemotherapy will be performed during second year of PROSPECT grant.

PROJECT 4

Work is on schedule. The major effort to date has been in initiating the clinical trial and setting-up the infrastructure needed. Now that this is active, we expect that accrual will be on schedule.

PROJECT 5

We have established both staining and quantification methods for using QD-based immunocytochemical and immunohistochemical analyses. Using this strategy, expression and cellular localization of EGFR and E-cad were compared between EGF-TKI sensitive and insensitive NSCLC and SCCHN cancer cell lines. Substantial differences in EGFR and E-cad expression and localization were identified among these cell lines both at the basal level and in response to EGF and EGFR-TKI,   Our observations suggest quantification of membrane expression of EGFR and E-cad may serve as biomarkers in predicting efficacy of EGFR-targeted therapy at least for one population of NSCLC and SCCHN patients. Our findings provide new biomarkers and QD methodology in predicting sensitivity to EGFR-targeting therapy which can be applied to tumor tissue specimens for clinical application. Furthermore, clarifying substantial differences between EGFR-TKI sensitive and insensitive cancer cells will help understand the mechanism of EGFR-targeted resistance and will facilitate development of new targeted therapies.

PATHOLOGY CORE

During the first year, the PROSPECT Pathology Core has achieved and exceeded its goals for the first year by identifying and processing a large number of frozen tissue specimens from NSCLC (N=736) and MPM (n=93) for DNA/RNA and protein extractions, including 153 NSCLC cases treated with neo-adjuvant chemotherapy. The goal for the retrospectively collected NSCLC was 150 cases. In addition, the prospective collection and processing of tissues (NSCLC=135) during the first year is an indication that the goal of 350 prospective NSCLC cases in four years will be achieved. The repository of NSCLC and MPM cell lines is in place.

BIOSTATISTICS AND DATA MANAGEMENT CORE

In collaboration with clinical investigators, research nurses, Biomarker Core, and basic scientists, the Biostatistics and Data Management Core has continued to deliver the biostatistics and data management support as proposed.

Appendices

Appendix A

Abstracts and Publications

2008 AACR Annual Meeting
April 12-16, 2008
San Diego, CA

Print this Page for Your Records Close Window

Abstract Number: 3937

Session Title: Proteomic Tumor Profiling 1

Presentation Title: Reverse-phase protein array (RPPA) profiling of response to taxanes and epidermal growth factor receptor (EGFR) inhibitors identifies an inverse correlation between markers of sensitivity to docetaxel and erlotinib in non-small cell lung cancer lines

Presentation Start/End Time: Tuesday, Apr 15, 2008, 8:00 AM -12:00 PM

Location: Exhibit Hall B-F, San Diego Convention Center

Poster Section: 26

Poster Board Number: 14

Author Block: *Lauren Averett Byers, Meera Nanjundan, Luc Girard, Kevin Coombes, Yang Xie, Michael Peyton, Sunny Zachariah, Stephanie Weber, Doris Siwak, Petros Nikolinakos, Ignacio Wistuba, Jack Roth, Gordon Mills, John Minna, John Heymach*. UT M.D. Anderson Cancer Center, Houston, TX, UT Southwestern Medical Center, Dallas, TX

Introduction: Non-small cell lung cancer (NSCLC) is a molecularly heterogeneous disease, with a variety of cell signaling pathways driving progression and therapeutic resistance. Using reverse-phase protein arrays (RPPA), a high-throughput technology that measures key signaling proteins, we profiled 45 NSCLC cell lines to derive proteomic signatures of response to taxanes (paclitaxel, docetaxel) and EGFR inhibitors (erlotinib, gefitinib, and cetuximab). RPPA is a quantitative, antibody-based assay that allows broad and simultaneous profiling of numerous therapeutically relevant targets from small amounts of protein (20ug). Unlike gene expression arrays, RPPA directly measures protein levels and can discern post-translational modifications such as phosphorylation, which reflects the activity level of signaling pathways. Methods: To determine sensitive and resistant cell lines for each drug, the concentration required for 50% growth inhibition (IC50) was determined by MTS assay in 45 cell lines. For RPPA, protein lysate from untreated cells was printed in serial dilutions onto nitrocellulose-coated glass slides. Each slide was then probed with one of 59 validated, monospecific antibodies. A single, representative logarithmic value was calculated for each protein based on the signal intensity-serial dilution curves. Results: Unsupervised hierarchical clustering of 15 drugs by cell line responsiveness grouped mechanistically-related drugs together, as demonstrated by clustering of the taxanes and of the EGFR inhibitors. Similarly, unsupervised clustering of RPPA proteomic expression profiles tightly clustered taxanes into one node and EGFR inhibitors in another. For each drug, no single marker was able to predict response better than chance; whereas, multivariate signatures predicted response to taxanes and EGFR inhibitors with ≥80% accuracy. Signatures of docetaxel and erlotinib response were inversely related, such that markers associated with docetaxel sensitivity were associated with erlotinib resistance (ex., Src, TSC2, LKB1, AMPK, CCNB1, gemin). Conclusions: RPPA proteomic profiling identified intracellular signaling pathways and proteins associated with sensitivity and resistance to the taxanes and EGFR-inhibitors in NSCLC. Moreover, markers of resistance to docetaxel predicted sensitivity to erlotinib. Since both drugs are commonly used as single agents in the second-line setting, these markers may have clinical application for selecting the best therapy for an individual patient. Response signatures will be validated in an independent set of NSCLC cell lines and in NSCLC tumors from patients treated with these agents.

2008 AACR Annual Meeting
April 12-16, 2008

Reverse-phase protein array (RPPA) profiling of non-small cell lung cancer lines identifies tumor signatures for sensitivity and resistance to chemotherapy and targeted agents

Lauren Averett Byers, Meera Nanjundan, Luc Girard, Kevin R. Coombes, Yang Xie, Michael Peyton, Yao Ma, Sunny Zachariah, Petros Nikolinakos, Ricardo Cigarroa, Gordon B. Mills, Jack A. Roth, John D. Minna, John V. Heymach.
M.D. Anderson Cancer Center, Houston, TX, UT Southwestern Medical Center, Dallas, TX

Introduction: Non-small cell lung cancer (NSCLC) is a molecularly heterogeneous disease, with a variety of cell signaling pathways driving progression and therapeutic resistance. Although agents are available that target many of these critical pathways, there is currently no biologically-based method for selecting the best drug for a patient. Using reverse phase protein array (RPPA), a high-throughput technology that systematically measures key signaling proteins, we profiled forty-four NSCLC cell lines for markers of sensitivity and resistance to fifteen cytotoxic and targeted agents. RPPA is a quantitative, antibody-based assay that allows broad and simultaneous profiling of numerous therapeutically relevant targets from small amounts of protein, as is obtained from routine biopsy. Unlike gene expression arrays, RPPAs directly measure protein levels and can discern specific post-translational modifications such as phosphorylation or cleavage. The ability to compare levels of phosphorylated versus non-phosphorylated proteins is particularly critical to determining the activity of signaling proteins such as tyrosine kinases.

Methods: The drug concentration required for 50% growth inhibition (IC50) was determined for 44 cell lines using MTS assays. For the RPPA, serial dilutions of pre-treatment cell lysates were printed on nitrocellulose-coated glass slides, and each slide incubated with one of 59 validated, monospecific antibodies. A single, representative logarithmic value for the signal intensity-serial dilution curve was then determined for each sample, representing the quantitative measure of a specific protein.

Results: Subsets of sensitive and resistant cell lines were identified for each drug, despite most cell lines having never been exposed to any treatment either in the patient from which they were derived or in vitro. When subjected to unsupervised clustering, mechanistically-related drugs grouped together (such as taxanes, platinum agents, and epidermal growth factor receptor inhibitors), with similar patterns of protein expression characterizing sensitivity or resistance. For example, resistance to cisplatin and carboplatin was associated with increased expression of cell adhesion molecules beta-catenin and E-cadherin and with Rab25, a GTPase previously correlated with worse outcome in breast and ovarian cancer. Cell lines treated with pemetrexed showed the greatest variation in IC50's, with a 1000-fold difference between sensitivity and resistance in 42 of the cell lines. Pemetrexed resistance was strongly associated with a number of proteins, including increased phospho-Rb (pRb) and PKCalpha. No single marker was able to predict pemetrexed resistance by itself. Rather, response to pemetrexed was predicted by a multivariate model which evaluated 10 markers for their "presence" or "absence," as determined by unique cutoff values for each protein defined in the model. For a given cell line, the more of these markers that were present, the more likely the cell line was resistant to pemetrexed. Finally, for PKCalpha, one of the non-phosphorylated protein markers in the model, we demonstrated that high PKCalpha mRNA levels correlated with resistance and with protein levels.

Conclusions: RPPA proteomic profiling identified intracellular signaling pathways and proteins associated with sensitivity and resistance to chemotherapies and targeted agents in NSCLC cell lines. These results suggest biologic mechanisms of therapeutic resistance. Our findings are being further investigated by correlating RPPA of tumor samples with clinical outcomes, with the goal of developing predictive markers that can guide treatment selection and identify new targets in NSCLC.

B178 Reverse-phase protein array (RPPA) profiling of non-small cell lung cancer lines identifies tumor signatures for sensitivity and resistance to chemotherapy and targeted agents. Lauren Averett Byers[1], Meera Nanjundan[1], Luc Girard[2], Kevin R. Coombes[1], Yang Xie[2], Michael Peyton[2], Yao Ma[2], Sunny Zachariah[2], Petros Nikolinakos[1], Ricardo Cigarroa[1], Gordon B. Mills[1], Jack A. Roth[1], John D. Minna[2], John V. Heymach[1]. [1]M. D. Anderson Cancer Center, Houston, TX; [2]UT Southwestern Medical Center, Dallas, TX.

Introduction: Non-small cell lung cancer (NSCLC) is a molecularly heterogeneous disease, with a variety of cell signaling pathways driving progression and therapeutic resistance. Although agents are available that target many of these critical pathways, there is currently no biologically-based method for selecting the best drug for a patient. Using reverse phase protein array (RPPA), a high-throughput technology that systematically measures key signaling proteins, we profiled forty-four NSCLC cell lines for markers of sensitivity and resistance to fifteen cytotoxic and targeted agents. RPPA is a quantitative, antibody-based assay that allows broad and simultaneous profiling of numerous therapeutically relevant targets from small amounts of protein, as is obtained from routine biopsy. Unlike gene expression arrays, RPPAs directly measure protein levels and can discern specific post-translational modifications such as phosphorylation or cleavage. The ability to compare levels of phosphorylated versus non-phosphorylated proteins is particularly critical to determining the activity of signaling proteins such as tyrosine kinases. Methods: The drug concentration required for 50% growth inhibition (IC_{50}) was determined for 44 cell lines using MTS assays. For the RPPA, serial dilutions of pre-treatment cell lysates were printed on nitrocellulose-coated glass slides, and each slide incubated with one of 59 validated, monospecific antibodies. A single, representative logarithmic value for the signal intensity-serial dilution curve was then determined for each sample, representing the quantitative measure of a specific protein. Results: Subsets of sensitive and resistant cell lines were identified for each drug, despite most cell lines having never been exposed to any treatment either in the patient from which they were derived or in vitro. When subjected to unsupervised clustering, mechanistically-related drugs grouped together (such as taxanes, platinum agents, and epidermal growth factor receptor inhibitors), with similar patterns of protein expression characterizing sensitivity or resistance. For example, resistance to cisplatin and carboplatin was associated with increased expression of cell adhesion molecules beta-catenin and E-cadherin and with Rab25, a GTPase previously correlated with worse outcome in breast and ovarian cancer. Cell lines treated with pemetrexed showed the greatest variation in IC_{50}'s, with a 1000-fold difference between sensitivity and resistance in 42 of the cell lines. Pemetrexed resistance was strongly associated with increased phospho-Rb (pRb) relative to Rb expression and with increased PKCalpha.

2008 AACR Annual Meeting
April 12-16, 2008
San Diego, CA

Print this Page for Your Records Close Window

Abstract Number:	3737
Session Title:	Imaging in Preclinical and Clinical Therapeutics
Presentation Title:	Using quantum dots to examine dynamic relocalization of EGFR, E-cadherin, and β-catenin in lung cancer cells upon treatment with EGFR-TKI
Presentation Start/End Time:	Tuesday, Apr 15, 2008, 8:00 AM -12:00 PM
Location:	Exhibit Hall B-F, San Diego Convention Center
Poster Section:	14
Poster Board Number:	17
Author Block:	*Donghai Huang, Ling Su, Xianghong Peng, Hongzheng Zhang, Fadlo Khuri, Dong M. Shin, Zhuo (Georgia) Chen.* Winship Cancer Institute of Emory University, Atlanta, GA

Quantum dots (QDs) provide sharper fluorescent signals than organic dyes and can detect multi-biomarkers simultaneously in the same material, allowing quantification and correlation of molecular signature with cellular response to targeted therapies. Recent data showed that cancer cells resistant to epidermal growth factor receptor-tyrosine kinase inhibitor (EGFR-TKI) expressed low level of E-cadherin (E-cad). However, the relationship between EGFR and E-cad in response to EGFR-TKI has not been well studied. In this study, we developed methods to detect E-cad, EGFR, and β-catenin simultaneously by using secondary antibodies- or streptavidine-conjugated QDs with 3 different emission wavelengths (QD565, QD605, and QD655) and compared cellular distribution of EGFR, E-cad, and β-catenin between EGFR-TKI sensitive (H292, H322) and resistant (H1703, H460) lung cancer cell lines. Relocalization of EGFR, E-cad, and β-catenin upon treatment with the EGFR-TKI erlotinib (0.5 - 2.5 μM) in the presence of EGF (100ng/ml) was also examined. The QD signals were quantified by CRi Nuance multi-spectral and/or Zeiss LSM 510 META confocal imaging system. The dynamic internalization of EGFR observed in the QD staining was confirmed by fluorescence-activated cell sorting (FACS). Our results showed that QD-based immunolabeling simultaneously detected EGFR, E-cad, and β-catenin signals. In the EGFR-TKI sensitive cells, EGFR, E-cad, and β-catenin were expressed mainly on the cell membrane, while in the resistant cells they were located mainly in the cytoplasm with reduced intensity. After induction with EGF, both EGFR and E-cad internalized to the cytoplasm, but the internalization signal in the EGFR-TKI sensitive cells was 2-4-fold greater than that in the resistant cells. Erlotinib at 0.5μM inhibited EGFR internalization up to 75%-85% in the EGFR-TKI sensitive cells as compared with the untreated control, whereas in the EGFR-TKI resistant cells the inhibition was only 10%-11%. Quantification also showed that in the EGFR-TKI sensitive cells, EGF induced E-cad internalization and reduced total levels of E-cad from 909±119.4 au (fluorescence intensity) to 586±119.3 au. In the EGFR-TKI resistant cells, the level of total E-cad was much lower than that in the sensitive cells (165±34.7 au). Addition of EGF neither induced internalization nor reduced the total level of E-cad. Our results suggest that there are substantial differences between EGFR-TKI sensitive and resistant cancer cells in EGFR and E-cad expression and localization both at the basal level and in response to EGF and EGFR-TKI. QD-based analysis of these differences facilitates understanding of the mechanism of resistance to EGFR-targeted therapy and can be used in the prediction of response during treatment. (Supported by DOD grant W81XWH07-1-0306 P5 to ZC and GCC Distinguished Scholar Award to FRK, DMS, and ZC).

2008 AACR Annual Meeting
April 12-16, 2008
San Diego, CA

Using Quantum Dots to Examine Dynamic Relocalization of EGFR and E-cadherin in Lung Cancer Cells upon Treatment with EGFR-TKI

Dong-hai Huang, Ling Su, Xiang-hong Peng, Hongzheng Zhang, Fadlo R. Khuri, Dong M. Shin, Zhuo (Georgia) Chen
Department of Hematology & Medical Oncology, Winship Cancer Institute, Emory University, Atlanta, GA

EMORY

EMORY UNIVERSITY
WINSHIP CANCER INSTITUTE

Abstract

Quantum dots (QDs) provide sharper fluorescent signals than organic dyes and can detect multi-biomarkers simultaneously in the same material, allowing quantification and correlation of molecular signature with cellular response to targeted therapies. Recent data showed that cancer cells resistant to epidermal growth factor receptor-tyrosine kinase inhibitor (EGFR-TKI) expressed low levels of E-cadherin (E-cad). However, the relationship between EGFR and E-cad in response to EGFR-TKI has not been well studied. In this study, we developed methods to detect E-cad and EGFR in the same cell samples simultaneously by using secondary antibodies-conjugated QDs with two different emission wavelengths (QD565 and QD605), and compared cellular distribution of EGFR and E-cad between EGFR-TKI sensitive (H292, H322) and insensitive (H1703, H460) lung cancer cell lines. Relocalization of EGFR and E-cad upon treatment with the EGFR-TKI erlotinib in the presence of EGF (100ng/ml) was also examined. The QD signals were quantified by Olympus Microscope 1×71 with CRi Nuance multi-spectral imaging and quantifying system. The dynamic internalization of EGFR observed in the QD staining was confirmed by fluorescence-activated cell sorting (FACS). Our results showed that QD-based immunolabeling simultaneously detected EGFR and E-cad signals. In the EGFR-TKI sensitive cells, EGFR and E-cad were expressed mainly on the cell membrane, while in the insensitive cells they were located mainly in the cytoplasm with reduced intensity. After induction with EGF, both EGFR and E-cad internalized to the cytoplasm, but the internalization capability in the EGFR-TKI sensitive cells was 1.49~1.67-fold greater than in the insensitive cells. Erlotinib at 0.5μM inhibited EGFR internalization up to 63.6%-48.4% in the EGFR-TKI sensitive cells as compared with the untreated control, whereas in the EGFR-TKI insensitive cells the inhibition was only 10.0%-11.5%. Quantification also showed that in the EGFR-TKI sensitive cells, EGFR induced E-cad internalization and reduced total levels of E-cad fro 0.574±0.052 a.u. (fluorescence average signal intensity per exposure time (ms)) to 0.077±0.021 a.u. In the EGFR-TKI insensitive cells, the level of total E-cad was much lower than that in the sensitive cells. Addition of EGF neither induced internalization nor reduced the total level of E-cad. Our results suggest that there are substantial differences between EGFR-TKI sensitive and insensitive cancer cells in EGFR and E-cad expression and localization both at the basal level and in response to EGF and EGFR-TKI. QD-based analysis of these differences facilitates understanding the mechanism of resistance to EGFR-targeted therapy and can be used in the prediction of response during treatment.

(Supported by DOD grant W81XWH-07-1-0306 Project 5 and GCC Distinguished Scholar Award to FRK, DMS, and ZC).

Study Aims

- To examine the localization of EGFR and E-cad simultaneously by using QD-based immunocytochemistry, and to develop a quantification method for the signal of QDs by Olympus Microscope 1×71 with CRi Nuance spectral imaging and quantifying system.
- To learn the internalization of EGFR and relocalization of E-cad simultaneously by using QD-based immunocytochemistry after stimulation with EGF, and the difference in effect of Erlotinib on the EGF-induced internalization between EGFR-TKI sensitive lung cancer cell lines (H292 and H322) and insensitive lung cancer cell lines (H1703 and H460).
- To confirm EGFR internalization in lung cancer cells by fluorescence-activated cell sorting (FACS), and to compare the results from FACS to those obtained from the QD quantification method.

Methods

1. QD-based immunocytochemistry: After starving the cells for 24 hours, the cells were incubated with Erlotinib for 2 hours and then stimulated with EGF for 30 minutes at 37°C. After a fixation, the cells were incubated with primary antibodies against E-cad and EGFR and then QD-2nd-antibodies (QD 565 and QD 605 from Invitrogen Corporation, Carlsbad, CA) in a cocktail solution for QDs-immunocytochemistry. (Figure 1)

2. Quantification of QDs signal: Olympus Microscope 1×71 with CRi Nuance spectral imaging and quantifying system was used to observe and quantify the QD signal (Figure 2). For QDs quantification, average membrane QDs signal was obtained by CRi Nuance software from manual quantification of 5 randomly selected fields in the slides. Average signal of each QDs was recorded. Relative of internalization was defined as [1-(membrane EGFR with EGF/membrane EGFR without EGF]×100%.

3. FACS analysis: After starving the cells for 24 hours, Erlotinib was added to the cells 2 hours before stimulation with EGF-fluorescence 488. Acetic acid at 0.2M was used to remove the uninternalized membrane receptor. Then EGFR internalization was examined with FACS. Relative of internalization was defined as (FITC+ cells / total cells)×100%.

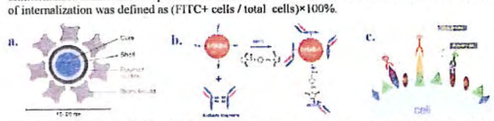

Fig. 1 Introduction of QDs-2nd-antibody-conjugates. a. Construction of QD (adapted from Invitrogen); b. QD conjugation to 2nd antibody fragments via disulphide and sulfhydryl-amine coupling; c. Immunocytochemistry by using QDs-2nd-antibody-conjugates.

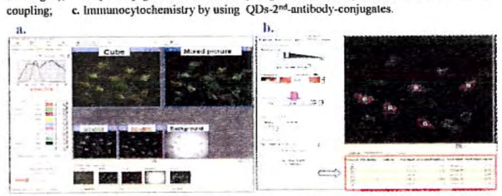

Fig. 2 Introduction of Olympus Microscope 1×71 with CRi Nuance spectral imaging and quantifying system. a. Obtaining the separated and the combined QDs signal after taken cube, established spectral library, and unmixed the cube; Two QDs signals were illustrated as an example (QD565 for E-cad, QD605 for EGFR); Removed background for accurate quantification of the QDs signals. b. Quantification of the QDs signal on cellular membrane manually by Nuance software.

Results

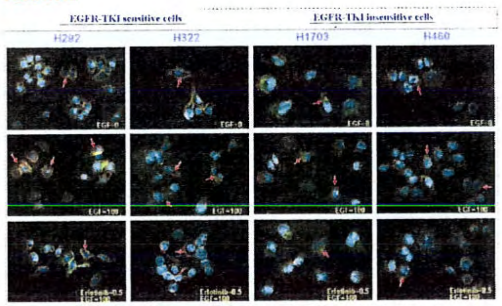

Fig. 3 Merged Image of E-cad (QD565, green) and EGFR (QD605, red) by Olympus Microscope 1×71 with CRi spectral imaging and quantifying system. E-cad and EGFR expression can be detected and localization of the two proteins can be tracked with different florescent signals simultaneously. In EGFR-TKI sensitive H292 and H322 cells, EGFR and E-cad expressions were detected mainly on the cellular membrane in the absence of EGF. EGF induced internalization of both EGFR and E-cad, which could be inhibited by Erlotinib in these cells. In contrast, in EGFR-TKI insensitive cells, these dynamic changes were not clearly observed due to low expression or cytoplasmic distribution of the both proteins.

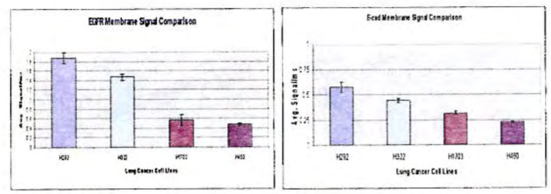

Fig. 4 Comparison of EGFR and E-cad membrane signals between EGFR-TKI sensitive and insensitive lung cancer cell lines quantified by CRi Nuance system. Average signal of each QD on membrane was quantified manually with CRi Nuance software. EGFR and E-cad levels were detected higher on cellular membrane in EGFR-TKI sensitive cell lines (H292 and H322) than those in EGFR-TKI insensitive cell lines (H1703 and H460).

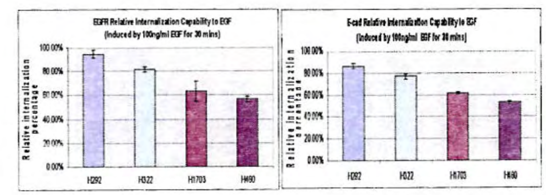

Fig. 5 Comparison of EGFR and E-cad internalization induced by EGF between EGFR-TKI sensitive and insensitive lung cancer cell lines by CRi Nuance system. EGFR-TKI sensitive cell lines (H292, H322) are more responsible for EGF induced EGFR and E-cad internalization than the EGFR-TKI insensitive cell lines (H1703 and H460).

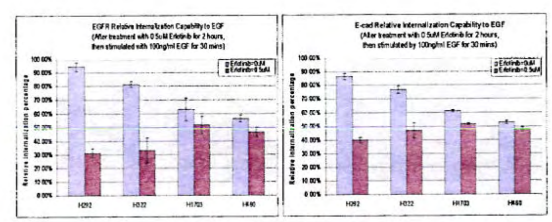

Fig. 6 Comparison of EGFR and E-cad relative internalization induced by EGF with or without Erlotinib between EGFR-TKI sensitive and insensitive lung cancer cell lines by CRi Nuance system. Erlotinib-mediated inhibition of EGF-induced EGFR and E-cad internalization is stronger in EGFR-TKI sensitive cells (H292 and H322) than that in EGFR-TKI insensitive cells (H1703 and H460).

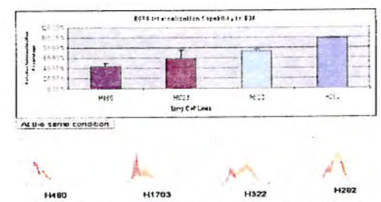

Fig. 7 Comparison of EGFR relative internalization induced by EGF between EGFR-TKI sensitive and insensitive lung cancer cell lines by FACS. FACS confirmed the quantification results by QDs-immunocytochemistry that EGF-induced EGFR internalization in EGFR-TKI sensitive cells (H292 and H322) was stronger than that in EGFR-TKI insensitive cells (H1703 and H460).

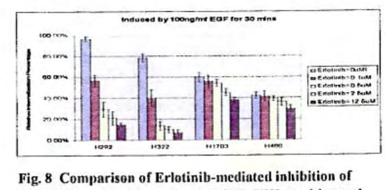

Fig. 8 Comparison of Erlotinib-mediated inhibition of EGFR internalization between EGFR-TKI sensitive and insensitive lung cancer cell lines using FACS method. EGFR-TKI sensitive cells (H292 and H322) were more sensitive to Erlotinib-mediated inhibition of EGF-induced EGFR internalization than the insensitive cells (H1703 and H460). Erlotinib at 0.5μM was enough to achieve more than 60% of the inhibition in the EGFR-TKI sensitive cells.

Conclusions

- Bioconjugated QDs can be used for multiplexed staining and image processing to localize each of proteins at the same time. Furthermore, their signals can be quantified simultaneously to profile biomarkers for correlating response to therapy.

- There are substantial differences between EGFR-TKI sensitive and insensitive cancer cells in EGFR and E-cad expression and localization both at the basal level and in response to EGF and EGFR-TKI.

NON-SMALL CELL LUNG CANCER PATIENT SURVIVAL WHEN ASSESSED AS A FIRST ORDER NONLINEAR PROCESS: EFFECT OF THERAPY AND STAGE

David J. Stewart

University of Texas MD Anderson Cancer Center

Send reprint requests to:

David J. Stewart, MD, FRCPC

Professor of Medicine

Deputy Chair, Department of Thoracic/Head & Neck Medical Oncology

University of Texas MD Anderson Cancer Center

1515 Holcombe Blvd, Unit 432

Houston, TX 77030

Telephone: (713) 692-6363

Fax: (713) 796-8655

E-mail: dstewart@mdanderson.org

Key words: log-linear plots, nonlinear regression analysis, non-small cell lung cancer

Running Title: NSCLC survival as a first-order process

Acknowledgements: This work was conducted under the auspices of the Lung Cancer Program of MD Anderson Cancer Center, and was supported in part by Cancer Center Support Grant number 5-P30 CA16672-32 and by Department of Defense grant number W81XWH-07-1-0306

ABSTRACT

Background: With first order kinetics, inflection points on semilog plots imply different limiting processes.

Methods: Kaplan-Meier overall and progression-free survival curve heights from selected NSCLC publications were measured manually. Nonlinear exponential decay was assessed using GraphPad Prism.

Results: Our preliminary observations, if confirmed, would suggest the following: *Palliative front-line chemotherapy:* Twelve of 15 curves for untreated controls and single agents were fit by 2-3-phase decay models while 42 of 48 curves for multidrug regimens were fit only by one-phase models. Rapid-decay-phase curves were convex in 0% vs 54%, respectively ($p<0.001$). The paucity of inflection points suggests outcome is driven primarily by continuous variables. Hence, individual patient outcome might be predicted better using continuous variables than by dichotomizing variables. Curve convexities suggest discontinuation of combination chemotherapy after 4-6 cycles "synchronizes" patient death. Characterizing patients dying along the leading convex edge might identify subgroups that would benefit from maintenance therapy. *Adjuvant Chemotherapy:* Overall half-life was longer with adjuvant chemotherapy than with matched controls ($p=0.03$), apparently more from a shift of rapid-phase patients into the potentially-cured slow-decay-phase fraction than from prolongation of survival of patients who die despite therapy. *Stage:* Two-phase-decay curves predominated for stage II-IV populations. Rapid-decay-phase half-life shortened while rapid-phase size increased with increasing stage ($p<0.04$), suggesting molecular characteristics that drive tumor cell growth rates determine not only patient survival time but also stage at presentation.

Conclusions: Future studies will explore adaptations of mixture distribution or nonlinear mixed effects modelling using individual patient data for multivariate nonlinear exponential decay survival analyses.

INTRODUCTION:

Survival analyses in cancer clinical trials generally use Kaplan-Meier plots in reporting survival. Differences between groups are generally assessed by comparing median overall survival time (OS), progression-free survival time (PFS), proportion of patients alive at a particular time (eg, 1 year) or by calculating hazard ratios, etc.

Biological processes such as drug disappearance[1] and enzymatic reactions[2] may follow first order kinetics, with disappearance of a given proportion of remaining drug, substance, etc, in a given time, rather than there being disappearance of a given quantity of substance per unit time. For processes such as drug disappearance that follow first order kinetics, plotting linear effect vs time will give a curved line, while plotting log effect vs time will give a straight line, and the slope of the line can be used to calculate the half-life[1]. In pharmacokinetic (PK) analyses, presence of an inflection point in the log-linear curve indicates a distinct process driving the rate of drug disappearance. For example, the rate of drug disappearance during the initial portion of the curve (the "distribution phase") is driven by drug uptake into tissues, the second portion (following the first inflection point) may be driven by metabolism/excretion, and the third portion (following a second inflection point) may be driven by saturation of metabolism/excretion processes, by redistribution of drug from tissues to blood, etc[1]. Additional inflection points and curve segments may also occur with some biological processes.

We hypothesized that patient survival variables may in many instances also follow first order kinetics, and in these instances, plotting log % OS, PFS, etc vs time should give a straight line. We hypothesized that dichotomous variables that drive prognosis (eg, variables that are present vs absent or that are above vs below a threshold) would give an inflection point on a plot of log % OS or PFS, etc, vs time in the same manner that different processes give inflection points on a PK curve, while continuous variables that affect prognosis would alter the slope of the survival curve without giving an inflection point. If these hypotheses were correct, then inflection points on semilog plots of survival variables could give insight into the minimum number of dichotomous variables that are driving prognosis, and nonlinear regression analyses analogous to compartmental PK analyses might permit one to define the proportion of the initial population accounted for by each subgroup and the half-life of each distinct subgroup.

With respect to standard analyses that use similar approaches, proportional hazards models generally average the entire curve, without deriving specific information from curve inflection points. Nonlinear mixed effects modelling[3] and mixture distribution analyses[4-6] have been used to estimate proportion of patients cured of a malignancy, and there is at least a limited experience using them to assess impact of therapy or prognostic variables[5, 7, 8].

In this manuscript, we used nonlinear regression exponential decay analyses of Kaplan-Meier OS and PFS curves from published non-small cell lung cancer (NSCLC) clinical trials as a preliminary feasibility assessment of the potential utility of such approaches in assessment of impact of treatment and prognostic variables on patient outcome. In embarking on the exercise, we anticipated that we would detect multiple inflection points on most curves, in keeping with there being several dichotomous variables driving prognosis.

METHODS:

In this preliminary feasibility assessment, we used OS and PFS curves from selected NSCLC published trials involving front-line chemotherapy in advanced disease[9-26], adjuvant chemotherapy in resected stage I-III disease[12, 27-37] and survival as a function of stage[10, 12, 20, 26-30, 32-44], and also used curves from best supportive care arms from 2 second line therapy trials[45, 46]. From printouts of these survival curves, height of curve above baseline was measured in mm for different time points from initiation of therapy. Height for each time point was converted to a percent of the curve height at time 0. We then used one-phase, 2-phase and 3-phase exponential decay programs in GraphPad Prism version 5.0 to model the data. The value of Y at time = 0 was set as a constant at 100% and the plateau phase (ie, the value of Y at time = infinity) was set as a constant at 0%. Curves were considered to conform to a one-phase model rather than a two-phase model (or to a two-phase model rather than a three-phase model) if one of the phases accounted for <1% of the patient population, or if half-lives for two phases differed by <10%.

Across studies, the median percent of patients in each decay phase and the median half-life of the rapid-decay phase were calculated for different groups. Groups were compared using Wilcoxon signed rank tests for matched groups (patients treated with adjuvant therapy vs control groups from the same study), and Kruskal-Wallis testing was used for comparisons of non-matched groups. Chi-square testing with Yates correction was used to compare groups with respect to proportion of curves fit by 2-3 phase decay models vs proportion fit by only one phase decay models, and with respect to proportion of curves with major convexities.

RESULTS:

Some typical curve shapes are outlined in Figure 1. Of 172 OS or PFS curves analyzed, 72 (42%) were fit by one-phase exponential decay models, 92 (53%) were fit by two-phase exponential decay models (single inflection point) and 8 (5%) were fit by three-phase exponential decay models (two inflection points). In Table 1 are characteristics of exponential decay curves for different patient groups. The total number in the table exceeds 172 since some curves were included both in assessments of effect of stage as well as assessment of effect of therapy.

Many of the curves had small shoulders at early follow-up time points. For OS, these small shoulders were probably related in part to selection of patients with relatively good performance status. For PFS, the small shoulders may have been related primarily to the fact that first re-evaluation of tumor status generally didn't occur until 6-8 weeks after therapy initiation. Refitting the data after omitting points on the early shoulder in most cases did not alter conclusions about number of curve inflection points (data not shown).

Overall, 41 of the curves (24%) had substantially more than just an initial shoulder, and appeared to be convex over much of the rapid decay phase. Examples are presented in Figure 2. Curve characteristics varied with therapy (Table 2). In patients on front-line chemotherapy trials for advanced disease, 12 of 15 (80%) OS or PFS curves from patients receiving best supportive care or single agent chemotherapy could be fit by 2-3 phase decay models, compared to only 6 of 48 (12.5%) curves from patients treated with regimens involving 2 or more agents ($p<0.001$). The proportion of curves fit by only a single phase decay model increased with the number of agents used in therapy. In addition, 54% of curves from patients treated with regimens involving ≥ 2

agents appeared to have convex rapid decay phases, compared to none of 15 curves for patients treated with best supportive care or single agent therapy (p<0.001).

Proportion of patients in the rapid-decay phase and rapid-decay phase half-lives for different patient groups are presented in Table 3. For 2- and 3-phase decay curves, the models frequently hit constraints with respect to the half-life of the slow-decay phase, and the slow-decay phase half-lives were generally very long with very wide 95% confidence intervals, and hence are not presented in this preliminary analysis. For curves that could be fit by either a 2- or 3-phase-decay model, data from the 2-phase-decay model were used for Table 3 and for the accompanying analyses. In therapy of advanced disease, the rapid-decay phase was larger, but the alpha half-life was longer with regimens involving $\geq$ 2 agents than with best supportive care or with single agent therapy, in keeping with the high proportion of curves from patients treated with multi-agent regimens that could be fit with only one-phase decay models.

With adjuvant chemotherapy, there was a smaller PFS rapid-decay phase with adjuvant chemotherapy than in control groups and a trend towards a smaller OS rapid-decay phase. Median alpha half-life (ie, half-life of the rapid-decay phase) was slightly longer with adjuvant chemotherapy for both OS and PFS, although this was not statistically significant. When one-phase exponential decay half-lives were calculated for OS and PFS from curves in studies of adjuvant chemotherapy vs matched controls, both OS and PFS half-lives were significantly longer in the adjuvant groups than in the matched control groups (Table 4).

With respect to stage, 6 of 10 (60%) OS curves from stage I untreated patients were best fit by one-phase decay models, compared to 4 of 22 (18%) OS curves from stage II-IV untreated patients (Table 1). Hence, stage I curves tended to be characterized by one-phase decay with very long half-life. For stages II-IV, the proportion of patients in the rapid decay phase increased and the half-life of the rapid decay phase decreased with increasing stage (Table 4).

DISCUSSION:

This preliminary assessment suggests that it may be feasible to use nonlinear exponential decay analysis to assess patient survival variables, and it also suggests that specific hypotheses may be generated by this approach, such as the ones outlined below. It is stressed that substantially more work will be needed to determine whether or not our observations were driven solely by methodology-related artefact, but the results suggest that adaptations of procedures such as mixture distribution analyses and nonlinear mixed effects modelling to permit nonlinear exponential decay analysis of censored individual patient data could potentially provide useful insights that might not be as apparent with more usual survival analysis approaches.

We had expected that we would routinely detect multiple inflection points on the curves, and we found substantially fewer inflection points than anticipated. The sparseness of curve inflection points suggests to us that most prognostic variables function as continuous variables affecting curve slope, rather than functioning as dichotomous variables that slot a patient into a specific patient subgroup. Hence, apparently dichotomous prognostic variables like gender may simply be surrogates for various continuous variables. Even with prognostic variables that are known to be continuous, it is common practice to dichotomize them around a cut-point. While this dichotomization may be useful in helping identify factors with prognostic significance, the paucity of survival curve inflection points would lead us to hypothesize that models that use continuous variables would do a better job of predicting outcome of individual patients than would models that dichotomize prognostic variables. For example, in NSCLC, it may be useful to consider actual tumor size rather than whether it is T1 (<3 cm diameter) or T2 (> 3cm), to consider number and bulk of nodes involved rather than just grouping them as N0 to N3, and to explore use of some measure of hormonal status rather than simply grouping patients as male vs female. Clinicians generally prefer to have simple "yes-no" rules in deciding management approaches, but it may be time to consider moving beyond this.

The higher proportion of advanced disease studies with curves conforming to one-phase decay curves when ≥ 2 drugs are used compared to when 0-1 drugs are used and when compared to assessments of impact of stage or effect of adjuvant chemotherapy for early stage disease could have arisen by chance, by inclusion of more than one curve from some studies, or through observer bias. However, one biologically plausible hypothesis that could explain it is that the routine practice of discontinuing chemotherapy after 3-6 cycles may be synchronizing patient death. Randomized trials have generally failed to identify a benefit of continuing chemotherapy beyond this point[47-50], but it is possible that there may be specific subpopulations that would benefit, and some studies of maintenance chemotherapy have suggested that it may be of benefit in some patients[51]. It would be of interest to assess tumor molecular characteristics and clinical features for patients dying along the leading edge of the convexity to determine if one might identify such a specific subpopulation that would benefit from maintenance chemotherapy.

Adjuvant chemotherapy was associated with longer OS and PFS half-lives compared to controls when only one-phase exponential decay models were used, in keeping with randomized trials[27, 37] and meta-analyses[52] that indicate a benefit of adjuvant chemotherapy in resected NSCLC. When we used for each study the model with the largest number of phases that could be fit successfully, adjuvant therapy (compared to untreated matched controls) was associated with a significant reduction in the proportion of patients in the rapid decay phase for PFS and a similar trend for OS. This suggests that the adjuvant chemotherapy is actually shifting patients into the cured fraction and not just prolonging survival. The slight trend towards prolongation of the alpha half-life would suggest that it also may be somewhat prolonging survival of patients who are not cured.

While proportion of patients in the rapid-decay phase decreased from stage II to stage IV, it was high in stage I patients. This is probably due to insufficient follow up time in several of the stage I studies to permit detection of a slower decay phase. The shortening of the alpha half-life as one goes from stage I to stage IV disease and the increase in proportion of patients in the rapid decay phase as one goes from stages II through IV suggests that molecular characteristics associated with rapid tumor cell growth increase the proportion of patients who are destined to die of disease while at the same time decreasing survival time of those who eventually die of NSCLC. Hence, one might hypothesize that a patient with recurrent stage I NSCLC would have more indolent disease than would a patient with equal bulk disease that was stage IV at presentation, and that the two would tend to have different molecular characteristics and possibly different treatment susceptibilities. In addition, this would suggest that molecular characteristics drive both prognosis and stage-ie, a patient with relatively indolent disease might tend to have it discovered when it was still in an early stage since it would stay at an early stage longer, while patients with more rapidly growing disease would be less likely to have the disease discovered by chance while it was still early stage. Hence, this is in keeping with the concept that stage at presentation is a surrogate for tumor cell growth rate in addition to being a surrogate for presence of micrometastatic disease, and that tumor cell molecular characteristics will eventually supplant stage as the important determinant of tumor management strategies.

Adaptations of methods such as mixture distribution or nonlinear mixed effects modelling to assess exponential survival decay using individual patient data could prove useful in a variety of ways. Instead of just assessing the impact of a prognostic or treatment variable on outcomes such as median survival or percent survival at a specific time, these approaches could potentially be used to assess impact of the variables on a variety of individual outcome components such as proportion of patients shifted from a poor outcome groups to better outcome groups, half-life of each subgroup, etc. It could also be used to estimate maximum achievable survival time for members of each subgroup, proportion of the total population accounted for by each subgroup at different time points along the survival curve, and time beyond which one may have a relatively homogeneous population of good prognosis patients. This ability to predict the point at which the population becomes homogeneous could be particularly useful in helping identify molecular factors associated with good prognosis. We plan to explore this further using individual patient data.

Table 1. Characteristics of exponential decay curves for different patient groups					
	No. Curves				
	1 phase decay	2 phase decay	3 phase decay	Rapid Phase Curve Convexity[a]	
				Yes	No
Front Line Chemotherapy for Advanced Disease:					
Overall survival:					
Best supportive care[b]	1	4	1	0	6
Single agent	2	3	0	0	5
Two-drug regimen	22	4	2	13	15
$\geq$ Three-drug regimen	7	0	0	5	2
Progression-free survival:					
Best supportive care[c]	0	2	0	0	2
Single agent	0	1	0	0	1
Two-drug regimen	11	0	0	6	5
$\geq$ Three-drug regimen	2	0	0	2	0
Adjuvant Chemotherapy for Stage I-III Resected Disease:					
Overall survival:					
Adjuvant chemotherapy	6	17	1	5	19
Control	8	12	1	3	18
Progression-free survival:					
Adjuvant chemotherapy	1	11	2	1	13
Control	1	11	0	0	12
Stage[d]:					
Overall survival:					
Stage I	6	5	0	1	10
Stage I-II[e]	0	1	0	0	1
Stage I-III[e]	1	8	0	0	9
Stage II	1	6	1	2	6
Stage III	2	6	2	2	8
Localized, incomplete resection	0	1	0	0	1
Stage IV	1	4	1	1	5
Progression-free survival:					
Stage I	1	1	0	0	2
Stage I-II[e]	0	1	0	0	1
Stage I-III[e]	0	2	0	0	2
Stage II	0	1	0	0	1
Stage III	0	2	0	0	2
Localized, incomplete resection	0	5	0	0	5
Stage IV	0	2	0	0	2
Other subgroup analyses:					
Overall survival	10	10	1	3	18
Progression-free survival	0	2	0	0	2

a. Convexity that is more that simply a shoulder on the initial part of the curve
b. Includes 2 curves from best supportive care arms of studies of second line therapies
c. Includes 1 curve from best supportive care arm of a study of second line therapy
d. From publications on survival vs stage and from control arms of adjuvant studies and best supportive care arms of studies of chemotherapy for advanced disease
e. Not broken down by individual stage

Table 2. Effect of therapy details on curve characteristics			
No. drugs	No. curves	No. with 2-3 phase decay[a]	No. with convexity[a]
0	8	7	0
1	7	5	0
2	39	6	19
≥ 3	9	0	7

a. $p < 0.001$ for 0-1 drugs vs ≥ 2 drugs (Chi-square with Yates correction)

Table 3. Comparison of proportion of patients in rapid-decay phase and rapid-decay-phase half-lives across groups.

Group	No. studies	% Rapid Decay Median	% Rapid Decay Range	p	Alpha half-life median	Alpha half-life range	p
First line chemotherapy for advanced NSCLC:							
OS: Best supportive care	6	96.7	82.6-100	0.006[a,b]	4.4	3.8-4.7	0.0008[a,b]
OS: Single Agent	5	94.8	66.4-100		4.9	1.5-7.1	
OS: Two Drugs	28	100	12.9-100		7.5	2.5-11.5	
OS: ≥ Three drugs	7	100	100-100		6.8	4.6-12.2	
PFS: Best supportive care	2	94.5	91.9-97.1	0.0019[a,b]	2.7	2.4-3.0	0.06[a,b]
PFS: Single Agent	1	14.6	-		2.2	-	
PFS: Two Drugs	11	100	100-100		3.9	3.2-5.2	
PFS: ≥ Three drugs	2	100	100-100		4.5	3.6-5.4	
Adjuvant chemotherapy vs control[e]:							
OS adjuvant chemo	24	89.3	1.3-100	0.12[c,d]	63.7	4.4-245.0	0.47[c,d]
OS controls	24	94.4	43.9-100		45.1	7.0-339.0	
PFS adjuvant chemo	13	68.2	29.9-100	0.02[c,d]	12.6	5.0-58.2	0.54[c,d]
PFS controls	13	85.0	44.0-100		10.9	5.1-98.6	
Survival by Stage[f]:							
OS: Stage I	11	100	40.6-100	0.23[a,b] (0.04[a,h])	105.6	15.3-339	0.0001[a,b] (0.0004[a,h])
OS: Stage I-II[g]	1	65.6	-		34.8	-	
OS: Stage I-III[g]	9	80.8	4.3-100		12.6	6.6-59.3	
OS: Stage II	8	79.1	49.4-100		19.1	12.7-58.5	
OS: Stage III	10	92.5	62.8-100		11.5	6.6-33.6	
OS: Stage IV	6	96.9	82.9-100		4.3	3.1-5.9	
PFS: Stage I	2	87.3	74.6-100	0.19[a,b]	69.4	40.1-98.6	0.13[a,b]
PFS: Stage I-II[g]	1	53.5	-		11.0	-	
PFS: Stage I-III[g]	2	33.7	23.3-44.0		8.5	6.1-10.9	
PFS: Stage II	1	72.0	-		13.2	-	
PFS: Stage III	2	77.5	77.5-85.0		8.0	6.0-10.0	
PFS: Stage IV	2	94.5	91.9-97.1		2.7	2.4-3.0	

a. Kruskal-Wallis
b. comparison across groups
c. Wilcoxon signed rank test
d. vs matched control group
e. Total numbers differ from Table 1 since control arms were included more than once here if compared to more than one chemotherapy arm from the same trial, while being included only once in Table 1. Total numbers differ from Table 3 since Table 3 included only single OS or PFS curves from each trial, while Table 4 also includes curves from subgroup analyses.

f. From studies on effect of stage or on untreated control arms from adjuvant therapy studies and studies of therapy for advanced disease
g. from studies for which data were not broken down by individual stages
h. comparison across stages II to IV

Table 4. Overall and progression-free survival half-lives with adjuvant chemotherapy for stage I-III disease[a]				
Group	No. Studies	Overall half-life		P
		Median	Range	
Overall survival:				
Adjuvant chemotherapy	13	61.9	20.2-299.0	0.0002[b]
Matched control	13	48.6	7.0-226.0	
Progression-free survival:				
Adjuvant chemotherapy	6	69.4	17.0-221.0	0.03[b]
Matched control	6	54.7	8.8-98.6	

a. Curves for adjuvant therapy compared to matched control curves, using half-lives derived from one-phase exponential decay models
b. Wilcoxon signed rank test comparing adjuvant therapy curve to matched control curve

Figure 1. Typical one-three phase decay survival curves showing both semilog plots and the corresponding linear plots

Figure 2. Examples of semilog plots with convex rapid phases (with and without a possible second phase), and corresponding linear plots

Figure 1. Representative curve types (linear vs semilog plots)

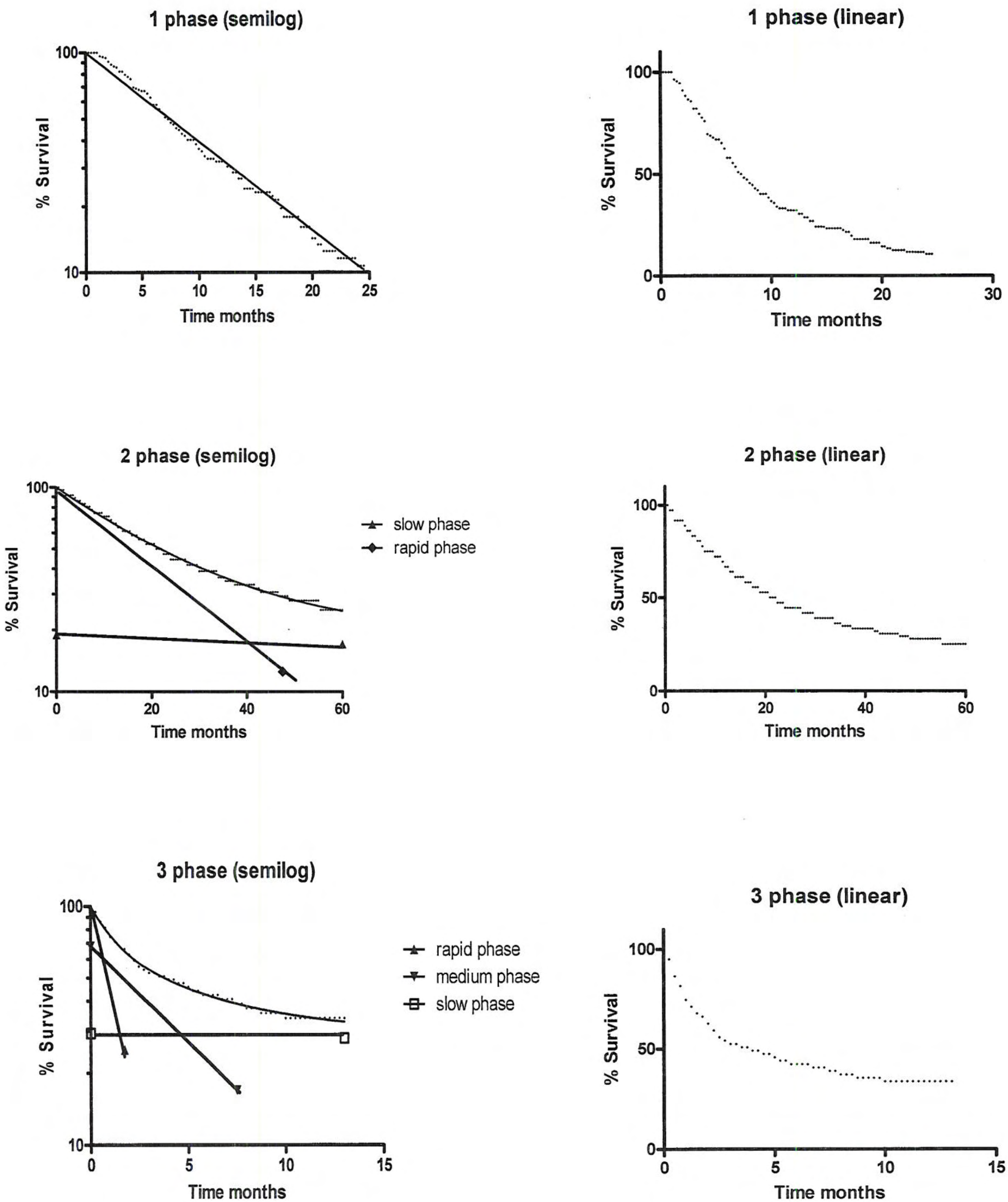

Figure 2. Examples of curves with convex rapid phase

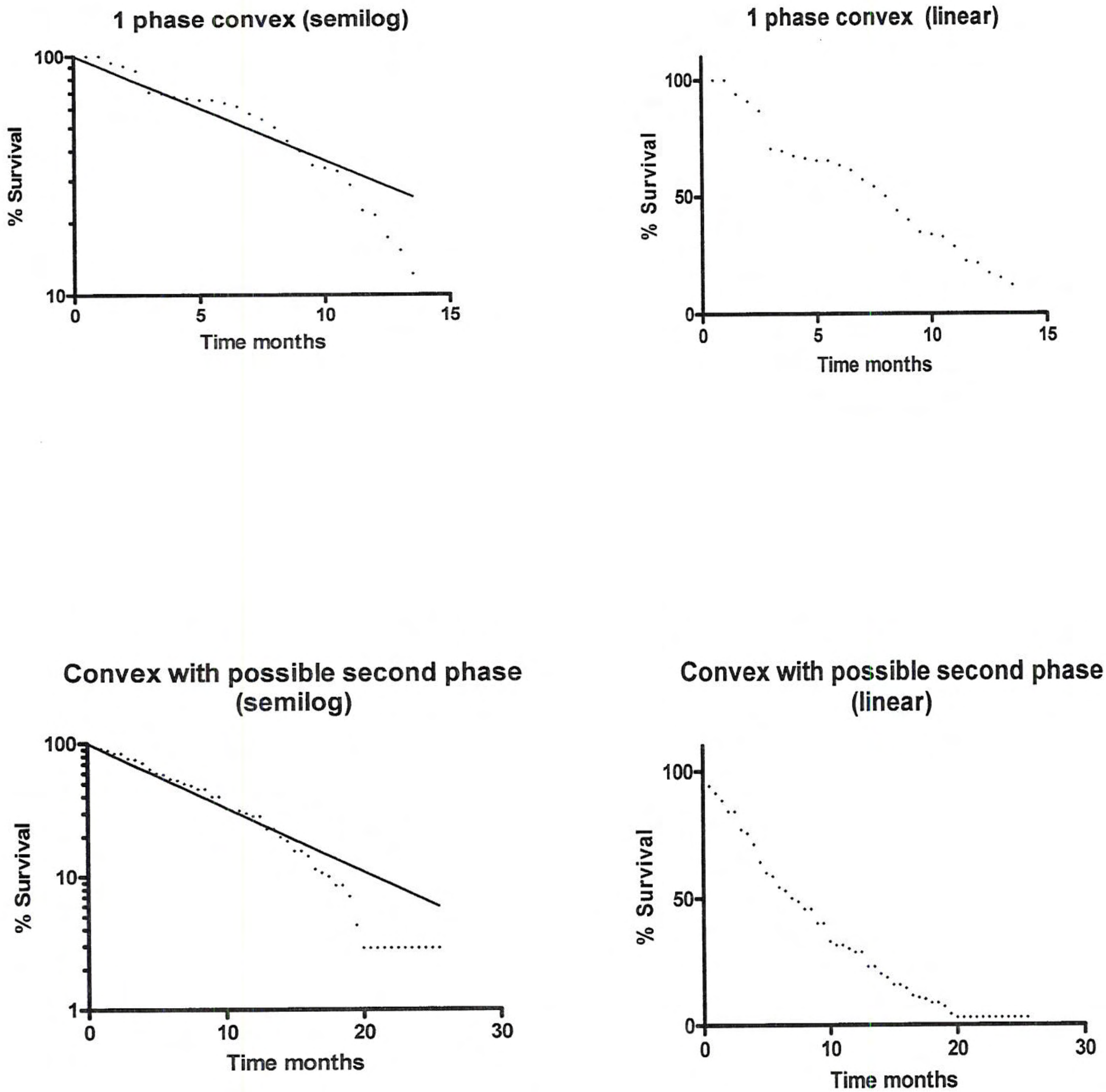

REFERENCES:

1. Benet L, Mitchell J, Sheiner L. Pharmacokinetics: The Dynamics of Drug Absorption, Distribution, and Elimination. In: Goodman Gilman A, Rall T, Nies A, Taylor P, eds. Goodman and Gilman's The Pharmacological Basis of Therapeutics. Eighth ed. New York, NY: Pergamon Press; 1990:3-32.
2. White A, Handler P, Smith E. Enzymes. II Kinetics, Inhibition, Metabolic Inhibitors, Control of Enzymatic Activity. In: White A, Handler P, Smith E, eds. Principles of Biochemistry. New York, NY: McGraw-Hill; 1968:223-46.
3. Law NJ, Taylor JM, Sandler H. The joint modeling of a longitudinal disease progression marker and the failure time process in the presence of cure. Biostatistics 2002;3(4):547-63.
4. Peng Y, Dear KB, Carriere KC. Testing for the presence of cured patients: a simulation study. Stat Med 2001;20(12):1783-96.
5. De Angelis R, Capocaccia R, Hakulinen T, Soderman B, Verdecchia A. Mixture models for cancer survival analysis: application to population-based data with covariates. Stat Med 1999;18(4):441-54.
6. Gordon NH. Application of the theory of finite mixtures for the estimation of 'cure' rates of treated cancer patients. Stat Med 1990;9(4):397-407.
7. McLean IW, Foster WD, Zimmerman LE. Uveal melanoma: location, size, cell type, and enucleation as risk factors in metastasis. Hum Pathol 1982;13(2):123-32.
8. Nie L, Chu H, Cole SR. A general approach for sample size and statistical power calculations assessing of interventions using a mixture model in the presence of detection limits. Contemp Clin Trials 2006;27(5):483-91.
9. Bonomi P, Kim K, Fairclough D, et al. Comparison of survival and quality of life in advanced non-small-cell lung cancer patients treated with two dose levels of paclitaxel combined with cisplatin versus etoposide with cisplatin: results of an Eastern Cooperative Oncology Group trial. J Clin Oncol 2000;18(3):623-31.
10. Buccheri G, Ferrigno D, Rosso A, Vola F. Further evidence in favour of chemotherapy for inoperable non-small cell lung cancer. Lung Cancer 1990;6:87-98.
11. Lilenbaum RC, Herndon JE, 2nd, List MA, et al. Single-agent versus combination chemotherapy in advanced non-small-cell lung cancer: the cancer and leukemia group B (study 9730). J Clin Oncol 2005;23(1):190-6.
12. Chemotherapy in non-small cell lung cancer: a meta-analysis using updated data on individual patients from 52 randomised clinical trials. Non-small Cell Lung Cancer Collaborative Group. Bmj 1995;311(7010):899-909.
13. Fossella F, Pereira JR, von Pawel J, et al. Randomized, multinational, phase III study of docetaxel plus platinum combinations versus vinorelbine plus cisplatin for advanced non-small-cell lung cancer: the TAX 326 study group. J Clin Oncol 2003;21(16):3016-24.
14. Fukuoka M, Masuda N, Furuse K, et al. A randomized trial in inoperable non-small-cell lung cancer: vindesine and cisplatin versus mitomycin, vindesine, and cisplatin versus etoposide and cisplatin alternating with vindesine and mitomycin. J Clin Oncol 1991;9(4):606-13.
15. Kelly K, Crowley J, Bunn PA, Jr., et al. Randomized phase III trial of paclitaxel plus carboplatin versus vinorelbine plus cisplatin in the treatment of patients with advanced non--small-cell lung cancer: a Southwest Oncology Group trial. J Clin Oncol 2001;19(13):3210-8.
16. Klastersky J, Sculier JP, Ravez P, et al. A randomized study comparing a high and a standard dose of cisplatin in combination with etoposide in the treatment of advanced non-small-cell lung carcinoma. J Clin Oncol 1986;4(12):1780-6.
17. Klastersky J, Sculier JP, Bureau G, et al. Cisplatin versus cisplatin plus etoposide in the treatment of advanced non-small-cell lung cancer. Lung Cancer Working Party, Belgium. J Clin Oncol 1989;7(8):1087-92.

18. Le Chevalier T, Brisgand D, Douillard JY, et al. Randomized study of vinorelbine and cisplatin versus vindesine and cisplatin versus vinorelbine alone in advanced non-small-cell lung cancer: results of a European multicenter trial including 612 patients. J Clin Oncol 1994;12(2):360-7.
19. Mylonakis N, Tsavaris N, Bacoyiannis C, et al. A randomized prospective study of cisplatin and vinblastine versus cisplatin, vinblastine and mitomycin in advanced non-small cell lung cancer. Ann Oncol 1992;3(2):127-30.
20. Rapp E, Pater JL, Willan A, et al. Chemotherapy can prolong survival in patients with advanced non-small-cell lung cancer--report of a Canadian multicenter randomized trial. J Clin Oncol 1988;6(4):633-41.
21. Rosso R, Ardizzoni A, Salvati F, et al. Etoposide v etoposide and cisplatin in the treatment of advanced non-small cell lung cancer: a FONICAP randomized study. Semin Oncol 1988;15(6 Suppl 7):49-51.
22. Sandler A, Gray R, Perry MC, et al. Paclitaxel-carboplatin alone or with bevacizumab for non-small-cell lung cancer. N Engl J Med 2006;355(24):2542-50.
23. Schiller JH, Harrington D, Belani CP, et al. Comparison of four chemotherapy regimens for advanced non-small-cell lung cancer. N Engl J Med 2002;346(2):92-8.
24. Shinkai T, Saijo N, Eguchi K, et al. Cisplatin and vindesine combination chemotherapy for non-small cell lung cancer: a randomized trial comparing two dosages of cisplatin. Jpn J Cancer Res 1986;77(8):782-9.
25. Veeder MH, Jett JR, Su JQ, et al. A phase III trial of mitomycin C alone versus mitomycin C, vinblastine, and cisplatin for metastatic squamous cell lung carcinoma. Cancer 1992;70(9):2281-7.
26. Woods RL, Williams CJ, Levi J, et al. A randomised trial of cisplatin and vindesine versus supportive care only in advanced non-small cell lung cancer. Br J Cancer 1990;61(4):608-11.
27. Arriagada R, Bergman B, Dunant A, Le Chevalier T, Pignon JP, Vansteenkiste J. Cisplatin-based adjuvant chemotherapy in patients with completely resected non-small-cell lung cancer. N Engl J Med 2004;350(4):351-60.
28. Douillard JY, Rosell R, De Lena M, et al. Adjuvant vinorelbine plus cisplatin versus observation in patients with completely resected stage IB-IIIA non-small-cell lung cancer (Adjuvant Navelbine International Trialist Association [ANITA]): a randomised controlled trial. Lancet Oncol 2006;7(9):719-27.
29. Imaizumi M. Postoperative adjuvant cisplatin, vindesine, plus uracil-tegafur chemotherapy increased survival of patients with completely resected p-stage I non-small cell lung cancer. Lung Cancer 2005;49(1):85-94.
30. Kato H, Ichinose Y, Ohta M, et al. A randomized trial of adjuvant chemotherapy with uracil-tegafur for adenocarcinoma of the lung. N Engl J Med 2004;350(17):1713-21.
31. The benefit of adjuvant treatment for resected locally advanced non-small-cell lung cancer. The Lung Cancer Study Group. J Clin Oncol 1988;6(1):9-17.
32. Nakagawa M, Tanaka F, Tsubota N, Ohta M, Takao M, Wada H. A randomized phase III trial of adjuvant chemotherapy with UFT for completely resected pathological stage I non-small-cell lung cancer: the West Japan Study Group for Lung Cancer Surgery (WJSG)--the 4th study. Ann Oncol 2005;16(1):75-80.
33. Olaussen KA, Dunant A, Fouret P, et al. DNA repair by ERCC1 in non-small-cell lung cancer and cisplatin-based adjuvant chemotherapy. N Engl J Med 2006;355(10):983-91.
34. Rosell R, Gomez-Codina J, Camps C, et al. A randomized trial comparing preoperative chemotherapy plus surgery with surgery alone in patients with non-small-cell lung cancer. N Engl J Med 1994;330(3):153-8.
35. Roth JA, Fossella F, Komaki R, et al. A randomized trial comparing perioperative chemotherapy and surgery with surgery alone in resectable stage IIIA non-small-cell lung cancer. J Natl Cancer Inst 1994;86(9):673-80.
36. Scagliotti GV, Fossati R, Torri V, et al. Randomized study of adjuvant chemotherapy for completely resected stage I, II, or IIIA non-small-cell Lung cancer. J Natl Cancer Inst 2003;95(19):1453-61.
37. Winton T, Livingston R, Johnson D, et al. Vinorelbine plus cisplatin vs. observation in resected non-small-cell lung cancer. N Engl J Med 2005;352(25):2589-97.
38. Betticher DC, Hsu Schmitz SF, Totsch M, et al. Prognostic factors affecting long-term outcomes in patients with resected stage IIIA pN2 non-small-cell lung cancer: 5-year follow-up of a phase II study. Br J Cancer 2006;94(8):1099-106.

39. Bonomi P, Faber L. Neoadjuvant chemoradiation therapy in non-small cell lung cancer: the Rush University experience. Lung Cancer 1993;9:383-90.
40. Gralla RJ. Preoperative and adjuvant chemotherapy in non-small cell lung cancer. Semin Oncol 1988;15(6 Suppl 7):8-12.
41. Lin E, Karp D. Color-matrix cancer staging and chemotherapy handbook. 2 ed. Houston, TX: The University of Texas M.D. Anderson Cancer Center; 2003.
42. Mountain CF. A new international staging system for lung cancer. Chest 1986;89(4 Suppl):225S-33S.
43. Wisnivesky JP, Yankelevitz D, Henschke CI. The effect of tumor size on curability of stage I non-small cell lung cancers. Chest 2004;126(3):761-5.
44. Wisnivesky JP, Henschke C, McGinn T, Iannuzzi MC. Prognosis of Stage II non-small cell lung cancer according to tumor and nodal status at diagnosis. Lung Cancer 2005;49(2):181-6.
45. Shepherd FA, Rodrigues Pereira J, Ciuleanu T, et al. Erlotinib in previously treated non-small-cell lung cancer. N Engl J Med 2005;353(2):123-32.
46. Thatcher N, Chang A, Parikh P, et al. Gefitinib plus best supportive care in previously treated patients with refractory advanced non-small-cell lung cancer: results from a randomised, placebo-controlled, multicentre study (Iressa Survival Evaluation in Lung Cancer). Lancet 2005;366(9496):1527-37.
47. von Plessen C, Bergman B, Andresen O, et al. Palliative chemotherapy beyond three courses conveys no survival or consistent quality-of-life benefits in advanced non-small-cell lung cancer. Br J Cancer 2006;95(8):966-73.
48. Westeel V, Quoix E, Moro-Sibilot D, et al. Randomized study of maintenance vinorelbine in responders with advanced non-small-cell lung cancer. J Natl Cancer Inst 2005;97(7):499-506.
49. Smith IE, O'Brien ME, Talbot DC, et al. Duration of chemotherapy in advanced non-small-cell lung cancer: a randomized trial of three versus six courses of mitomycin, vinblastine, and cisplatin. J Clin Oncol 2001;19(5):1336-43.
50. Buccheri GF, Ferrigno D, Curcio A, Vola F, Rosso A. Continuation of chemotherapy versus supportive care alone in patients with inoperable non-small cell lung cancer and stable disease after two or three cycles of MACC. Results of a randomized prospective study. Cancer 1989;63(3):428-32.
51. Rinaldi M, Belvedere O, Cauchi C, Defferrari C, Viola G, Grossi F. Maintenance chemotherapy in non-small cell lung cancer. Ann Oncol 2006;17 Suppl 2:ii67-70.
52. Berghmans T, Paesmans M, Meert AP, et al. Survival improvement in resectable non-small cell lung cancer with (neo)adjuvant chemotherapy: results of a meta-analysis of the literature. Lung Cancer 2005;49(1):13-23.

Appendix B

PROSPECT Database Screenshots

Appendix B: PROSPECT Database Screenshots

Clinical module

1) Patient Information, Social History, Medical History

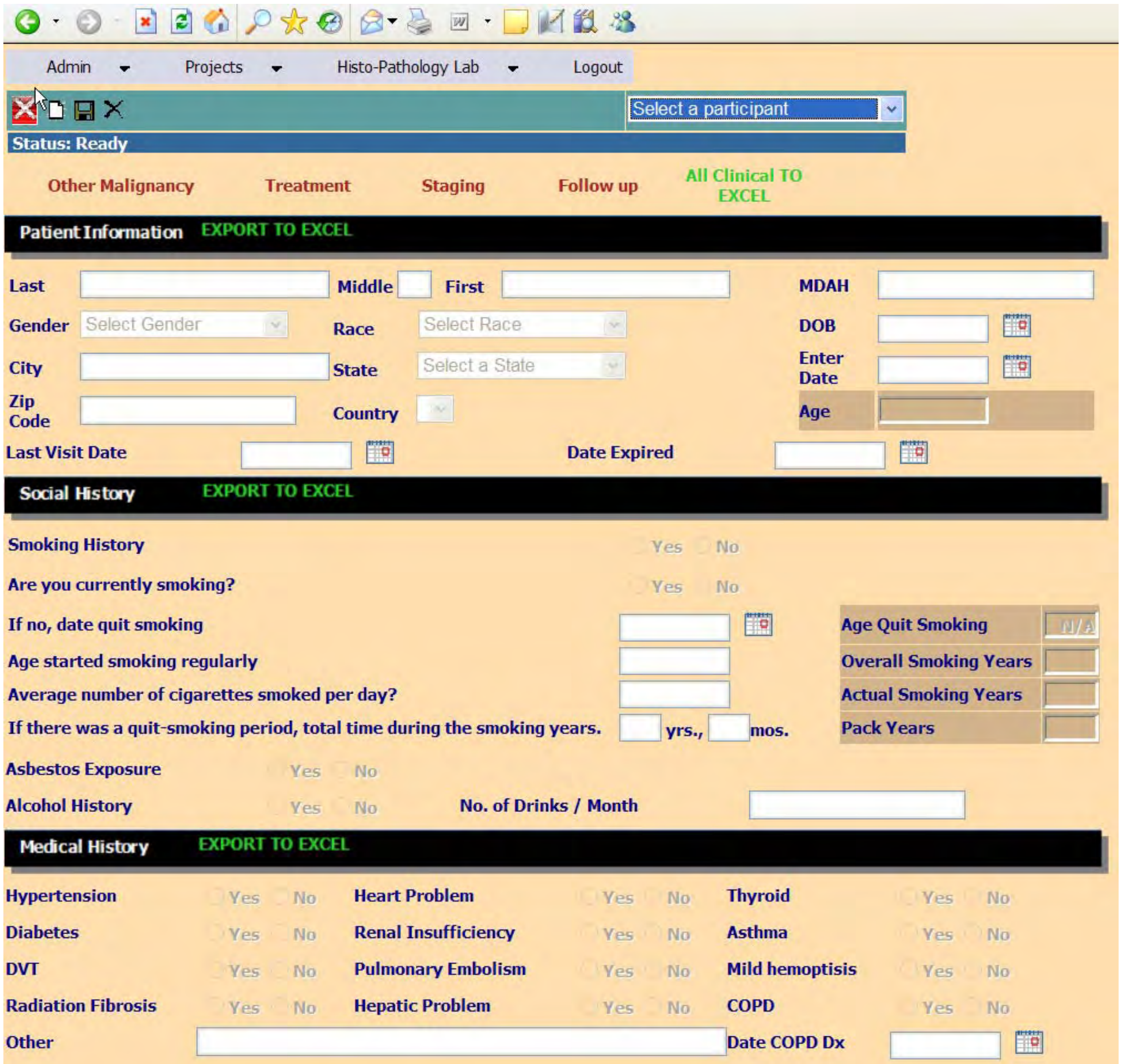

2) Other Malignancy

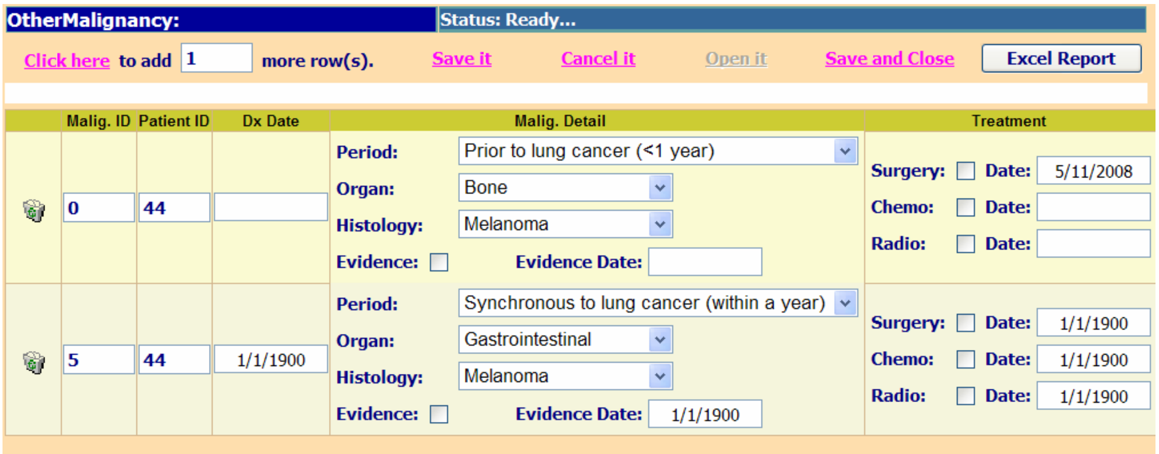

3) Treatment: Surgery, Chemotherapy, Radiotherapy and Other Treatments.

4) Staging

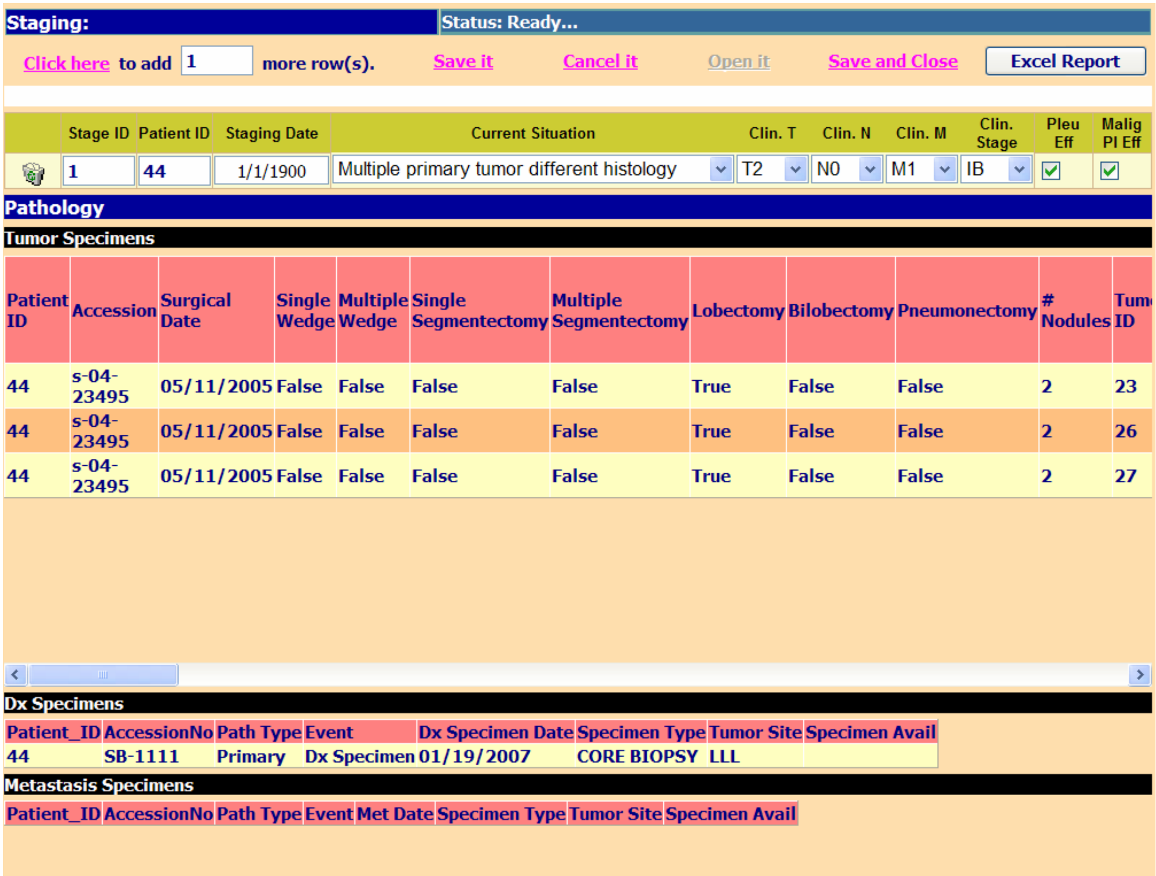

Staging:
Status: Ready...
Click here to add 1 more row(s).
Save it
Cancel it
Open it
Save and Close
Excel Report
Stage ID | Patient ID | Staging Date | Current Situation | Clin. T | Clin. N | Clin. M | Clin. Stage | Pleu Eff | Malig Pl Eff
1 | 44 | 1/1/1900 | Multiple primary tumor different histology | T2 | N0 | M1 | IB
Pathology
Tumor Specimens
Patient ID | Accession | Surgical Date | Single Wedge | Multiple Wedge | Single Segmentectomy | Multiple Segmentectomy | Lobectomy | Bilobectomy | Pneumonectomy | # Nodules | Tum ID
44 | s-04-23495 | 05/11/2005 | False | False | False | False | True | False | False | 2 | 23
44 | s-04-23495 | 05/11/2005 | False | False | False | False | True | False | False | 2 | 26
44 | s-04-23495 | 05/11/2005 | False | False | False | False | True | False | False | 2 | 27
Dx Specimens
Patient_ID | AccessionNo | Path Type | Event | Dx Specimen Date | Specimen Type | Tumor Site | Specimen Avail
44 | SB-1111 | Primary | Dx Specimen | 01/19/2007 | CORE BIOPSY | LLL
Metastasis Specimens
Patient_ID | AccessionNo | Path Type | Event | Met Date | Specimen Type | Tumor Site | Specimen Avail

5) Follow-up

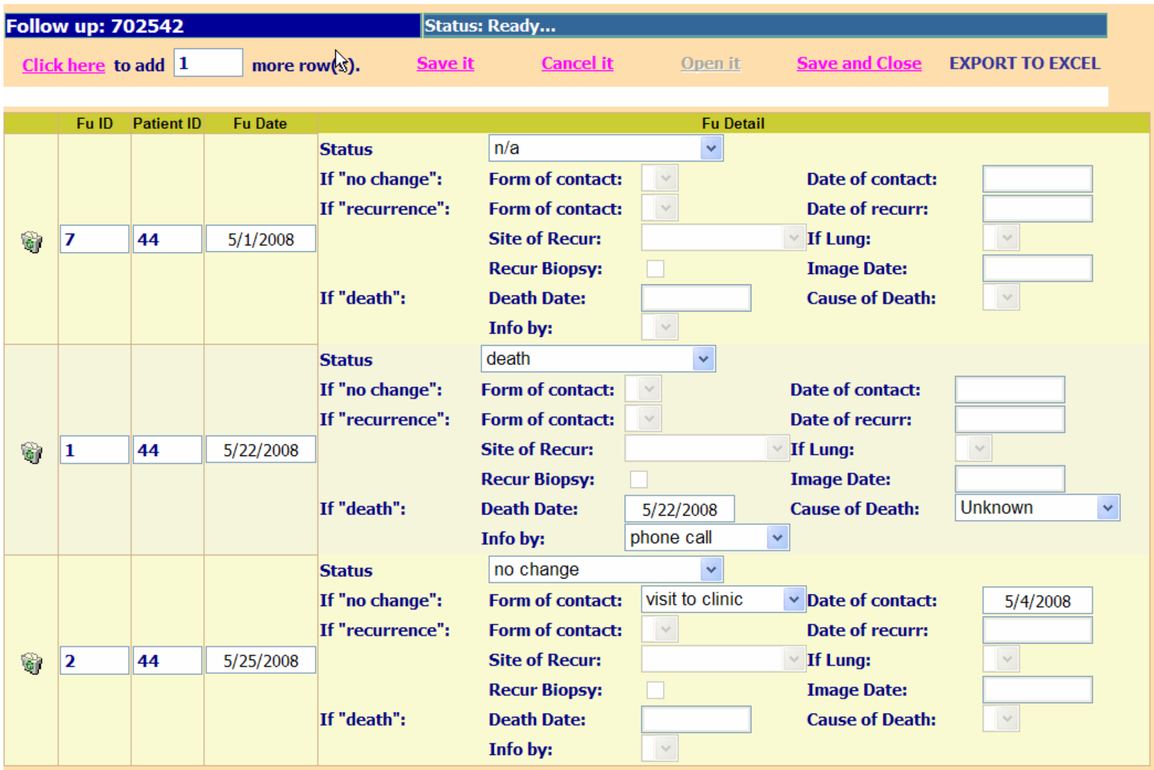
Follow up: 702542
Status: Ready...
Click here to add 1 more row(s).
Save it
Cancel it
Open it
Save and Close
EXPORT TO EXCEL
Fu ID
Patient ID
Fu Date
Fu Detail
7
44
5/1/2008
Status
n/a
If "no change":
Form of contact:
Date of contact:
If "recurrence":
Form of contact:
Date of recurr:
Site of Recur:
If Lung:
Recur Biopsy:
Image Date:
If "death":
Death Date:
Cause of Death:
Info by:
1
44
5/22/2008
Status
death
If "no change":
Form of contact:
Date of contact:
If "recurrence":
Form of contact:
Date of recurr:
Site of Recur:
If Lung:
Recur Biopsy:
Image Date:
If "death":
Death Date:
5/22/2008
Cause of Death:
Unknown
Info by:
phone call
2
44
5/25/2008
Status
no change
If "no change":
Form of contact:
visit to clinic
Date of contact:
5/4/2008
If "recurrence":
Form of contact:
Date of recurr:
Site of Recur:
If Lung:
Recur Biopsy:
Image Date:
If "death":
Death Date:
Cause of Death:
Info by:

Pathological module

1) Tissue Pathological Data

- Primary Dx specimen
- Primary Surgical Specimen
- Metastasis Dx Specimen
- Metastasis Surgical specimen

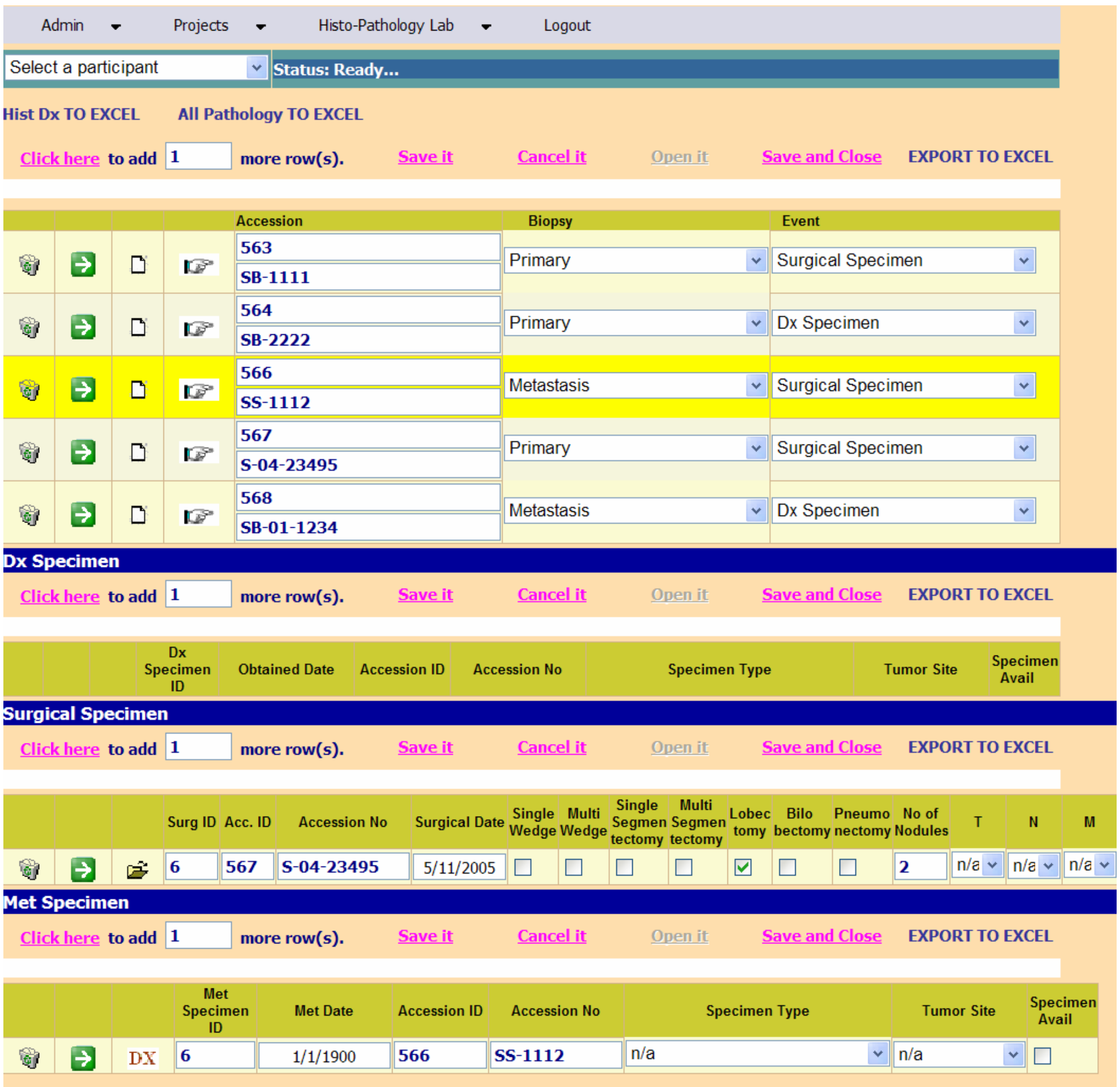

2) Histology

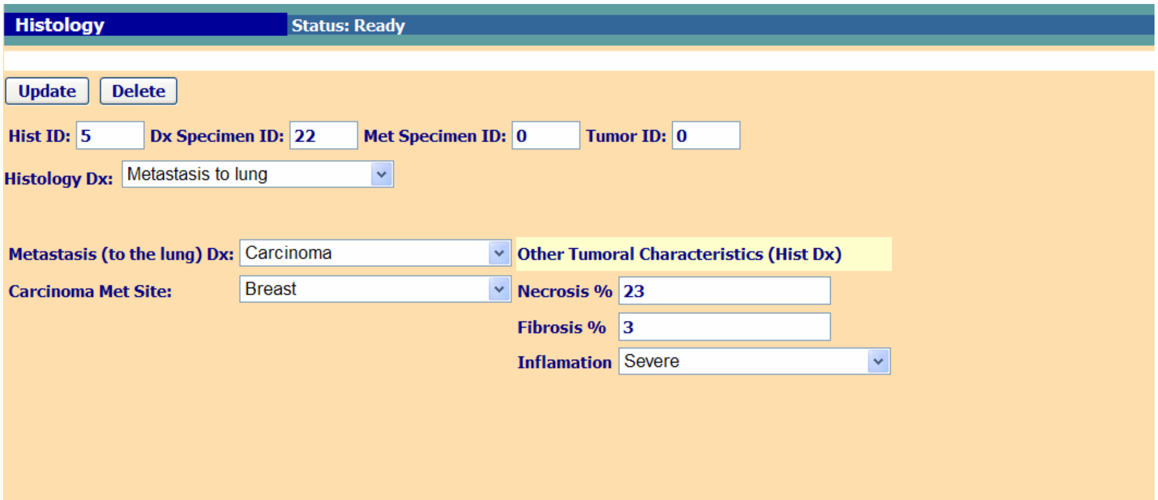
Histology
Status: Ready
Update
Delete
Hist ID: 5
Dx Specimen ID: 22
Met Specimen ID: 0
Tumor ID: 0
Histology Dx: Metastasis to lung
Metastasis (to the lung) Dx: Carcinoma
Other Tumoral Characteristics (Hist Dx)
Carcinoma Met Site: Breast
Necrosis % 23
Fibrosis % 3
Inflamation Severe

3) Staging and Tumor Information

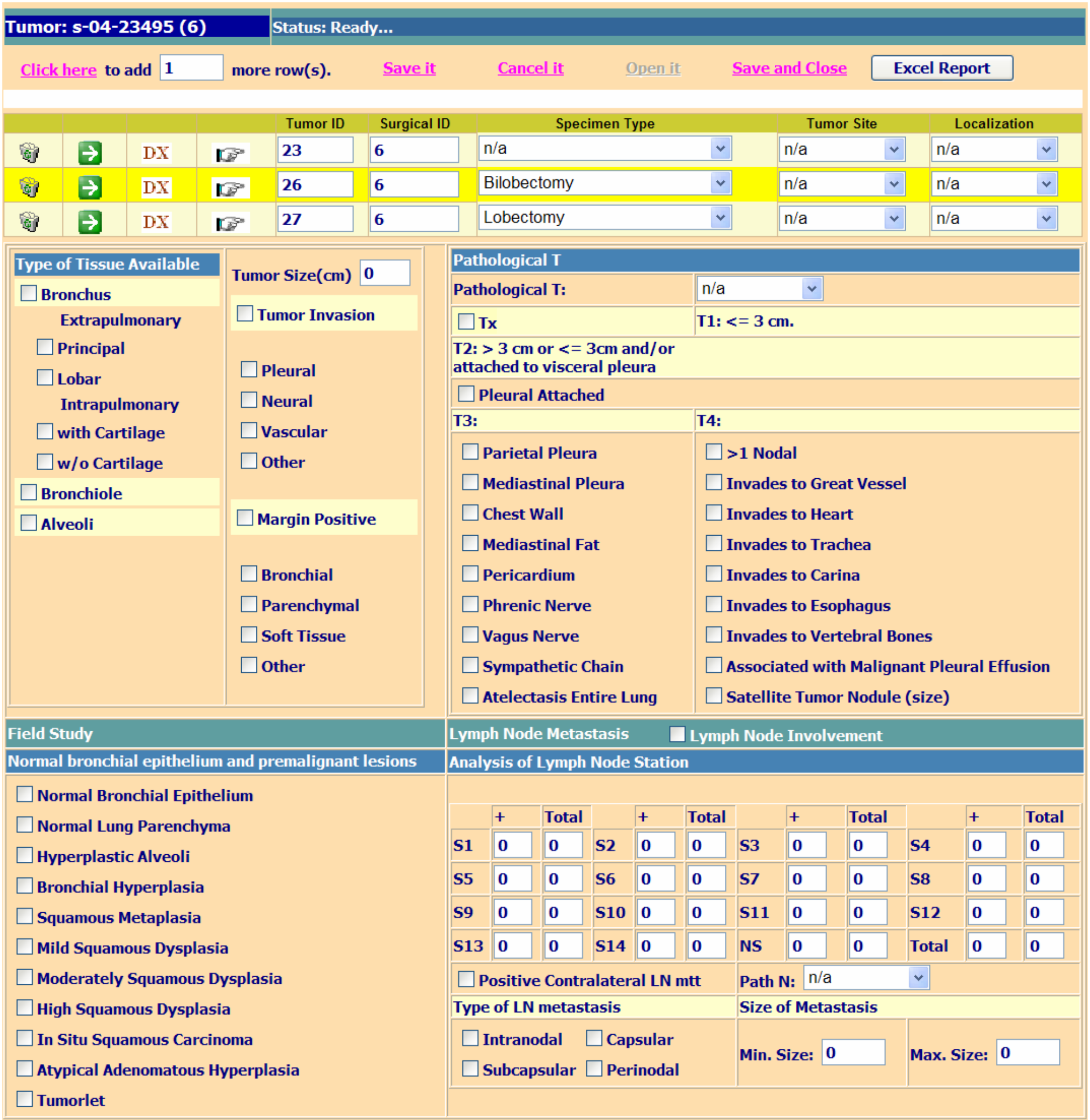

4) Tissue Bank (Frozen and Paraffin)

Dictionaries

Admin Projects Histo-Pathology Lab Logout

Dictionaries

Country Update

Page 1 [2] [3] [4] [5] [...]

	Dictionaries	Set Order
+		
	Afghanistan	1
	Albania	2
	Algeria	3
	American Samoa	4
	Andorra	5
	Angola	6
	Anguilla	7
	Antarctica	8
	Antigua and Barbuda	9
	Arctic Ocean	10
	Argentina	11
	Armenia	12
	Aruba	13
	Ashmore and Cartier Islands	14
	Atlantic Ocean	15
	Australia	16
	Austria	17
	Azerbaijan	18
	Bahamas	19

Page 1 [2] [3] [4] [5] [...]

Page 1of 14

Excel Reports

	K	L	M	N	O	P	Q
1	**Specimen Avail**	**Surgical Date**	**Single Wedge**	**Multiple Wedge**	**Single Segmentectomy**	**Multiple Segmentectomy**	**Lobectomy**
2							
3							
4							
5		5/11/2005 0:00	FALSE	FALSE	FALSE	FALSE	TRUE
6		5/11/2005 0:00	FALSE	FALSE	FALSE	FALSE	TRUE
7		5/11/2005 0:00	FALSE	FALSE	FALSE	FALSE	TRUE
8		5/11/2005 0:00	FALSE	FALSE	FALSE	FALSE	TRUE
9							
10							
11							
12							
13		1/1/1900 0:00	FALSE	TRUE	TRUE	FALSE	FALSE
14		1/1/1900 0:00	FALSE	TRUE	TRUE	FALSE	FALSE
15	FALSE						
16	TRUE						
17							
18							
19		1/1/1900 0:00	FALSE	FALSE	FALSE	FALSE	FALSE
20							
21							
22							
23							
24							
25							
26		1/1/1900 0:00	FALSE	FALSE	FALSE	FALSE	FALSE
27							
28							
29							
30							
31							
32							
33							
34							
35							